

https://dspace.org/

Process Simulation for Biofuels Production from Castor Oil

Maluleke, Lethabo

2025-07
University of the Witwatersrand, Johannesburg
https://hdl.handle.net/10539/49749
Maluleke, Lethabo. (2025). Process Simulation for Biofuels Production from Castor Oil. [Master's dissertation, University of the Witwatersrand, Johannesburg]. WIReDSpace. https://hdl.handle.net/10539/49749

Downloaded from a DSpace repository. https://dspace.org/



Process Simulation for Biofuels Production from Castor Oil

Master of Science CHMT7008A RESEARCH REPORT

Prepared by

Lethabo Maluleke

9901419F

Submitted to

School of Chemical and Metallurgical Engineering, Faculty of Engineering and the Built Environment Environment, University of the Witwatersrand, Johannesburg, South Africa

Supervisor(s): Dr Saeideh Babaee

July 2025

Abstract

In this study, the process simulation for producing biofuels from castor oil was developed with remarkable success. The objectives were to simulate the mass and energy balance for different catalysts consisting of Alumina and Nickel composites at various temperatures and pressures, with applicable conversion rates. The Alumina catalyst was used for hydrotreating at 345˚C and 30bar for green diesel production and hydrocracking at 240˚C and 60bar for bio-jet fuel and bio-gasoline production. Nickel-based 25%NiSAPO-11 was used for the hydrotreating process at 300˚C and 30bar, 25%Ni/ZSN-5 was used in the hydrocracking process at 300˚C and 30 bar for bio-jet fuel and bio-gasoline production.

Green diesel was produced from the two catalysts with a similar flowsheet. The quality of the green diesel is aligned with the commercial diesel and thus provides confidence for the green diesel to be produced commercially. There are tail gases produced as waste streams during this process, which can be environmentally unfriendly; however, their impact is less than that of using fossil fuels for fuel. The tail gas contains carbon dioxide, which is a greenhouse gas. Carbon capture and storage technology can be used to store the gas and eliminate negative environmental impact. The carbon capture technology is not covered in the study.

Based on the results, the green diesel process was scaled up in mass flow to larger larger-sized process plant without any complications. The scaling is proportionate in nature to the ratio of the pilot initially studied. Product qualities remain the same, and the demand for feedstock and energy scales in proportion to the castor oil feed rate. The waste streams are also proportionate. Hydrogen as a feedstock is consumed in the process; the production process for hydrogen was not explored, although the use of green hydrogen in the process would be ideal. The energy requirement for the green diesel process is for the hydrogen compressor, which generates elevated temperatures for the hydrotreating reactor.

In this study, the green diesel flowsheet was further developed to produce bio-jet fuel in the hydrocracking reactor. With the application of Alumina catalyst and 25%Ni/ZSN, these processes were developed first for the 100kg/hr of castor oil and then for the 1000kg/hr of castor oil feed. In addition, the process flowsheets were identical, with a variation in process reactor conversions, pressure, and temperature conditions. The Bio-jet fuel was produced through green diesel cracking with hydrogen, forming short alkanes. The products were separated in a RadFrac distillation column. The Bio-jet fuel

was the heavy fraction of C8 to C15, and the light liquid hydrocarbons streams were the top products.

The bio-jet fuel produced was compatible with commercial jet fuel, which can thus be produced for commercial applications. The energy consumption of the bio-jet fuel is in addition to the green diesel process, although energy recovery is possible through process integration between the heaters and coolers. Pinch technology principles were applied in the integration of the process streams. There was a hydrogen compressor installed for the supply of hydrogen into the cracking process. A turbine was installed to recover the unreacted hydrogen and gases, integrating them into the green diesel process. Based on the results, the bio-jet fuel process was scaled up without compromising the product quality. The hydrogen recovery process was integrated with the green diesel hydrogen system.

The bio-gasoline production process was achieved through optimisation of the separation section of the bio-jet fuel production process. The hydrocracking reactor produces a varied range of hydrocarbons from C3 to C16, and the bio-gasoline was composed of C4 to C12. Therefore, various distillation optimisations can be embarked on to determine the product slate for either bio-jet fuel or bio-gasoline. Bio-jet fuel composition includes C7 to C15 components.

The bio-gasoline process also produced petroleum gas as a byproduct. In the RadFrac column separation stage, bio-gasoline was produced as a bottom's product, and the top products were liquid and gas streams. These top streams had comparable properties to petroleum gas with high percentages of propane and traces of butane. Residual hydrogen from the hydrocracking reactor also appeared in the gaseous stream.

Table of Contents

Abstract 1
Chapter 1: Research Background 10
1.1 Introduction 10
1.2 Problem Statement 16
1.3 Research aims and objectives. 16
Chapter 2: Literature Review 17
2.1 Biofuels 17
2.1.1 Biodiesel ***vs.*** Renewable/Green Diesel Properties 17
2.1.2 Gasoline Properties 18
2.1.3 Bio-jet fuel vs Commercial Jet fuel properties 19
2.2 Methods for Biofuel Production from Castor Oil 20
2.2.1. Transesterification (Alcoholysis) 20
2.2.2. Pyrolysis 20
2.2.3. Hydrocracking 20
2.3 Process Design - Flowsheet Development for Hydrocracking 21
2.4 Simulation of biofuels in Aspen Plus 21
2.4.1 Simulation and optimization of a bio-jet fuel production process from castor oil 21
2.4.2 Simulation of the soybean oil hydrotreating process for green diesel production 22
2.5 Catalyst for the Biofuels production from Castor Oil 22
2.5.1 Alumina Catalyst 22
2.5.2 Nickel on Different Acidic Zeolite Catalysts 23
Chapter 3: Methodology 25
3.1 Process Flow Description 25
3.1.1 Pre-treatment 25
3.1.2 Hydrotreating 26
3.1.3 Intermediate Separation 28
3.1.4 Isomerisation and hydrocracking 28
3.1.5 Final Separation 29
3.2 Simulation 30
3.2.1 Aspen Plus 30
3.2.2 Green Diesel Production Model 30
3.2.2.1. Component Description 31

3.2.2.2. Thermodynamic Methods 32
3.2.2.3. Feed Supply 32
3.2.2.4. Feed Pre-Cooler 33
3.2.2.5. Hydrodeoxygenation Reactor 33
3.2.2.6. Stearic Acid Conversion 34
3.2.2.7. Linoleic Acid Conversion 34
3.2.2.8. Ricinoleic Acid Conversion 34
3.2.2.9. Oleic Acid Conversion 35
3.2.2.10. Hexadecanoic Acid Conversion 35
3.2.2.11. Product Cooling 35
3.2.2.12. Product Separation 36
3.2.3 Bio-jet Fuel Production Model 38
3.2.3.1 Hydrocracking Reactor 39
3.2.3.2 Pentadecane cracking reactions 39
3.2.3.3 Hexadecane cracking reactions 39
3.2.3.4 Heptadecane cracking reactions 40
3.2.3.5 Octadecane cracking reactions 40
3.2.3.6 Hydrogen feed 41
3.2.3.7 Product separation 41
3.2.3.8 Distillation 43
3.2.3.9 Streams 43
3.2.3.10 Pressure Inputs 44
3.2.4 Sensitivity Studies 44
3.2.4.1 Flow Rate 44
3.2.4.2 Temperature and pressure for different catalysts 45
3.2.5 Energy Efficiency 45
3.2.5.1 Pinch Technology 45
3.2.5.2 Energy consumption comparison to petroleum refineries 47
Chapter 4: Results and Discussion 48
4.1 Process Flowsheets for Green Diesel Production 48
4.1.1 Material Balance in Hydrotreating Reactor 50
4.1.2 Product Separation 51
4.1.2.1 Green Diesel 51

4.1.2.2 Water 52
4.1.2.3 Tail gas 52
4.1.3 Optimisation 53
4.1.3.1 Energy Consumption 53
4.1.3.2 Scalability 54
4.1.3.3 Sensitivity Analysis for Hydrogen Consumption 58
4.1.3.4 Energy Consumption for scaling 60
4.2 Process Flowsheet for Bio-jet fuel production 61
4.2.1Hydrocracking Reactor Material Balance 61
4.2.2 Final Products 63
4.2.3 Waste Streams 64
4.2.4 Scalability 64
4.2.4.1 Product quality 65
4.2.4.2 Hydrogen Consumption 74
4.2.5 Energy Efficiency 75
4.2.5.1 Hydrotreating Pinch Analysis 75
4.2.5.2 Hydrocracking Pinch Analysis 76
4.2.5.3 Distillation Pinch 77
4.2.5.4 Comparison to petroleum refining energy consumption 78
4.2.6 Distillation 79
4.2.6.1 Product Streams 80
4.2.7 Bio-gasoline production process. 81
Chapter 5: Conclusions 85
Chapter 6: Recommendations 86
References 87
Appendix A: Catalysis research on hydrotreating of vegetable oils, waste cooking oil 90
Appendix B: Distillation profiles 91

List of Figures

Figure 2.1. The molecular structure of Castor Oil (Ogunniyi, 2005).

Figure 2.2: Demonstration of Castor oil conversion to various fuels over a nickel-based catalyst. (Liu, et al., 2015)

Figure 3.1: Typical process for hydrotreated vegetable oil (Szeto & Leung, 2022)

Figure 3.2: Reactions for Hydrodeoxygenation, Decarboxylation and Decarbonylation

Figure 3.3: Green Diesel production flowsheet in Aspen Plus

Figure 3.4: A list of components loaded onto the Aspen Simulation.

Figure 3.5: Thermodynamic method

Figure 3.6: Castor Oil in feed stream

Figure 3.7: Feed Pre-cool to 345˚C

Figure 3.8: Reactor operating pressure and temperature

Figure 3.9: Stearic acid hydrogenation reactions in Aspen

Figure 3.10: Linoleic acid hydrogenation reactions in Aspen

Figure 3.11: Ricinoleic acid hydrogenation reactions in Aspen

Figure 3.12: Oleic Acid hydrogenation reactions in Aspen

Figure 3.13: The Hexadecanoic acid hydrogenation reactions in Aspen

Figure 3.14: Product cooling and flash drum conditions

Figure 3.15: Final product Cooler

Figure 3.16: Pressure valve dropping pressure to 2bar.

Figure 3.17: Flash drum conditions for final product separation

Figure 3.18: The hydrogen split fraction in Stream 16

Figure 3.19: Fresh Hydrogen make-up stream

Figure 3.20: Hydrogen Compressor

Figure 3.21: Process flowsheet for hydrocracking section

Figure 3.22: The green diesel is pumped and preheated before the reactor.

Figure 3.23: Reactions for Pentadecane hydrocracking into shorter alkanes in Aspen.

Figure 3.24: Reactions for Hexadecane hydrocracking into shorter alkanes in Aspen.

Figure 3.25: Reactions for Heptadecane hydrocracking into shorter alkanes in Aspen.

Figure 3.26: Reactions for Octadecane hydrocracking into shorter alkanes in Aspen.

Figure 3.27: Hydrogen feed to the Hydrocracking Section

Figure 3.28: Hydrocracking hydrogen feed

Figure 3.29: Cooling and flash drum conditions for product separation

Figure 3.30: The isentropic turbine installed for pressure reduction.

Figure 3.31: The pressure changing valve for the product stream.

Figure 3.32: Pre-distillation heater for product stream

Figure 3.33: Configuration for distillation column

Figure 3.34: Distillation Streams configuration

Figure 3.35: Pressure in the column

Figure 3.36: Condenser specifications

Figure 3.37: Example Using hot and cold composite curves to determine energy targets (March, 1998)

Figure 3.38: Pinch Principle (March, 1998)

Figure 4.1 Green Diesel production flowsheet

Figure 4.2: Hydrogen consumption vs recycle stream size for the 100kg/hr case of NiSapo.

Figure 4.3: Hydrogen consumption vs recycle stream size for NiSapo.

Figure 4.4 Hydrocracking flowsheet

Figure 4.5: Hydrocarbon distribution to the final product stream

Figure 4.6: Bio-jet fuel production process for 100kg/hr of castor oil with Alumina

Figure 4.7: Bio-jet fuel production process for 1000kg/hr of castor oil with Alumina.

Figure 4.8: Bio-jet fuel production process for 100kg/hr of castor oil with Ni/ZSM-5.

Figure 4.9: Bio-jet fuel production process for 1000kg/hr of castor oil with Ni/ZSM-5.

Figure 4.10: Heat integration illustrated on the Castor Oil Aspen Simulation

Figure 4.11: Separation process of Bio-jet/Bio-gasoline fuel

Figure 4.12: Distillation 1 column specifications

Figure 4.13: Distillation 2, second and final distillation column specification

List of Tables

Table 1.1: Classification of biofuels (Rodionova, 2017)

Table 1.2 Various Vegetable oils (Navale, et al., 2011).

Table 2.1: Fatty acid profile of Castor oil (Orozco, et al., 2017)

Table 2.2: Physical properties of castor oil (Molefe, et al., 2019).

Table 2.3: Typical properties of biodiesel compared to petroleum diesel and renewable diesel (Hoekman, et al., 2012)

Table 2.4: Typical Gasoline properties (Veza, et al., 2019).

Table 2.5: Typical Bio-jet fuel properties (Wu, et al., 2016)

Table 2.6: Hydro conversion of castor oil on Ni supported on different strengths of zeolites (Liu, et al., 2015)

Table 4.1 Scenarios for Green Diesel modelling

Table 4.2 Base Case: Mass and Energy Balance 100kg/hr with Alumina Catalyst

Table 4.3: Material balance across the hydrotreating reactor

Table 4.4 Green Diesel Quality

Table 4.5: Tail Gas Composition

Table 4.6 Hydrogen Compressor Energy Requirement

Table 4.7 Case 1: Mass and Energy Balance for 1000kg/hr with Alumina Catalyst

Table 4.8 Case 2: Mass and Energy Balance 100kg/hr of 25% Ni/SAPO-11

Table 4.9 Case 3: Mass and Energy Balance 1000kg/hr of 25% Ni/SAPO-11

Table 4.10 Green Diesel Product Quality Analysis for different cases.

Table 4.11: Compressor results for the NiSapo 100kg/hr and 1000kg/hr.

Table 4.12: Material balance in the hydrocracking reactor.

Table 4.13: Turbine and compressor for Hydrocracking for 100kg/hr Ni/SAPO-11

Table 4.14: Typical Bio-jet fuel properties (Wu, et al., 2016)

Table 4.15: Scenarios for Process Optimisation

Table 4.16 Mass and Energy Balance Alumina 100kg/hr

Table 4.17: Alumina 100kg/hr Summary of Feedstock and Final Products

Table 4.18 Alumina 1000kg/hr Mass and Energy Balance

Table 4.19: Alumina 1000kg/hr Feedstock and Final Products

Table 4.20: Ni/ZSM-5 100kg/hr Mass and Energy Balance

Table 4.21: Ni/ZSM-5 100kg/hr Feedstock and Product Analysis

Table 4.22: Ni/ZSM-5 1000kg/hr Mass and Energy Balance

Table 4.23: Ni/ZSM-5 1000kg/hr Feedstock and Product Quality Analysis

Table 4.24: Material balance across the hydrocracking reactor for the 1000kg/hr Ni/ZSM-5 case.

Table 4.25: Turbine and compressor for 1000kg/hr Ni/ZSM-5

Table 4.26: Hot streams for the hydrotreating section.

Table 4.27: Hot and Cold Stream temperatures

Table 4.28: Distillation column cold and hot streams

Table 4.29 Split fractions in the Distillation column for the 100kg/hr Ni/ZSM-5

Table 4.30: Bio-jet fuel product comparison

Table A.1: Condenser/Top Stage performance

Table A.2: Reboiler/Bottom stage performance.

Chapter 1: Research Background

1.1 Introduction

Economic development is faced with a lot of challenges, considering the depletion of natural resources as well as the environmental legislation that requires compliance while developing the natural resources into final products. South Africa (SA) had approximately 0.95 thousand barrels per day of crude oil reserves as of September 2021, according to the World Data Atlas (Atlas, 2022). SA's daily crude oil production sits at approximately 0.55 million barrels per day as of December 2020, while petroleum consumption is approximately 0.49 million barrels per day, according to the same reference (Atlas, 2022). Approximately 64% of our daily oil consumption is imported oil. This makes the SA economy quite vulnerable to the fluctuating oil prices in the world, and yet, oil demand continues to increase as the industrial sector and civilisation expand. Dwindling natural resources, accompanied by increasing concerns about the negative environmental impact of greenhouse gas emissions, have encouraged the exploration of alternative energy sources (Linganiso, et al., 2022).

The negative environmental impact, as a main concern, is greenhouse gas emissions into the atmosphere, which causes global warming. Global warming is the increase in the overall temperature of the Earth's surface beyond the normal increases. Greenhouse gases cause global warming by capturing heat in the atmosphere. Carbon dioxide (CO_2) is the main gas that is believed to be a contributor to global warming. Of the gases emitted in 2004, 56 % was carbon monoxide (CO) caused by using fossil fuels, and the second part came from CO_2 due to deforestation (Tvaronaviciene, 2021). It is well known that CO_2 from industries like power generation, motor vehicles, and chemical processes also contribute to the overall emissions. It has thus become imperative for organisations to reduce greenhouse gas emissions for the future sustainability of the planet. Sustainability means utilising today's resources without negatively impacting the environment, so that the planet's resources will then be available for future generations. Global warming has a ripple effect on other areas that are disruptive to the planet, i.e., changing precipitation patterns, increasing evaporation due to warming, and increasing temperature extremes (Tvaronaviciene, 2021). Alternative energy sources such as biofuels do not contribute to global warming as compared to petroleum fuels. CO_2 emitted from fossil fuels stays in the atmosphere, whereas CO_2 from biofuels is reabsorbed through photosynthesis by plants. Therefore, CO_2 is naturally balanced. Biofuels are thus a renewable source of energy (Navale, et al., 2011). A further discussion of the carbon dioxide emissions from biodiesel compared with diesel fuel would require an analysis of the total system. Biodiesel production requires agricultural land and energy for tillage, chemicals,

machinery, harvesting, transport, storage, and labour. Processing requires energy to operate mixers and pumps, presses, the production of storage vessels, and labour. The fuel would also require transportation to its point of use. (Peterson & Hustrulid, 1997) Assuming that the energy requirements for the development and processing of biofuels are from another biofuels source, it remains a preferable source of energy than fossil fuels from a global warming perspective.

The biofuels production drive has additional benefits besides the climate change sustainability benefit. The growing interest in many African countries can be explained by factors such as high crude oil prices, fluctuations in prices due to geopolitical uncertainties, local and global environmental impacts of fossil fuels, opportunities for job creation, new research and technological advances, economic development, and the need to increase the access to energy services (Visagie & Prasad, 2006). The use of African land to grow biofuels crops can assist in poverty alleviation and economic development for the continent. Several African countries have signed agreements with foreign investors to devote large parcels of land for biofuel production (UNIDO, 2009). A balancing act between food supply and industrial development of biofuels from the same land should be carefully considered.

Biofuels are energy-rich chemicals produced through biological processes or obtained from the chemical conversion of biomass from former living organisms. Biofuels are produced from photosynthetic organisms such as photosynthetic bacteria, micro- and macro-algae, and vascular land plants. The primary products of biofuel may be in a gas, liquid, or solid form. These products can be further converted by biochemical, physical, and thermochemical methods. Biofuels can be classified into two categories: primary and secondary biofuels. The primary biofuels are unprocessed, directly produced from burning wood or cellulosic plant material and dry animal waste. Secondary biofuels undergo chemical processing and can be classified into three generations that are each indirectly generated from plant and animal material. The third generation is the biofuels generated from cyanobacteria, microalgae, and other microbes, which is the most promising approach to meet the global energy demands (Rodionova, 2017). Table 1.1 shows the classification of biofuels.

Table 1.1: Classification of biofuels (Rodionova, 2017)

Biofuels			
Primary	Secondary		
	First generation	Second generation	Third generation
Firewood, wood chips, pellets, animal waste, forest and crop residues, landfill gas.	Bioethanol or butanol by fermentation of starch (from wheat, barley, corn, potato) or sugars (from sugarance and sugar beet.) Biodiesel by transesterification of oil crops (rapeseed, soybeans, sunflower, palm, coconut, used cooking oil, and animal fats.)	Bioethanol and biodiesel produced from Conventional technologies but based on novel starch, oil and sugar crops such as *Jatropha*, cassava or *Miscanthus*; Bioethanol, biobutanol, syndiesel produced from lignocellulosic materials (e.g. straw, wood and grass)	Biodiesel from microalgae Bioethanol from microalgae and seaweeds Hydrogen from green microalgae and microbes

The vegetable and animal-derived feedstocks used to produce biofuels are known as triglycerides (Hoekman, et al., 2012). The vegetable oils are favourable as sources of biofuels due to their ease of conversion from triglycerides to liquid transportation fuels as compared to other biomass sources. They are high-energy liquids that contain less oxygen. (Ong & Bhatia, 2010) (Taufiqurrahmi & Bhatia, 2011).

It is important to ensure that food security is not threatened when driving the production of fuels from vegetable oils. Thus, the use of non-edible vegetable oils in chemical processing is preferred. In developing countries, biofuel sources are more focused on non-edible vegetable oils as alternative fuels to diesel because edible vegetables are used in our day-to-day life (Navale, et al., 2011). Table 1.2 below shows a list of edible and non-edible vegetable oils that are potential sources for biofuel feedstock.

Table 1.2 Potential Vegetable oils (Navale, et al., 2011) for Biofuel production.

Edible Vegetable Oils	**Non-edible Vegetable Oils**
Peanut	Jatropha curcas
Safflower	Karanjia (pongamia glabra)
Palm	Pongamia pinnata
Soybean	Mahua
Sesame	Neem
Rapeseed/Canola	Pine seeds
Sunflower	Castor
Mustard	Nagchmaba
Linseed	Kusum
Coconut	Ark (Calotropis gigantea)

The choice of vegetable oil depends particularly on its availability, cost, and climate in each country (Taufiqurrahmi & Bhatia, 2011). For the African context, the castor oil plant (Ricinus communis) is preferred. It is a plant species of the Euphorbiaceae that originates in Africa, but it is found in both wild and cultivated states in all the tropical and subtropical countries of the world (Forero, 2004). The comparative advantage of Ricinus communis is that its growing period is much shorter than that of Jatropha curcas and Pongamia pinnata, and there is greater experience and awareness among farmers about its cultivation (Rajagopal, 2007). Ricinus communis is an ideal candidate for production of high value, industrial oil feedstocks because of the very high oil content (48%–60%) of the seed, and the extremely high levels of potential oil production (500 to1000 litres of oil per acre) (Dermibas, et al., 2016).

Castor seeds are poisonous to humans and animals because they contain ricin, ricinine, and certain allergens that are lethally toxic. If a seed is ingested accidentally, it causes abdominal pain, vomiting, and diarrhoea. It is claimed that as little as one milligram of ricin can kill an adult (Woodend, 1993). This makes castor oil a good selection for biofuels production as the use of castor seeds does not threaten food security. Castor oil has various other applications which include usage in chemical industries as a raw material for paints and coatings, in cosmetics, hairdressing, ointments, and as an ingredient of soaps and polishes amongst other uses (D.S., 2005).

Castor oil, like all other vegetable oils, has different physical and chemical properties that vary with the method of extraction. The different methods for castor oil extraction from castor seeds include traditional extraction, solvent extraction, and cold pressing. The traditional extraction method is regarded as inefficient and time-consuming, as it only yields 20% of the oil (Oluwe, et al., 2012). Cold-pressed castor oil has a low acid value, low iodine value, and a slightly higher saponification value than the solvent-extracted oil, and it is lighter in colour. Also, the oil is insoluble in alcohol (Ogunniyi, 2005). The composition for castor oil is presented in Table 2.1 below:

Table 2.1: Fatty acid profile of Castor oil (Orozco, et al., 2017).

Fatty Acid	Composition(w/w%)
Ricinoleic acid	87.0
Oleic acid	7.42
Linoleic acid	3.10
Stearic Acid	1,03
Palmitic Acid	0.91

The chemistry of castor oil is centred on its high content of ricinoleic acid as in Table 2.1 The ricinoleic acid($C_{18}H_{34}O_3$) gives characteristics such as high viscosity, high miscibility, low iodine content, low freezing point, which make it an appropriate raw material to produce biofuel (Osorio-Gonzalez, et al., 2020). Table 2.2 below shows the Physical properties of castor oil.

Table 2.2: Physical properties of castor oil (Molefe, et al., 2019).

Physical Properties	Units	Values
Viscosity	mm2s-1	6.27-8.84
Density	g/mL	0.957-0.961
Thermal Conductivity	W/m°C	4.727
Specific Heat	kJ/kgK	0.089
Flash Point	°C	145
Pour Point	°C	2.7
Melting Point	°C	-2 to -5
Refractive index		1.472 -1.480

R. communis meets most of the properties considered desirable to produce useful feedstocks in biodiesel production, except for the high viscosity of oil that may limit its use. The high viscosity of Ricinus communis oil adds to its poor atomization of the fuel, incomplete combustion, choking of the fuel injectors, and ring carbonisation (Baroutian, et al., 2010). The molecular structure of castor oil is shown in Figure 2.1 below (Ogunniyi, 2005):

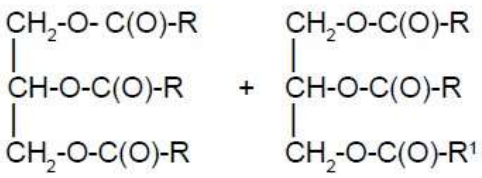


Figure 2.1*. The molecular structure of Castor Oil (Ogunniyi, 2005).*

R displays - (CH2)7-CH=CH- CH2-CH(OH)-(CH2)5-CH3 and R1 shows other fatty acid derivatives

According to (Amigun et al., 2010), there are no operational large-scale (commercial) biodiesel plants on the African continent. This is echoed by (Pradhan & Mbohwa, 2014) South Africa has stalled in the legislative process, and no large-scale commercial biofuel project has materialised yet. Developing biofuels, especially using food grain, is a challenge to the government of South Africa due to issues related to food security, commodity prices, economic and social concerns, and impacts of land use changes on the environment. (Pradhan & Mbohwa, 2014) The biodiesel market in Africa is mainly characterised by several small- and medium-scale producers. Most of the countries in Africa, except South Africa, Mozambique, and Zimbabwe, are still in the first stage of biodiesel development. South Africa's biodiesel market is characterised by several small- and medium-scale producers, while Zimbabwe recently inaugurated Africa's first-ever commercial biodiesel plant. The 6 million US dollar biodiesel plant, which processes Jatropha, cotton seed, sunflower, and soya, among other feedstocks, can produce 100ML annually. The plant was expected to save up to US$80 million a year in foreign currency from the importation of diesel. However, the plant is operating at less than 5% capacity, which is attributed to an acute shortage of feedstock.

The production and commercialisation of biodiesel in Africa could provide an opportunity to diversify energy and agricultural activity, reduce dependence on fossil fuels (oil), and sustainably contribute to economic growth (Amigun et al., 2008). World-leading biofuels producers for the period 2007 – 2017 are from North America, South & Central America, Europe, and Asia Pacific. The biofuels production from these regions showed a growth rate of 11.4% annually. Biofuels production and consumption data for the 12 years of 2007-2017 showed that in most of the surveyed countries, biofuels policies played an important role in developing and growing regional and national biofuels markets. (Ebadian, van dyk, McMillan, & Saddler, 2020)

Molefe, et al., 2019 reviewed the various methods to determine the simultaneous production of bio-gasoline and bio-jet fuels from Castor oil. (Molefe, et al., 2019). The methods included Hydrocracking, pyrolysis, and transesterification. Although transesterification is common, hydrocracking is ideal for producing high-quality bio-jet and bio-gasoline with a single catalyst. The study will focus on producing bio-jet fuel and bio-gasoline from castor oil through hydrodeoxygenation and hydrocracking. Green diesel production will be an intermediate product.

1.2 Problem Statement

Energy is essential for both development and economic growth. The use of fossil fuels for energy remains an environmental concern due to greenhouse gas emissions, as the major contributor to carbon dioxide emissions. Environmentally friendly energy sources are needed.

The challenge with biofuels is the large industrial scale production of fuels, which is underdeveloped, especially in Africa. The challenge is due to issues related to food security, commodity prices, economic and social concerns, and impacts of land use changes on the environment. (Pradhan & Mbohwa, 2014) . These impacts have halted the development of biofuels on a large scale.

The lack of economic development and jobs in Africa remains a concern for the well-being and prosperity of the African continent. Growing and developing alternative technologies are vital to enable economic growth. Africa's substantial land capacity permits the cultivation of energy crops, which can serve as feedstock for biofuel production facilities. The modelling of the production process at different capacities encourages development in making technical information available for feasibility studies by aspiring entrepreneurs. In addition, modelling castor oil feedstock as a non-edible crop makes information available to eliminate the concern of food security challenges to policymakers. The lifecycle emissions of a castor oil production process can be evaluated based on the modelling results.

1.3 Research aims and objectives.

The research aims to develop a flowsheet for the pilot-scale production of green diesel, bio-jet fuel, and bio-gasoline from castor oil using hydrotreating and hydrocracking in the presence of catalysts, including alumina and nickel-based composites.

The research objectives are detailed below:

a. To develop an Aspen Model for green diesel, bio-gasoline, and bio-jet fuel production from castor oil using hydrotreating and hydrocracking. Green diesel is the intermediate product in the production of bio-gasoline and bio-jet fuel.

b. To model the mass and energy balances of the different catalyst effects on Aspen Plus and evaluate the effect of castor oil mass flow rate on yield and product slate.

c. To optimise and recommend an energy-efficient process through heat integration from the mass and energy balances performed.

Chapter 2: Literature Review

2.1 Biofuels

This study will consider renewable/green diesel, bio-jet fuel, and bio-gasoline as biofuels.

2.1.1 Biodiesel *vs.* Renewable/Green Diesel Properties

Biodiesel is defined by ASTM as a fuel comprised of mono-alkyl esters of long-chain fatty acids derived from vegetable oils or animal fats, designated as B100. Biodiesel is produced via transesterification, where triglycerides react with alcohol and a catalyst. A by-product of transesterification is glycerine, also known as glycerol. Since the most common alcohol used to produce biodiesel is methanol, another name for biodiesel is fatty acid methyl esters (FAME) (Hoekman, et al., 2012)

Renewable diesel is produced by catalytic hydroprocessing of triglyceride feedstock to produce biodiesel. In this process, alcohol is not utilised, the resulting products are hydrocarbons instead of fatty acid alkyl esters, and glycerol is not generated (Hoekman et al., 2012). Table 2.3 below shows a comparative study of typical biodiesel, petroleum diesel, and renewable diesel.

Table 2.3: Typical properties of biodiesel compared to petroleum diesel and renewable diesel (Hoekman, et al., 2012).

Property	Petroleum diesel	Biodiesel (FAME)	Renewable Diesel
Carbon, wt.%	86.8	76.2	84.9
Hydrogen, wt.%	13.2	12.6	15.1
Oxygen, wt.%	0.0	11.2	0.0
Specific gravity	0.85	0.88	0.78
Cetane No.	40-45	45-55	70-90
T90°C	300-330	330-360	290-300
Viscosity, mm^2/s, at40°C	2-3	4-5	3-4
Mass basis, MJ/Kg	43	39	44
Mass basis, 1000BTU/gal	18500	16600	18900
Vol basis,1000BTU/gal	130	121	122

Table 2.3 shows Biodiesel (FAME) to have a higher oxygen content and lower carbon content because it has a lower hydrogen and carbon content as compared to the other

forms of diesel. The higher oxygen content in the fuel is not desirable as it contributes to the oxidative instability of the fuel.

The viscosity of most biodiesel is higher than that of petroleum fuel by a factor of 2.

Renewable diesel is closely comparable to petroleum diesel in most properties. The specific gravity is lower with a higher viscosity than that of petroleum diesel. The cetane number is higher than that of petroleum diesel (Hoekman, et al., 2012). Cetane number is a relative measure of the interval between the beginning of injection and auto ignition of the fuel. The higher the cetane number, the shorter the delay interval and the greater its combustibility (Navale, et al., 2011). Renewable diesel is an intermediate product in the production of bio-jet fuel and bio-gasoline from vegetable oils through hydrocracking.

2.1.2 Gasoline Properties

The properties of petroleum gasoline are shown in Table 2.4 below.

Table 2.4: Typical Gasoline properties (Veza, et al., 2019).

Property	Gasoline
Chemical formula	C4-C12
Octane number	88-99
Cetane number	0-10
C/H atom ratio	0.44(octane)
Oxygen content(wt.%)	-
Density at 288K(g/mL)	0.77
Lower heating value (MJ/Kg)	43.40
Energy Density (MJ/L)	31.0-33.2
Viscosity at 413K(mm2/s)	0-49
Stoichiometry AFR	14.70
Boiling point C	38-204
Auto-ignition temperature(K)	300
Latent Heat at 298K(kJ/kg)	380-500
Saturation pressure(kPa) at 38C	31.00
Lamina flame speed(cm/s)	33

The octane number, as in Table 2.4, is a critical parameter for a gasoline product. Octane number (ON) is a measure of the ignition quality or flammability of gasoline (Dermibas, et al., 2015). The gasoline should also not contain any oxygen, as outlined in Table 2.5 for oxidative stability.

2.1.3 Bio-jet fuel vs Commercial Jet fuel properties

Bio-jet fuel production was demonstrated by the transformation of vegetable oil into bio-jet fuels through catalytic cracking over an HZSM-5 catalyst.C6-C9 aromatics were obtained. (Wu, et al., 2016). Table 2.5 below shows the typical properties of bio-jet fuel obtained.

Table 2.5: Typical Bio-jet fuel properties (Wu, et al., 2016).

Properties	Commercial Jet fuel	Bio-jet Fuel I*	Bio-jet fuel II**
Heat of combustion (MJ/kg)	43.3	42.5	44.9
Density(g/cm3)	0.797	0.87	0.81
Carbon content(wt.%)	86.3	89.7	85.7
Hydrogen content(wt.%)	13.4	10.3	14.3
Total Oxygen(wt.%)	-	0.03	ud[+]
Total sulphur(wt.%)	0.04	ud	Ud
Average carbon number	11.0	11.5	11.6
H/C (mol ratio)	1.98	1.4	1.9
Average molecular weight	C11H21	C11.5H15.7	C11.9H21.9

* Aromatic biofuel produced by the catalytic cracking of vegetable oil over HZSM-5(80) at 500°C, followed by the alkylation of aromatics.

** Cycloparaffins biofuel is produced by the hydrogenation of aromatics.

[+] undetermined.

The bio-jet fuels presented in Table 2.5 are closely comparable to the commercial jet fuel. Traces of oxygen have been detected in Bio-jet Fuel I, resulting in a decrease in hydrogen content. The bio-jet fuels show undetected levels of Sulphur as compared to the commercial jet fuel.

2.2 Methods for Biofuel Production from Castor Oil

(Molefe, et al., 2019) reviewed the various methods to determine the simultaneous production of bio-gasoline and bio-jet fuels from Castor oil. The methods included Hydrocracking, pyrolysis, and transesterification. Although transesterification is common, hydrocracking is ideal for producing high-quality bio-jet and bio-gasoline with a single catalyst.

2.2.1. Transesterification (Alcoholysis)

Transesterification (Alcoholysis) involves using methanol, butanol, or ethanol in the presence of a catalyst such as sodium hydroxide (NaOH) or potassium hydroxide (KOH) to break the molecule of the raw renewable oil chemically into methyl or ethyl esters of the renewable oil with glycerol as a byproduct (Dermirbas, 2003). The biodiesel produced through transesterification from edible and nonedible vegetable oils involves five steps i.e. 1) heating of the oil, 2) preparation of the alkaline mixture, 3) adding of alkaline alcohol to the oil and stirring the mixtures, 4) settling of the separation of glycerol, and 5) washing of ethyl ester with water. This process converts the oil into its corresponding ether to make it more suitable for use in diesel engines. The process overcomes the viscosity issue faced with using the oil in its purest form (Shrirame, et al., 2011).

2.2.2. Pyrolysis

Pyrolysis is the conversion of a substance using heat or a catalyst, with heat for thermal catalytic cracking. Pyrolysis is reported to favour the production of bio-gasoline rather than biodiesel (Ma & Hanna, 1999).

2.2.3. Hydrocracking

Hydrocracking is a catalytic cracking process that requires hydrogen-rich conditions as well as a suitable catalyst. It is a severe form of hydrotreating (De & Luque, 2014). Hydrocracking involves hydrotreating first, as the products should contain fewer impurities. Hydrotreating involves the saturation of olefins for a particular petroleum feed as well as the removal of sulphur, nitrogen, and other impurities (Gary, et al., 2007). Biofuel feedstock has low sulphur and nitrogen content. The feed contains a high level of oxygen, which must be eliminated. Therefore, the focus for hydrotreating will not be on Hydrodesulphurisation (HDS) or Hydrodenitrogenation (HDN) but on Hydrodeoxygenation (HDO) (Molefe, et al., 2019). For bio-gasoline and bio-jet fuel production from castor oil, the solid acid catalyst, such as HZSM-5 or composite, is promising (Molefe, et al., 2019). Extensive catalysis research also went into the various catalysts used at different process conditions to produce the various products from vegetable oils, as in Appendix A (Lovas, et al., 2015). HZSM-5 catalyst was used to hydro-

treat Waste Cooking oil in a batch reactor at 400-420°C and 10 bar pressure. The product slate included Gas oil 30.55 -36.3% as well as 15.57-16.76% gasoline and 9.99-11.83% kerosene.

2.3 Process Design - Flowsheet Development for Hydrocracking

UOP Honeywell developed and patented a process flowsheet to produce biofuels from a renewable feedstock. The key stages of the process flowsheet are detailed below (McCall et al., 2011):

- Hydrogenating, deoxygenating, isomerizing, and selectively hydrocracking the renewable feedstock in a reaction zone in the presence of hydrogen and at the suitable reaction conditions, by contacting the renewable feedstock with a multifunctional catalyst or a set of catalysts having hydrogenation, deoxygenation, isomerization, and selective hydrocracking functions to provide a reaction effluent comprising water, carbon oxides, light hydrocarbon gasses, hydrogen and paraffinic hydrocarbons wherein the deoxygenating comprises at least hydrodeoxygenation.
- Separating the water, carbon oxides, light hydrocarbon gases, and hydrogen from the reaction effluent to generate a stream comprising the paraffinic hydrocarbons.
- Separating the stream comprising the paraffinic hydrocarbons to generate the hydrocarbon product comprising hydrocarbons having boiling points in the aviation fuel range; an overhead stream comprising naphtha; and a bottoms stream comprising components having boiling points higher than the aviation fuel boiling point range.
- Recycling a portion of the bottoms stream to the reaction zone wherein the volume ratio of recycle to feedstock is in the range of about 0.1:1 to about 8:1.
- Recovering the hydrocarbon product stream.

2.4 Simulation of biofuels in Aspen Plus

The previous simulation work on Aspen Plus evaluated for this study is outlined below:

2.4.1 Simulation and optimization of a bio-jet fuel production process from castor oil

The modelling to produce bio-jet fuels was carried out in Aspen Plus with castor oil as a feedstock. A castor oil feedstock with a flow stream of 100 kg/h, with composition of palmitic acid (1.1 kg/h), stearic acid (3.1 kg/h), oleic acid (4.9 kg/h), linoleic acid (1.3 kg/h) and ricinoleic acid (89.6 kg/h). Due to the confidentiality of the kinetic model or type of catalyst involved in the UOP Honeywell, the hydrotreating reaction was estimated with the kinetic model developed for the hydrotreating of cottonseed oil. For the hydrotreating reaction, operating conditions of 345˚C and 30bar, and conversion of

99.36% was achieved. For the hydrocracking reaction at 240˚C and 60bar, conversion of 82% was achieved. (Gutierrez-Antonio, Gomez-Castro, Segovia-Hernandez, & Brionez-Ramirez, 2013).

2.4.2 Simulation of the soybean oil hydrotreating process for green diesel production

The process was simulated in Aspen Plus v10 presents a model for the hydrotreating of soybean oil to produce green diesel. The decarboxylation, decarbonylation, and hydrodeoxygenation reactions were carried out in a stoichiometric reactor in the presence of NiMo/Al_2O_3 catalyst. In addition to the cracking reactions and fractionation, the fuels produced green diesel, aviation biofuel, and light gases. Brazilian soybean oil was used as the raw material to produce green diesel. On the distillation optimisation, the best results were chosen when the distillation column was configured with 22 stages, feed at stage 12, and a reflux equal to 0.8. The hydrogen/soybean oil ratio was 0.031. The energy used in the process was 1181kW/hr. More than 80% of the soybean oil was converted to renewable fuels, with approximately 65% to green diesel. (Cavalcanti, Ravagnani, Stragevitch, Carvalho, & Pimentel, 2022)

2.5 Catalyst for the Biofuels production from Castor Oil

2.5.1 Alumina Catalyst

Alumina (Al_2O_3, aluminium oxide) is an important ceramic material, which, because of its hardness, high melting point, and low electrical conductivity, has many technological applications in electronics, optics, biomedicine, and mechanical engineering. In catalysis, gamma alumina (γ-Al_2O_3) is the most widely used support because it has a high mechanical strength, can be prepared with a high surface area, and is quite inexpensive to produce. In addition, alumina is used as a catalyst itself because its surface contains acidic and basic groups. (Kovarik, et al., 2021)

Alumina as a support or co-catalyst is used in many catalytic processes such as isomerisation, catalytic cracking, alkylation, hydroforming, etc (Pines & Haag, 1959). The Alumina as a catalyst for treating triglycerides into fuel production was used by (Sebos, et al., 2009). The hydrotreating process occurs optimally at 30 bar and 345 °C, and the hydrocracking reaction occurs at 60 bar and 240 °C with Alumina as a catalyst. Reaction Conversions of 99.35% and 82% were obtained, respectively, for the hydrotreating and hydrocracking reactions.

2.5.2 Nickel on Different Acidic Zeolite Catalysts

Different fuel range alkanes can be synthesised from hydro processing castor oil by Nickel supported on different acidic zeolites, and bio-aviation fuel can be obtained by Nickel supported on moderate acidic strength zeolites (Liu, et al., 2015) as illustrated in Figure 2.2 below

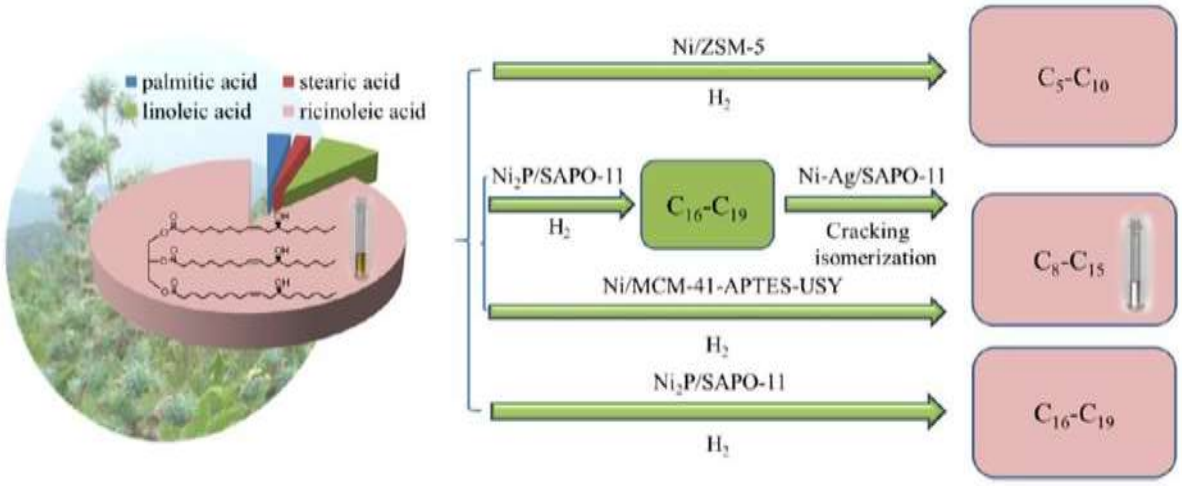


Figure 2.2: Demonstration of Castor oil conversion to various fuels over a nickel-based catalyst. (Liu, et al., 2015)

Renewable bio-aviation fuel was produced by hydro processing castor oil using bifunctional catalysts with differing acid strength. By employing the two-step and one-pot processes that we designed, bifunctional catalysts with moderate acidity could promote the conversion of castor oil or C_{16}-C_{19} alkanes into high yields of bio-aviation fuel with high isomerisation selectivity. (Liu, et al., 2015).

Bio-aviation fuel was first synthesised by hydro processing castor oil in a continuous flow fixed-bed microreactor with the main objective to obtain a high yield of aviation fuel and determine the elemental compositions of the product phases as well as the reaction mechanism. Highest aviation range alkane yields (91.6 wt.%) were achieved with high isomer/n-alkane ratio (i/n) 4.4–7.2 over Ni supported on acidic zeolites. The outcome of this study is summarized in Table 2.6 below.

Table 2.6: Hydro conversion of castor oil on Ni supported on different strengths of zeolites (Liu, et al., 2015).

Entry	Catalyst	Feed	T(°C)	Yield% (lighter)	Yield% (C5-C7)	Yield% (C8-C15)	Yield% (C16-C19)	Conv (%)	i/n ratio (C8C15)
1	a)25% Ni/SAPO-11	Castor Oil	300	0.2	1.2	3.2	95.4	99	0.1
2	b)25% Ni_2P/SAPO-11	Castor Oil	300	0.3	4.9	2.5	92.3	99	0.1
3	25% NiAg/SAPO-11 (molar Ni/Ag:44)	Product I	360	0.3	3.8	91.6	4.3	98	6.8
4	25% NiAg/SAPO-11 (molar Ni/Ag:44)	Product II	360	0.3	5.6	88.9	5.2	98	7.2
5	25% Ni/H-Beta	Castor Oil	300	0.8	97.7	1.5	0	99	0
6	25%Ni/ZSM-5(Si/Al:38)	Castor Oil	300	1.2	96.8	2.0	0	99	0
7	25%Ni/ZSM-5(Si/Al:50)	Castor Oil	300	0.9	93.4	3.2	2.3	99	0.5
8	25%Ni/ZSM-5(Si/Al:100)	Castor Oil	300	0.7	58.8	25.3	15.2	99	2.4
9	25%Ni/USY	Castor Oil	300	0.6	79.4	19.2	0.8	99	5.3
10	25%Ni/USY-APTES-MCM-41(APTES:7.5)	Castor Oil	300	0.5	13.8	80.3	5.4	99	4.4

i/n ratio(C_8-C_{15}) = ratio of isomers and normal(n) alkanes.3MPa, WHSV=2hr^{-1}

Product1:C_{16}-C_{19}(hydro processing castor oil by 25% Ni/SAPO-11)

Product11:C_{16}-C_{19}(hydro processing castor oil by 25% NiP/SAPO-1)

Lighter products:C_1-C_4, CO, CO2

Chapter 3: Methodology

The simulation will be performed as a simulation on Aspen Plus; there will be no physical equipment installed, or laboratory experiments performed for the completion of this study. A predetermined quality of castor oil will be used as feed into the Aspen Simulation as discussed previously in Chapter 2. Castor oil extraction will not be included in the study.

3.1 Process Flow Description

A feed of 100kg/hr (Gutierrez-Antonio, et al., 2013) of castor oil was used in the simulation for all the simulations in this study. A typical process for hydrotreated vegetable oil, which will be simulated, is presented in Figure 3.1 below:

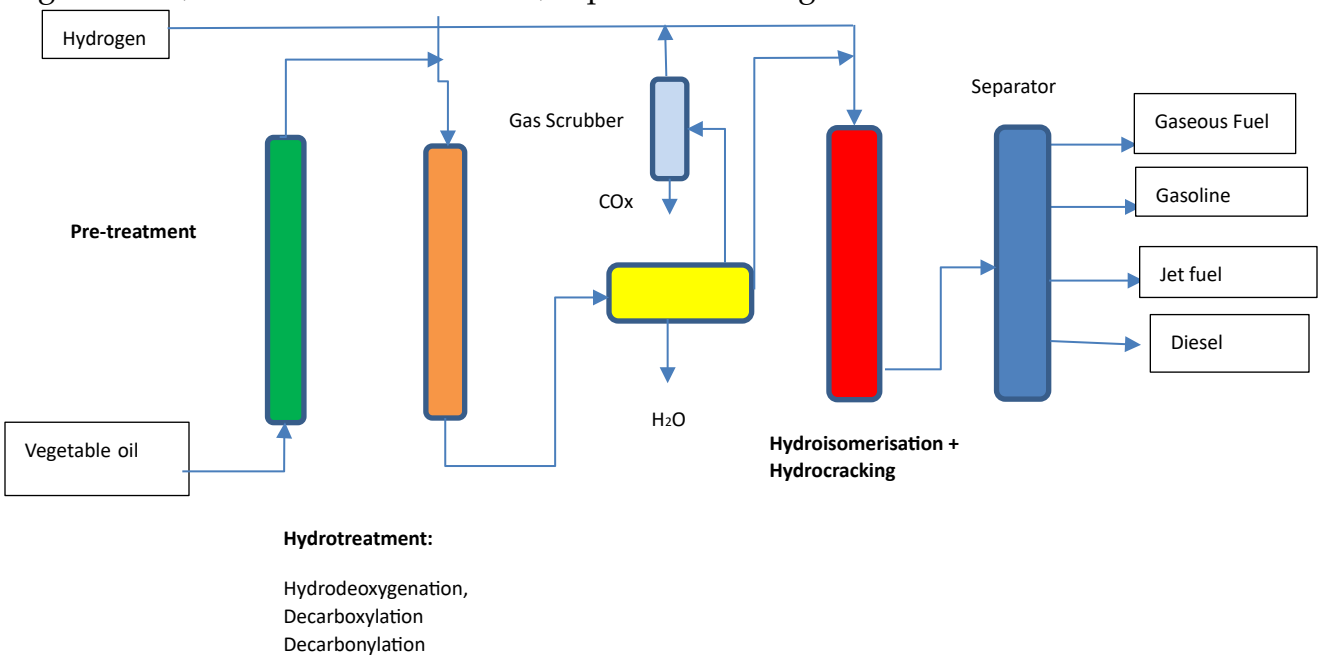


Figure 3.1: Typical process for hydrotreated vegetable oil (Szeto & Leung, 2022).

The process steps for Figure 3.1 are discussed below:

3.1.1 Pre-treatment

Pre-treatment involves the removal of any solid or food (in case of waste cooking oil) particles from the vegetable stream to ensure a uniform feedstock into the process.

3.1.2 Hydrotreating

Hydrotreating favours the production of fuel in the petroleum diesel range as it removes heteroatoms and saturates the C-C bonds with the number of atoms still intact (De & Luque, 2014). Hydrodeoxygenation, Decarboxylation, and decarbonylation occur in the hydrotreating step. Hydrodeoxygenation (HDO) is the process of removing oxygen from oxygenated feedstock in the form of water to increase the energy value of the oil. It is preferred under low temperatures(300-345°C) and high hydrogen pressures(30bar) (Mohammad, et al., 2013). The removal of oxygen also improves the thermal stability of the fuel (Gutierrez-Antonio, et al., 2013). HDO yields hydrocarbons with the same number of carbon atoms, along with water and propane.

Decarboxylation and decarbonylation yield paraffin with one carbon atom less than the initial fatty acid and release CO_2 and CO, respectively (Mohammad, et al., 2013). The reactions for HDO, Decarboxylation, and decarbonylation are presented in Figure 3.2 below (Douvartzides, et al., 2019):

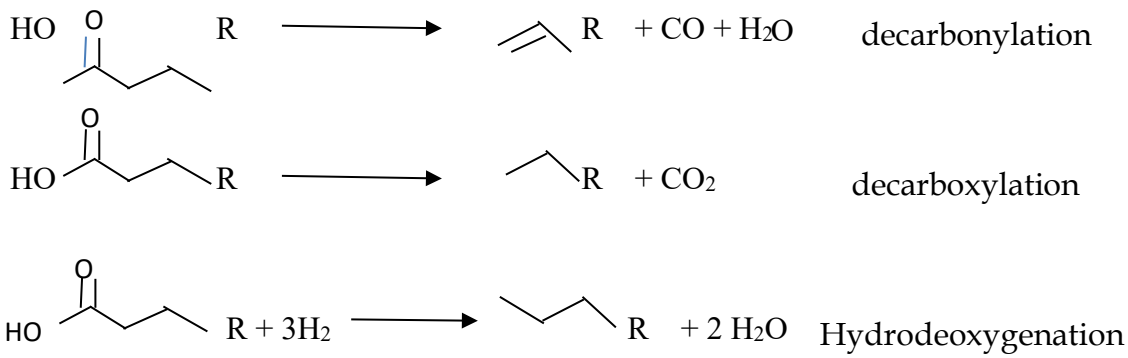


Figure 3.2: Reactions for Hydrodeoxygenation, Decarboxylation, and Decarbonylation.

The deoxygenation of triglycerides provides a green diesel consisting of normal (straight chain) saturated hydrocarbons in the C15–C18 range. These hydrocarbons have a high cetane number but poor cold flow properties since they have a high freezing point above 15°C (Douvartzides, et al., 2019). One solution to this problem is to blend green diesel with petroleum diesel as a cetane number improver. Another solution to this problem comes with the hydro isomerisation of the normal saturated hydrocarbons into branched-chain isomers with lower freezing points appropriate for use in engines under cold weather and cold start conditions, though with the cost of lower cetane numbers (Sotelo-Boyas, et al., 2012) (Murzin, 2013).

Through the process of decarbonylation and decarboxylation, CO_2 and CO can form as byproducts. The reaction pathways for castor oil components in the hydrotreating reactions are presented below:

Stearic Acid:

Hydrodeoxygenation: $C_{18}H_{36}O_2 + 3H_2 \rightarrow C_{18}H_{38} + 2H_2O$ (3.1)

Decarboxylation: $C_{18}H_{36}O_2 \rightarrow C_{17}H_{36} + CO_2$ (3.2)

Decarbonylation: $C_{18}H_{36}O_2 + H_2 \rightarrow C_{17}H_{36} + CO + H_2O$ (3.3)

Linoleic Acid:

Hydrodeoxygenation: $C_{18}H_{32}O_2 + 5H_2 \rightarrow C_{18}H_{38} + 2H_2O$ (3.4)

Decarboxylation: $C_{18}H_{32}O_2 + 2H_2 \rightarrow C_{17}H_{36} + CO_2$ (3.5)

Decarbonylation: $C_{18}H_{32}O_2 + 3H_2 \rightarrow C_{17}H_{36} + CO + H_2O$ (3.6)

Ricinoleic Acid:

Hydrodeoxygenation: $C_{18}H_{34}O_3 + 5H_2 \rightarrow C_{18}H_{38} + 3H_2O$ (3.7)

Decarbonylation: $C_{18}H_{34}O_3 + 3H_2 \rightarrow C_{17}H_{36} + CO + 2H_2O$ (3.8)

Oleic Acid:

Hydrodeoxygenation: $C_{18}H_{34}O_2 + 4H_2 \rightarrow C_{18}H_{38} + 2H_2O$ (3.9)

Decarboxylation: $C_{18}H_{34}O_2 + H_2 \rightarrow C_{17}H_{36} + CO_2$ (3.10)

Decarbonylation: $C_{18}H_{34}O_2 + 2H_2 \rightarrow C_{17}H_{36} + CO + H_2O$ (3.11)

Palmitic (Hexadecanoic) Acid:

Hydrodeoxygenation: $C_{16}H_{32}O_2 + 3H_2 \rightarrow C_{16}H_{34} + 2H_2O$ (3.12)

Decarboxylation: $C_{16}H_{32}O_2 \rightarrow C_{15}H_{32} + CO_2$ (3.13)

Decarbonylation: $C_{16}H_{32}O_2 + H_2 \rightarrow C_{15}H_{32} + CO + H_2O$ (3.14)

Hydrodeoxygenation occurs at process conditions of 280°C and 3.5MPa (Kubicka & Tukac, 2013). The main products from the hydrodeoxygenation of Castor oil are Pentadecane ($C_{15}H_{32}$), Hexadecane($C_{16}H_{34}$), Heptadecane($C_{17}H_{36}$) and Octadecane($C_{18}H_{38}$) with Water (H_2O), Carbon dioxide (CO_2) and Carbon Monoxide (CO) as byproducts.

3.1.3 Intermediate Separation

The by-products (H_2O, CO_2, CO) formed from the HDO, decarboxylation, and decarbonylation reactions are removed from the green diesel produced through the deoxygenation of the triglycerides before the isomerisation and hydrocracking step. The water is removed through a three-phase separator, and the gas stream containing CO_2 and CO is further treated in a gas scrubber to remove the CO_2 and CO.

3.1.4 Isomerisation and hydrocracking

Isomerisation changes the structure of a molecule, leaving its molecular weight the same. Given that saturated hydrocarbons are not prone to direct isomerisation, they must be processed appropriately, and hydroisomerization is an appropriate technique in this direction. The hydro isomerisation of a saturated hydrocarbon takes place in three steps, starting with its dehydrogenation into the same carbon atom alkene, and proceeds with the skeletal isomerisation of the alkene and its final hydrogenation into the branched isomer saturated hydrocarbon. This three-step process is feasible in light saturated hydrocarbons with less than 7 carbon atoms, but it is difficult for heavier molecules without some extent of hydrocracking (Klerk, 2011).

In the case of the heavy saturated hydrocarbons of the green diesel, isomerisation needs a balanced action of hydro-isomerisation and hydrocracking over an appropriate heterogeneous catalyst that can increase selectivity to the desired isomer hydrocarbons (Douvartzides, et al., 2019). Thus, renewable diesel can be converted into bio-gasoline and bio-jet fuel through hydrocracking. Hydrocracking simply forms alkanes with shorter chains (Mohammad, et al., 2013). The hydrocracking product properties vary as the cracking severity and selectivity are dependent on the hydrogen pressure, the catalyst used, temperature, and the nature of the feedstock (Molefe, et al., 2019). The products of the hydrogenation from Equation (3.1) to (3.14) are cracked into shorter alkanes in hydrocracking, a combination of reactions involved are below:

Pentadecane Cracking:

$$C_{15}H_{32} + H_2 \rightarrow C_3H_8 + C_{12}H_{26} \quad (3.15)$$

$$C_{15}H_{32} + H_2 \rightarrow C_4H_{10} + C_{11}H_{26} \quad (3.16)$$

$$C_{15}H_{32} + H_2 \rightarrow C_5H_{12} + C_{10}H_{22} \quad (3.17)$$

$$C_{15}H_{32} + H_2 \rightarrow C_6H_{14} + C_7H_{20} \quad (3.18)$$

$$C_{15}H_{32} + H_2 \rightarrow C_7H_{16} + C_8H_{18} \quad (3.19)$$

Hexadecane Cracking:

$$C_{16}H_{34} + H_2 \rightarrow C_3H_8 + C_{13}H_{26} \quad (3.20)$$

$$C_{16}H_{34} + H_2 \rightarrow C_4H_{10} + C_{12}H_{26} \quad (3.21)$$

$$C_{16}H_{34} + H_2 \rightarrow C_5H_{12} + C_{11}H_{22} \quad (3.22)$$

$$C_{16}H_{34} + H_2 \rightarrow C_6H_{14} + C_{10}H_{20} \quad (3.23)$$

$$C_{16}H_{34} + H_2 \rightarrow C_7H_{16} + C_9H_{20} \quad (3.24)$$

$$C_{16}H_{34} + H_2 \rightarrow 2C_8H_{18} \quad (3.25)$$

Heptadecane Cracking:

$$C_{17}H_{36} + H_2 \rightarrow C_3H_8 + C_{14}H_{26} \quad (3.26)$$

$$C_{17}H_{36} + H_2 \rightarrow C_4H_{10} + C_{13}H_{26} \quad (3.27)$$

$$C_{17}H_{36} + H_2 \rightarrow C_5H_{12} + C_{12}H_{22} \quad (3.28)$$

$$C_{17}H_{36} + H_2 \rightarrow C_6H_{14} + C_{11}H_{20} \quad (3.29)$$

$$C_{17}H_{36} + H_2 \rightarrow C_7H_{16} + C_{10}H_{20} \quad (3.30)$$

$$C_{17}H_{36} + H_2 \rightarrow C_8H_{18} + C_9H_{20} \quad (3.31)$$

Octadecane Cracking:

$$C_{18}H_{38} + H_2 \rightarrow C_3H_8 + C_{15}H_{32} \quad (3.32)$$

$$C_{18}H_{38} + H_2 \rightarrow C_4H_{10} + C_{14}H_{30} \quad (3.33)$$

$$C_{18}H_{38} + H_2 \rightarrow C_5H_{12} + C_{13}H_{28} \quad (3.34)$$

$$C_{18}H_{38} + H_2 \rightarrow C_6H_{14} + C_{12}H_{26} \quad (3.35)$$

$$C_{18}H_{38} + H_2 \rightarrow C_7H_{16} + C_{11}H_{24} \quad (3.36)$$

$$C_{18}H_{38} + H_2 \rightarrow C_8H_{18} + C_{10}H_{22} \quad (3.37)$$

$$C_{18}H_{38} + H_2 \rightarrow 2C_9H_{20} \quad (3.38)$$

3.1.5 Final Separation

The separation of various hydrocarbon products into product slates occurs through distillation with gaseous fuels as bioproduct, then gasoline, jet fuel, and diesel range.

3.2 Simulation

For this study, two simulations were developed in Aspen Plus Version 14, the first to produce green diesel from castor oil, and the second simulation the produce bio-jet fuel. The production of green diesel is the primary process developed from castor oil. The green diesel undergoes hydrocracking to yield bio-jet fuel.

3.2.1 Aspen Plus

Aspen Plus is a Chemical Engineering Application used in the modelling and simulation of chemical processes for optimisation and design purposes. It is a software developed in 1982, by Aspen Technology, founded in 1981.
MIT's chemical engineering group received a U.S. Department of Energy grant to study technical innovation in the process industries in response to the 1970s energy crisis. Aspen Plus is the first product developed by Aspen Technology (Aspen, 2024). Aspen Plus has continually improved over the years. Aspen v14 was used to model biofuel production from castor oil.

Aspen Tech launched Aspen Plus (a commercial version of Aspen) with innovative first-of-its-kind capabilities for the chemical engineering industry, including modelling capabilities for three-phase/reactive distillation, non-ideal physical properties, electrolytes, polymers, and flowsheet optimisation. (Aspen, 2024)

Given a process design and an appropriate selection of thermodynamic models, Aspen Plus uses mathematical models to predict the performance of the process. Aspen Plus has an existing database of species and their pure/binary regressed parameters. It can handle complex processes such as multiple-column separation processes, Chemical Reactors, Distillation of chemically reactive compounds, electrolyte solutions such as the Chlor-Alkali Industry, and Complex Recycle Bypass Steam processes. (ChemEngGuy, 2024)

3.2.2 Green Diesel Production Model

A model was built in Aspen Plus to process the castor oil and produce green diesel. The flowsheet developed in this study is presented below in Figure 3.3.

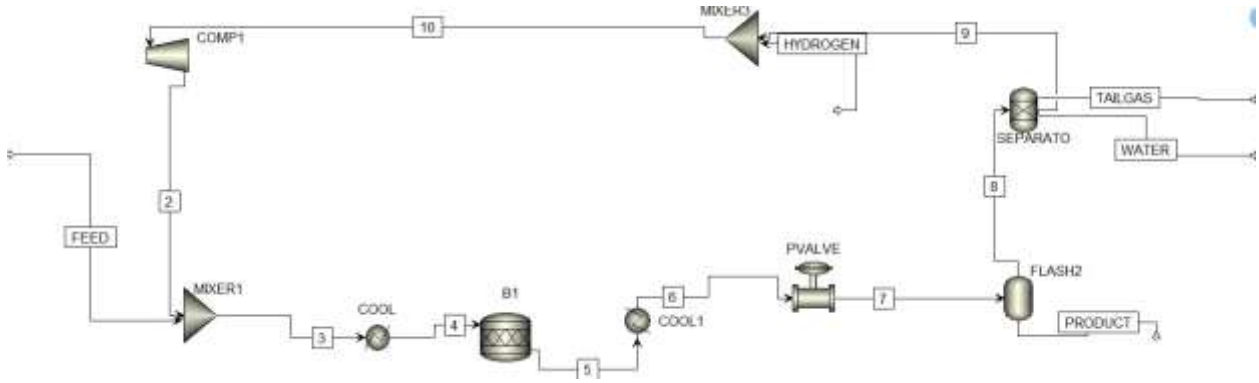


Figure 3.3: Green Diesel production flowsheet in Aspen Plus.

3.2.2.1. Component Description

The list of various components used in the simulation was loaded onto Aspen as listed in Figure 3.4 below. The components include the castor oil composition, i.e., Ricinoleic acid($C_{18}H_{34}O_3$), Linoleic Acid($C_{18}H_{32}O_2$), Stearic Acid($C_{18}H_{36}O_2$), Oleic Acid($C_{18}H_{34}O_2$), and Palmitic acid, also known as Hexadecanoic Acid($C_{16}H_{32}O_2$), the hydrogen(H2) as feedstock. From the hydrogenation reaction, water (H_2O), Carbon Monoxide (CO), and Carbon Dioxide (CO_2) as byproducts, and the final products being Pentadecane ($C_{15}H_{32}$), Hexadecane($C_{16}H_{34}$), Heptadecane($C_{17}H_{36}$), and Octadecane($C_{18}H_{38}$)

Selection | Petroleum | Nonconventional | Enterprise Database | Comments

Select components

Component ID	Type	Component name	Alias	CAS number
STEAR-01	Conventional	STEARIC-ACID	C18H36O2	57-11-4
N-HEP-01	Conventional	N-HEPTADECANE	C17H36	629-78-7
N-OCT-01	Conventional	N-OCTADECANE	C18H38	593-45-3
HYDRO-01	Conventional	HYDROGEN	H2	1333-74-0
WATER	Conventional	WATER	H2O	7732-18-5
CARBO-01	Conventional	CARBON-DIOXIDE	CO2	124-38-9
CARBO-02	Conventional	CARBON-MONOXIDE	CO	630-08-0
N-PEN-01	Conventional	N-PENTADECANE	C15H32	629-62-9
RICIN-01	Conventional	RICINOLEIC-ACID	C18H34O3	141-22-0
LINOL-01	Conventional	LINOLEIC-ACID	C18H32O2	60-33-3
OLEIC-01	Conventional	OLEIC-ACID	C18H34O2	112-80-1
N-HEX-01	Conventional	N-HEXADECANOIC-ACID	C16H32O2	57-10-3
N-HEX-02	Conventional	N-HEXADECANE	C16H34	544-76-3

Figure 3.4: A list of components loaded onto the Aspen Simulation.

3.2.2.2. Thermodynamic Methods

The thermodynamic method used for the simulation is Soave Redling Kong due to the presence of hydrocarbons, light gases, carbon dioxide, and hydrogen (Cavalcanti, et al., 2022). This method is suitable in regions of high temperatures and pressures, it is commonly applied to hydrocarbon processing, and it was successfully applied in the soybean oil simulation work by (Cavalcanti, Ravagnani, Stragevitch, Carvalho, & Pimentel, 2022). SteamNBS was used for the free-water method as illustrated in Figure 3.5 below.

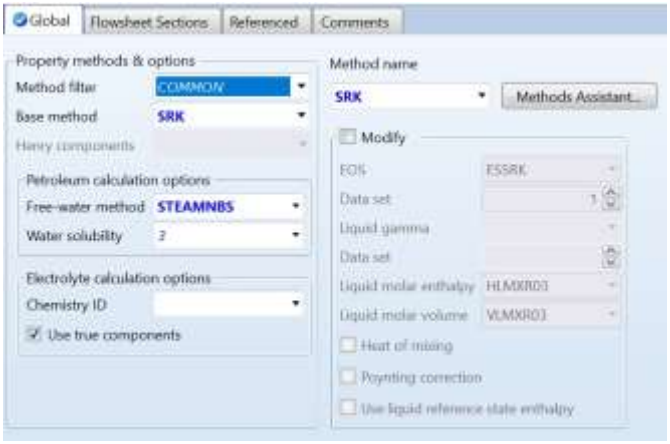


Figure 3.5: Thermodynamic method.

3.2.2.3. Feed Supply

A 100kg/hr of Castor Oil was fed into the simulation at 30 bar and 25 °C as described in Figure 3.6 below.

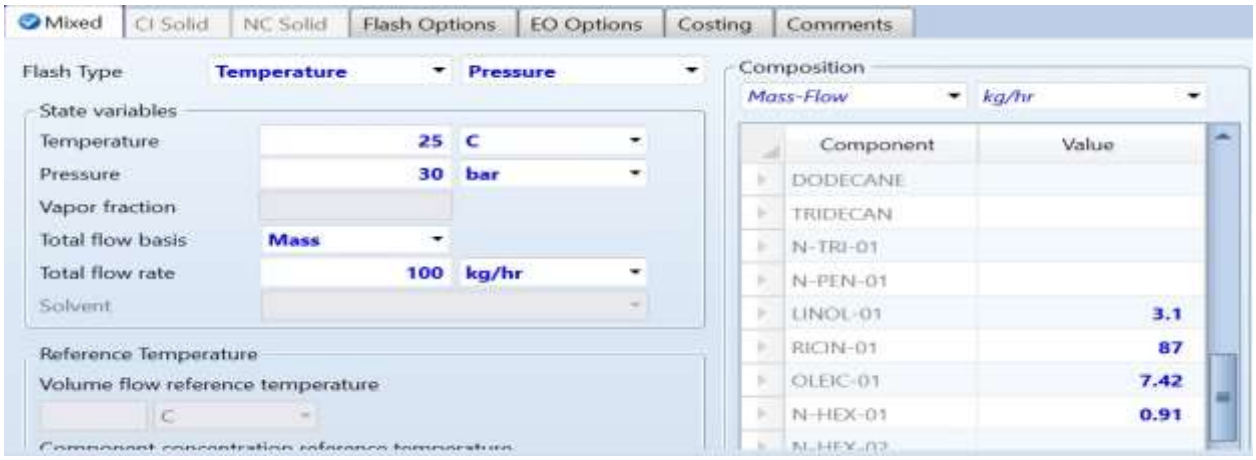


Figure 3.6: Castor Oil in feed stream.

3.2.2.4. Feed Pre-Cooler

The Castor Oil stream is combined with the Hydrogen in Recycle Stream 2 within the Mixer block and heated in the heat exchanger before entering the Reactor. The Castor Oil and Hydrogen mixture is cooled via heat exchange with the reactor product stream prior to being fed into the reactor at 345˚C and 30 bar, utilising an Alumina Catalyst (Gutierrez Antonio, et al., 2013). Refer to Figure 3.7 below.

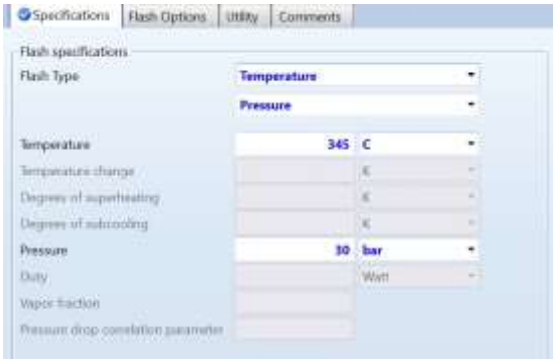


Figure 3.7: Feed Pre-cool to 345˚C.

3.2.2.5. Hydrodeoxygenation Reactor

A RStoich reactor was used to model the reactions occurring in the hydrodeoxygenation reactor. The reactor operates at 345°C and 30 bar with Alumina Catalyst (Gutierrez Antonio, et al., 2013) as shown in Figure 3.8 below.

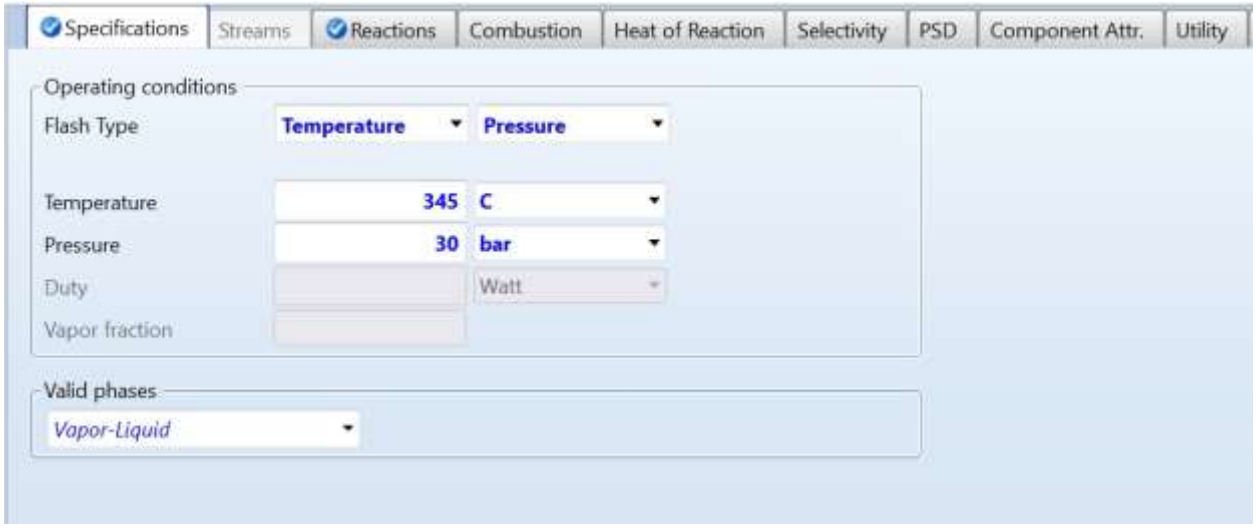


Figure 3.8: Reactor operating pressure and temperature.

The hydrodeoxygenation reactions Equations (1) to (14) as stipulated in Chapter 2 were loaded onto Aspen according to the respective stoichiometries. The fractional conversion

of castor oil is 99% and thus, the fractional conversion of each component was specified as 99%.

3.2.2.6. Stearic Acid Conversion

To achieve 99% conversion of Stearic Acid, the conversion was split equally amongst the three reactions (1-3), and 0.33 fractional conversion was applied to each reaction as illustrated in Figure 3.9 below.

Reactions

	Rxn No.	Specification type	Molar extent	Units	Fractional conversion	Fractional Conversion of Component	Stoichiometry
	1	Frac. conversion		kmol/hr	0.33	STEAR-01	STEAR-01 + 3 HYDRO-01 --> N-OCT-01(MIXED) + 2 WATER(MIXED)
	2	Frac. conversion		kmol/hr	0.33	STEAR-01	STEAR-01 --> N-HEP-01(MIXED) + CARBO-01(MIXED)
	3	Frac. conversion		kmol/hr	0.33	STEAR-01	STEAR-01 + HYDRO-01 --> N-HEP-01(MIXED) + CARBO-02(MIXED) + WATER(MIXED)

Figure 3.9: Stearic acid hydrogenation reactions in Aspen.

3.2.2.7. Linoleic Acid Conversion

To achieve 99% conversion of Linoleic Acid, the conversion was split equally amongst the three reactions (4) to (6), and 0.33 fractional conversion was applied to each reaction as illustrated in Figure 3.10 below.

Reactions

	Rxn No.	Specification type	Molar extent	Units	Fractional conversion	Fractional Conversion of Component	Stoichiometry
	4	Frac. conversion		kmol/hr	0.33	LINOL-01	LINOL-01 + 5 HYDRO-01 --> N-OCT-01(MIXED) + 2 WATER(MIXED)
	5	Frac. conversion		kmol/hr	0.33	LINOL-01	LINOL-01 + 2 HYDRO-01 --> N-HEP-01(MIXED) + CARBO-01(MIXED)
	6	Frac. conversion		kmol/hr	0.33	LINOL-01	LINOL-01 + 3 HYDRO-01 --> N-HEP-01(MIXED) + CARBO-02(MIXED) + WATER(MIXED)

Figure 3.10: Linoleic acid hydrogenation reactions in Aspen.

3.2.2.8. Ricinoleic Acid Conversion

To achieve 99% conversion of Linoleic Acid, the conversion was split equally amongst the two reactions (7) to (8), and 0.495 fractional conversion was applied to each reaction as illustrated in Figure 3.11 below. For Ricinoleic acid, only the hydrodeoxygenation (7) and decarbonylation (8) reactions are possible.

Reactions

	Rxn No.	Specification type	Molar extent	Units	Fractional conversion	Fractional Conversion of Component	Stoichiometry
	7	Frac. conversion		kmol/hr	0.495	RICIN-01	RICIN-01 + 5 HYDRO-01 --> N-OCT-01(MIXED) + 3 WATER(MIXED)
	8	Frac. conversion		kmol/hr	0.495	RICIN-01	RICIN-01 + 3 HYDRO-01 --> N-HEP-01(MIXED) + CARBO-02(MIXED) + 2 WATER(MIXED)

Figure 3.11: Ricinoleic acid hydrogenation reactions in Aspen.

3.2.2.9. Oleic Acid Conversion

To achieve 99% conversion of Oleic Acid, the conversion was split equally amongst the three reactions (9), (10), and (11), and 0.33 fractional conversion was applied to each reaction as illustrated in Figure 3.12 below.

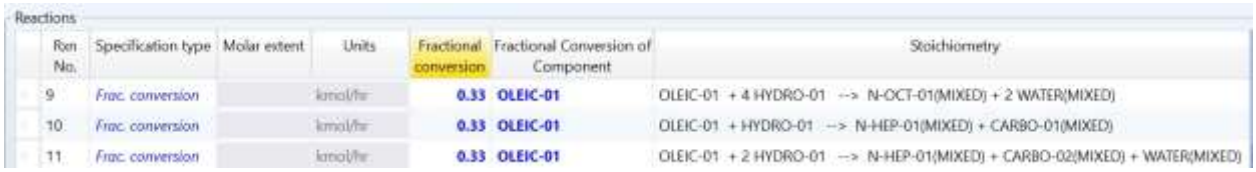


Figure 3.12: Oleic Acid hydrogenation reactions in Aspen.

3.2.2.10. Hexadecanoic Acid Conversion

To achieve 99% conversion of Hexadecanoic Acid, the conversion was split equally amongst the three reactions (12), (13), and (14), and 0.33 fractional conversion was applied to each reaction as illustrated in Figure 3.13 below.

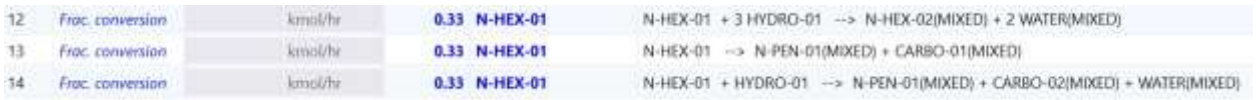


Figure 3.13: The Hexadecanoic acid hydrogenation reactions in Aspen.

3.2.2.11. Product Cooling

The reactor final product stream is cooled to 20˚C as illustrated in Figure 3.14 below in a cooler before separation in the flash drum.

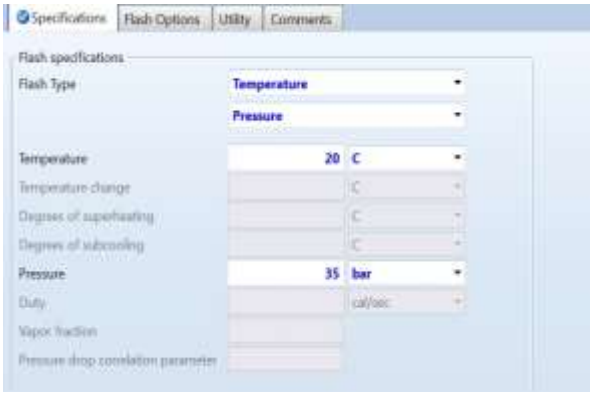


Figure 3.14: Product Cooler.

3.2.2.12. Product Separation

The cooled product stream is depressurised to 2bar with a pressure valve as illustrated in Figure 3.15 below and fed to the flash drum for final separation.

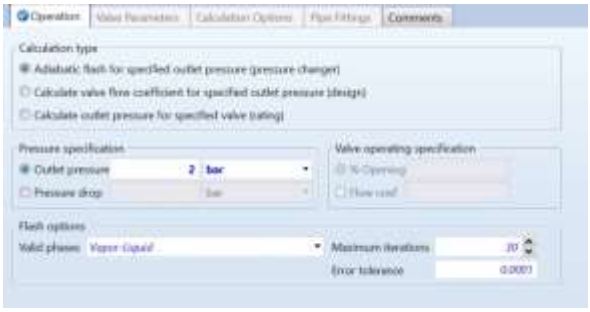


Figure 3.15: Pressure valve dropping pressure to 2bar.

The flash drum separates the final product, residual hydrogen, and byproducts at 20˚C and 2bar as illustrated in Figure 3.16 below.

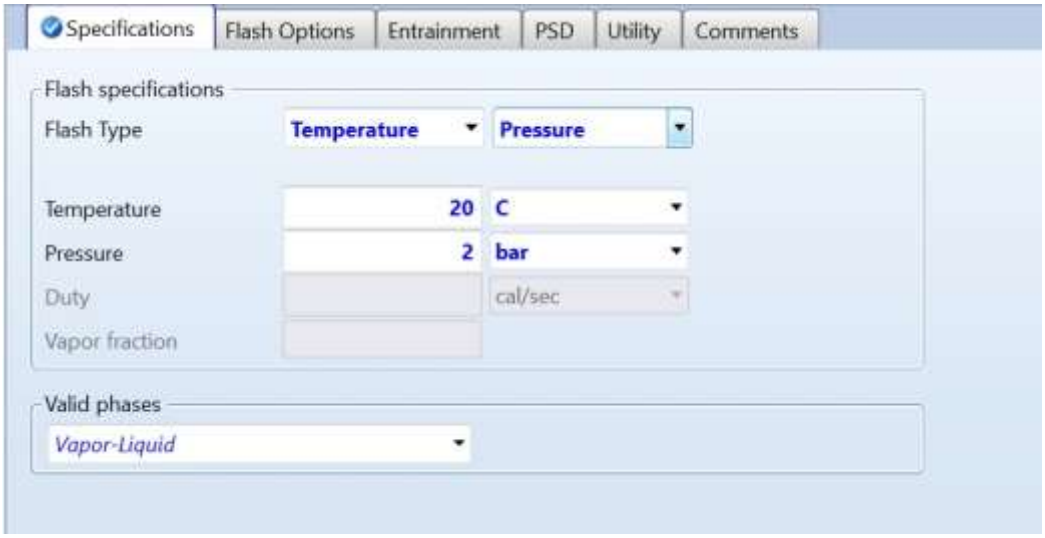


Figure 3.16: Flash drum conditions for final product separation.

The final green diesel product is produced at the bottom liquid stream of the flash drum. The top vapour stream of the flash drum is processed further in the 3-phase separator upstream. The three-phase separator is presented in Figure 3.17 below. The 100% split fraction of hydrogen in Stream 16 is specified as a means of recovering the feedstock. The separator also separates the water and tail gases, which include carbon monoxide and carbon dioxide.

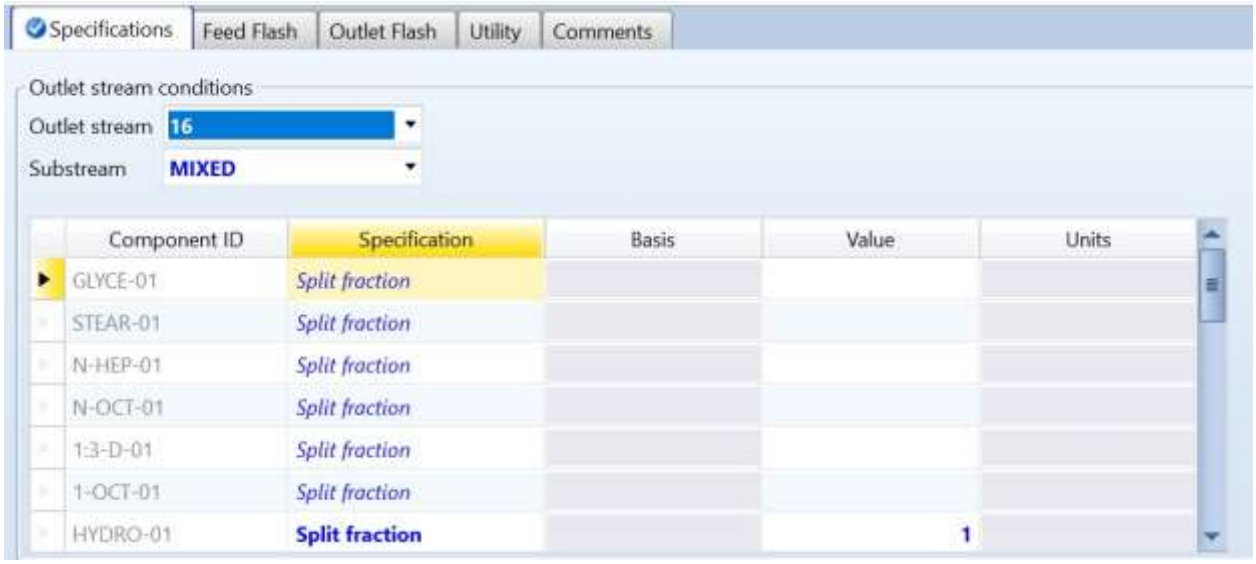


Figure 3.17: The hydrogen split fraction in Stream 16.

The recovered Hydrogen is recycled and mixed with a fresh hydrogen make-up stream. The fresh hydrogen stream is specified in Figure 3.18 below at 2bar and 25˚C.

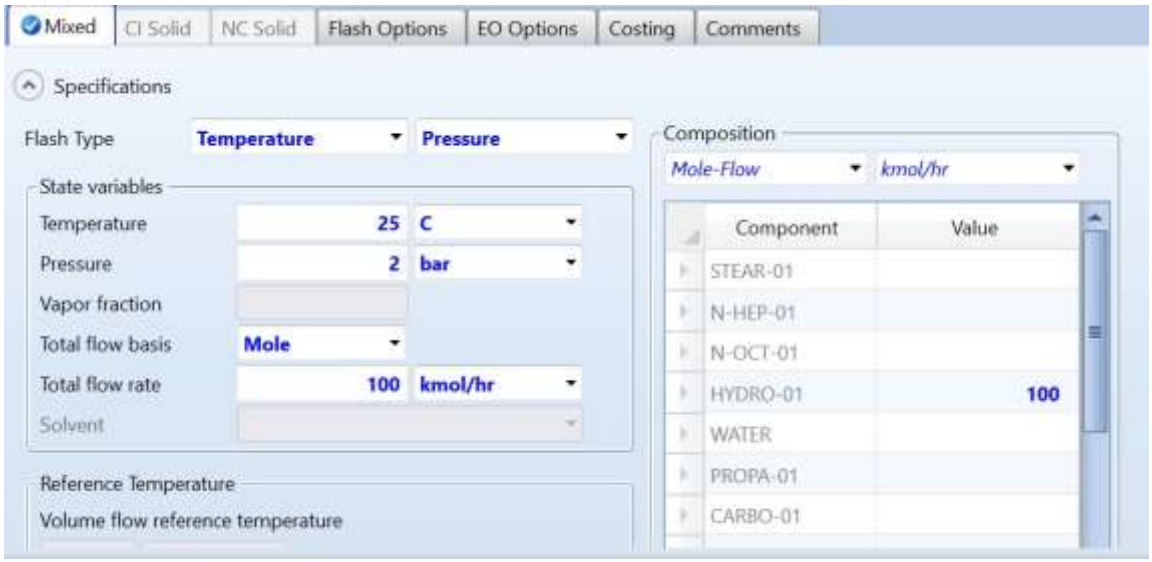


Figure 3.18: Fresh Hydrogen make-up stream.

The combined hydrogen streams are sent to the compressor to produce hydrogen at 35bar as in Figure 3.19 below.

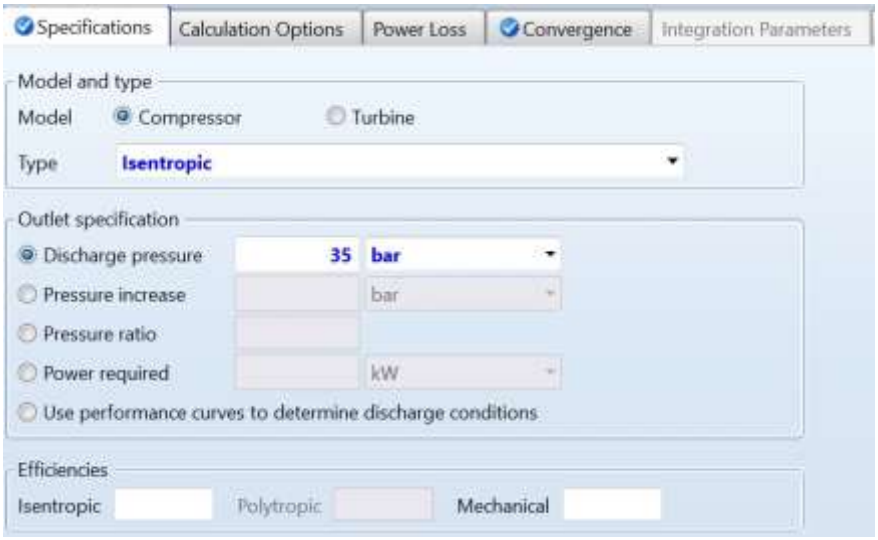


Figure 3.19: Hydrogen Compressor.

The outlet stream of the compressor with hydrogen joins the castor oil feed stream as a recycle stream, and the process loop is closed.

3.2.3 Bio-jet Fuel Production Model

Bio-jet fuel is produced through the further processing of green diesel through a cracking process with hydrogen to produce shorter alkanes. The process flowsheet developed in Aspen is presented in Figure 3.20 below, and a detailed description of each equipment is provided.

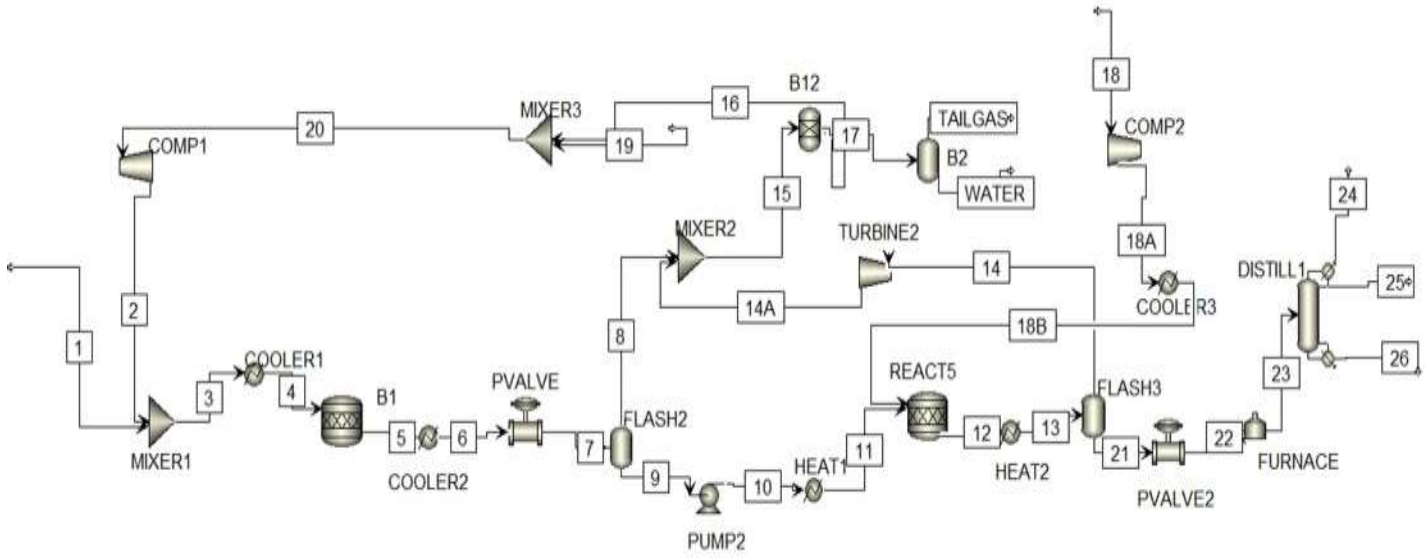


Figure 3.20: Process flowsheet for hydrocracking section.

Green diesel is further processed to produce jet fuel and light products. The Green Diesel from Flash 2 is pumped to 60bar and heated to 240˚C for the hydrocracking reactor, as the Alumina catalyst process conditions are illustrated in Figure 3.21 below.



Figure 3.21: The green diesel is pumped and preheated before the hydrocracking reactor.

3.2.3.1 Hydrocracking Reactor

The products (Pentadecane, Hexadecane, Heptadecane, Octadecane) from the hydrotreating process undergo further processing in a hydrocracking reactor to produce various other compounds. Each component will be explored next.

3.2.3.2 Pentadecane cracking reactions

There are five reactions possible for the cracking of pentadecane into shorter alkanes, as illustrated in Equations (3.15) to (3.19). The fractional conversion was uniformly distributed across the six reactions, with each reaction contributing 0.18, as depicted in Figure 3.22 below. The overall conversion of pentadecane is 0.90.

Reactions

Rxn No.	Specification type	Molar extent	Units	Fractional conversion	Fractional Conversion of Component	Stoichiometry
14	Frac. conversion		kmol/hr	0.18	N-PEN-01	N-PEN-01 + HYDRO-01 --> PROPA-01(MIXED) + DODECANE(MIXED)
15	Frac. conversion		kmol/hr	0.18	N-PEN-01	N-PEN-01 + HYDRO-01 --> BUTANE(MIXED) + UNDECANE(MIXED)
16	Frac. conversion		kmol/hr	0.18	N-PEN-01	N-PEN-01 + HYDRO-01 --> HEXANE(MIXED) + NONANE(MIXED)
18	Frac. conversion		kmol/hr	0.18	N-PEN-01	N-PEN-01 + HYDRO-01 --> PENTANE(MIXED) + DECANE(MIXED)
19	Frac. conversion		kmol/hr	0.18	N-PEN-01	N-PEN-01 + HYDRO-01 --> HEPTANE(MIXED) + OCTANE(MIXED)

Figure 3.22: Reactions for Pentadecane hydrocracking into shorter alkanes in Aspen.

3.2.3.3 Hexadecane cracking reactions

There are six reactions possible for the cracking of hexadecane into shorter alkanes, as illustrated in Equations (3.20) to (3.25). The fractional conversion was distributed evenly across the six reactions, with 0.16 per reaction, as shown in Figure 3.23 below. The overall conversion of hexadecane is 0.96.

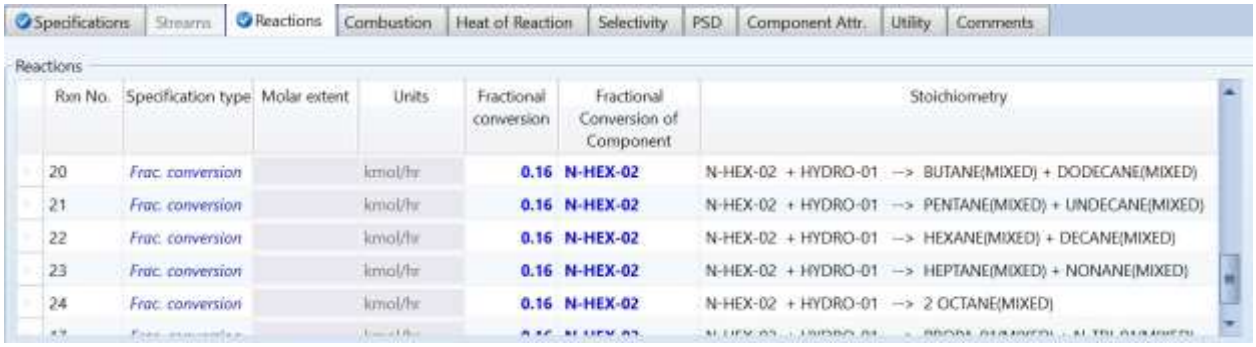


Figure 3.23: Reactions for Hexadecane hydrocracking into shorter alkanes in Aspen.

3.2.3.4 Heptadecane cracking reactions

There are six reactions possible for the cracking of heptadecane into shorter alkanes, as illustrated in Equations (3.26) to (3.31). Each of the six reactions had a fractional conversion of 0.16, as shown in Figure 3.24 below.

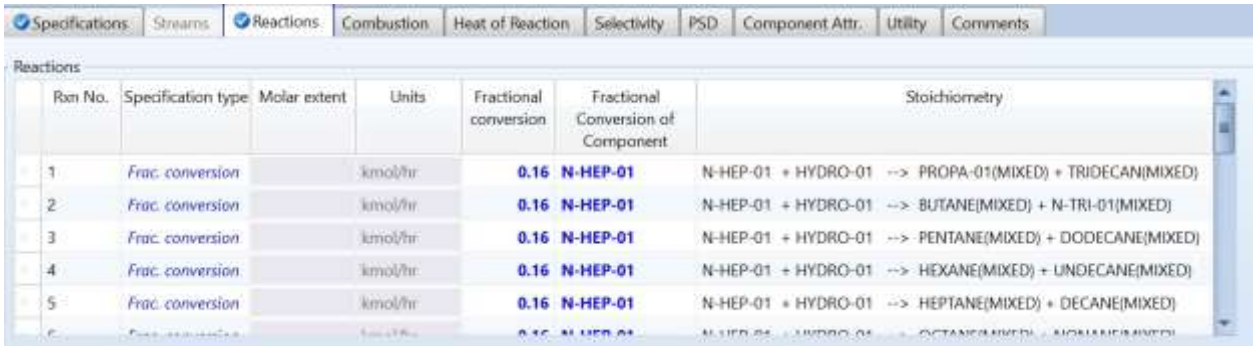


Figure 3.24: Reactions for Heptadecane hydrocracking into shorter alkanes in Aspen.

3.2.3.5 Octadecane cracking reactions

There are seven reactions possible for the cracking of octadecane into shorter alkanes, as illustrated in Equations (3.32) to (3.38). The fractional conversion was equally distributed among the six reactions, with 0.14 per reaction, as shown in Figure 3.25 below. The overall conversion of octadecane is 0.98.



Figure 3.25: Reactions for Octadecane hydrocracking into shorter alkanes in Aspen.

3.2.3.6 Hydrogen feed

Stream 18 delivers 5 Kmol/hr of hydrogen to the hydrocracking section at 1 bar and 25˚C, as seen in Figure 3.26.



Figure 3.26: Hydrogen feed to the Hydrocracking Section.

The stream is compressed to 60 bar and cooled to 240˚C, as shown in Figure 3.27 below.

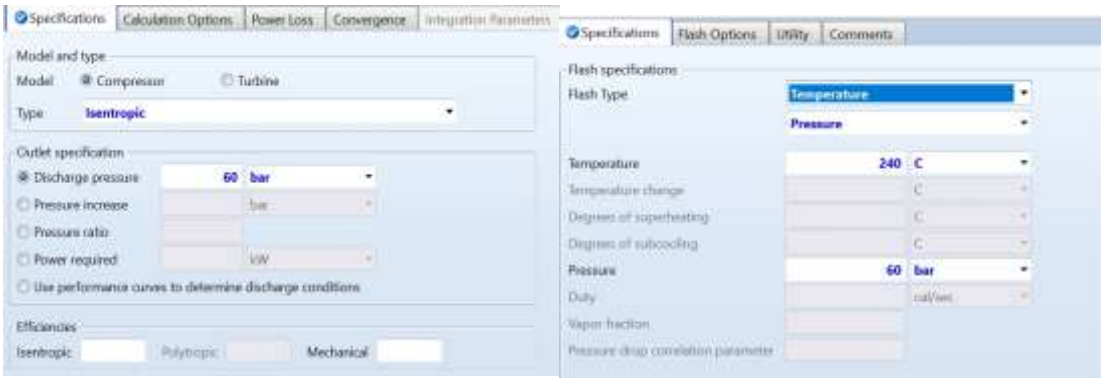


Figure 3.27: Hydrocracking hydrogen feed.

3.2.3.7 Product separation

The hydrocracking products are cooled and then separated in the flash drum as in Figure 3.28 below. The vapour stream contains residual hydrogen from the hydrocracking reactor.

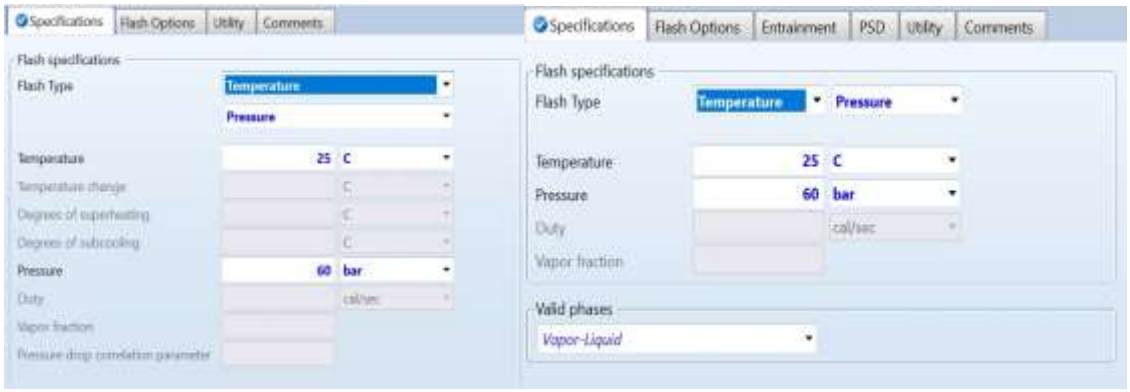


Figure 3.28: Cooling and flash drum conditions for product separation.

A turbine is installed to reduce pressure in the vapour stream from 35bar to 2bar as in Figure 3.29 below.



Figure 3.29: The isentropic turbine installed for pressure reduction.

The hydrogen vapour stream(14A) then joins the residual hydrogen from the hydrotreating section stream (8) for hydrogen recovery and recycling. The liquid from the flash drum is depressurised to 2 bar in the pressure valve, as shown in Figure 3.30, before product separation in the upstream distillation column.

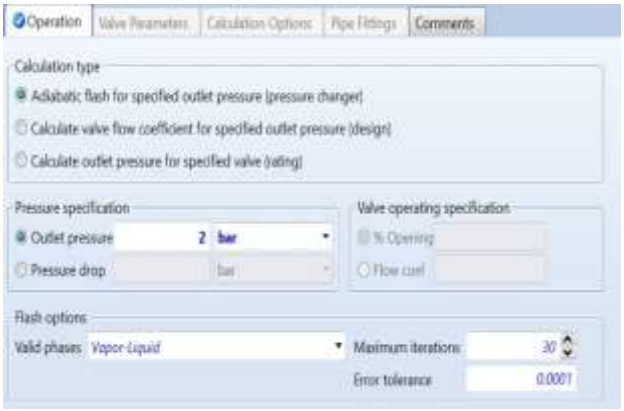


Figure 3.30: The pressure changing valve for the product stream.

The product stream is further pre-heated to 60˚C in preparation for separation in the distillation column, as shown in Figure 3.31 below.



Figure 3.31: Pre-distillation heater for product stream.

3.2.3.8 Distillation

The distillation column has 50 stages, and the condenser is partial-vapour-liquid as shown in Figure 3.32 below. The operations specifications are the reflux ratio and distillate to feed ratio.



Figure 3.32: Configuration for distillation column.

3.2.3.9 Streams

The feed stream is above stage 15 in the column with 50 stages; the 1st stage has both vapor and liquid, as in Figure 3.33 below.

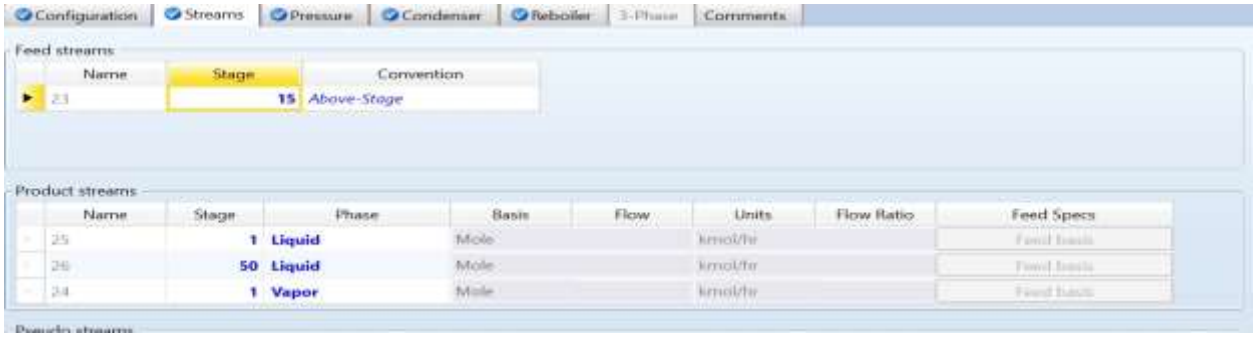


Figure 3.33: Distillation Streams configuration.

3.2.3.10 Pressure Inputs

The pressure in the distillation column is at 2bar with minimal pressure drop across the stage as illustrated in Figure 3.34 below.



Figure 3.34: Pressure in the column.

The condenser specifies the distillate vapour fraction as shown in Figure 3.35 below.



Figure 3.35: Condenser specifications.

3.2.4 Sensitivity Studies

Sensitivity studies will be conducted to determine the impact of various conditions on the product quality. The studies will evaluate various flow rates to determine the scalability of the process, the temperature, and pressure conditions for various catalysts:

3.2.4.1 Flow Rate

The process must be scaled to higher flows for commercialisation. Although the initial feed into the process was 100kg/hr, which is a pilot, the simulation will then be scaled to 1ton per hour to confirm the scalability of the process. Mass and energy balances for this process will be made available for the various plant scales that entrepreneurs may be interested in.

- 100kg/hr
- 1000kg/hr

3.2.4.2 Temperature and pressure for different catalysts

Hydrodeoxygenation Process Conditions

Various authors recommend different temperature ranges for the hydrodeoxygenation and hydrocracking reactions. For the hydrodeoxygenation reactions, temperature ranges are as below:

- 280˚C and 3.5 MPa (Kubicka & Tukac, 2013)
- 345˚C and 30bar, Alumina Al_2O_3 (Gutierrez-Antonio, et al., 2013)
- 300˚C and 30bar, 25% Ni/SAPO-11 (Liu, et al., 2015)

Hydrocracking Process Conditions

- 240˚C and 60bar, Alumina Al_2O_3 (Gutierrez-Antonio, et al., 2013)
- 300˚C and 30bar,25%Ni/ZSM-5(Si/Al:100) (Liu, et al., 2015)

3.2.5 Energy Efficiency

3.2.5.1 Pinch Technology

Energy efficiency for the process will be determined using the Pinch technology principle as illustrated by (March, 1998). After the heat and material balance is established, targets for energy saving can be set before the design of the heat exchanger network. Pinch technology provides a consistent methodology for energy saving from the basic heat and material balance to the total utility site. The process for pinch analysis is illustrated below:

a. Data Extraction – extraction of information required for Pinch analysis from a given process heat and material balance, in this case from the Aspen simulations for Biofuels production from Castor Oil.
b. Thermal Data – identify hot streams that need cooling and hot streams that require heating, and the heat capacity flowrate (kW/˚C) for the streams involved.
c. Construction of composite curves- energy targets are obtained using a tool called the "composite Curves", from the thermal data for a process, pinch analysis provides a target for the minimum energy consumption.
d. Determining the energy targets- composite curves provide a counter-current picture of heat transfer and can be used to determine the minimum energy target for the process, as illustrated in Figure 3.36 below, for example.

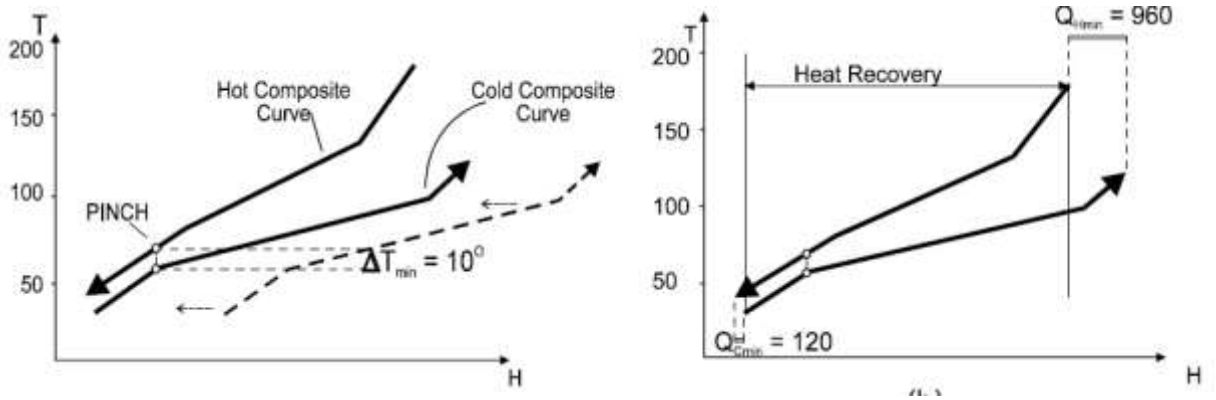


Figure 3.36: Example Using hot and cold composite curves to determine energy targets (March, 1998).

e. Pinch principle – from the composite curves, the point where Dtmin is observed is known as the "pinch." The following rules must be applied to achieve minimum energy targets for a process, as illustrated in Figure 3.37 below:

- Heat must not be transferred across the pinch.
- There must be no external cooling above the pinch.
- There must be no external heating below the pinch.

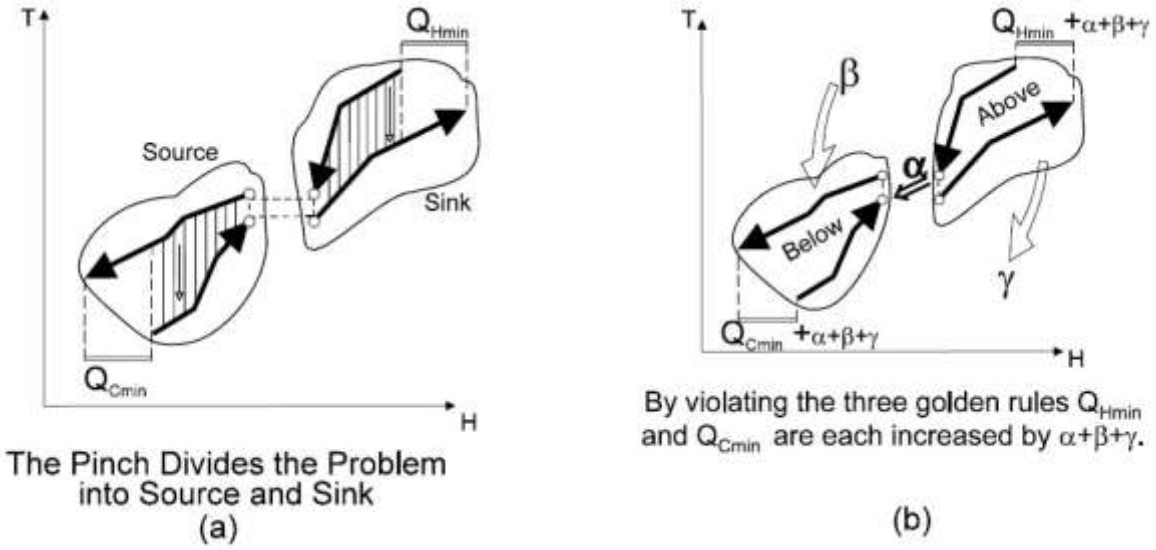


Figure 3.37: Pinch Principle (March, 1998).

In Figure 3.37(b), α amount of heat is transferred from above the pinch to below the pinch. The system above the pinch, which was before in heat balance with QHmin, now loses α units of heat to the system below the pinch. To restore the heat balance, the hot utility must be increased by the same amount, that is, α units. Below the pinch, α units of heat are added to the system that had an excess of heat; therefore, the cold utility requirement

also increases byα units. In conclusion, the consequence of a *cross-pinch heat transfer* (α) is that both the hot and cold utilities will increase by the cross-pinch duty (α) (March, 1998)

Figure 3.37(b) also shows γ amount of external cooling above the pinch and β amount of external heating below the pinch. The external cooling above the pinch of γ amount increases the hot utility demand by the same amount. Therefore, on an overall basis, both the hot and cold utilities are increased by γ amount. Similarly, external heating below the pinch of β amount increases the overall hot and cold utility requirement by the same amount (i.e. β)(March, 1998).

3.2.5.2 Energy consumption comparison to petroleum refineries

The process of refining crude oil to refined products can be achieved via a diverse range of refinery configurations. These configurations can be generalised into four types: simple, compound, complex and petrochemical. The simplest type consists of crude distillation, catalytic reforming and refining processes. The compound type includes the simple refinery units and units for vacuum distillation and catalytic cracking. The complex refineries have a complete slate of products, including the production of lube oils. Lastly, the petrochemical type includes petrochemical plants and those which produce aromatic hydrocarbons. (Bergh, 2012)
The castor oil process to be modelled consists of catalytic hydrotreating, catalytic hydrocracking and atmospheric distillation to produce green diesel, bio jet fuel, bio-gasoline and LPG. For catalytic hydrotreating, catalytic hydrocracking and atmospheric distillation sections in petroleum refineries, the energy consumption is illustrated in Table 3.1 below.

Table 3.1: Energy Use by Refinery Process (Bergh, 2012)

Process	**Specific Energy Use (MJ/bbl)**	**Average Use (MJ/bbl)**
Catalytic Hydrotreating	64 - 173	126.6
Catalytic Hydrocracking	168 - 339	253.2
Atmospheric Distillation	87-196	120.1

The three processes listed in Table 3.1 above represent 50% of energy consumption in a complex refinery. Other processes, such as the lube oil production process.

Chapter 4: Results and Discussion

4.1 Process Flowsheets for Green Diesel Production

The flowsheet, as displayed in Figure 4.1, illustrates the production process flowsheet for Green Diesel production developed in Aspen Plus. The flowsheet applies to all the scenarios that were modelled as listed in Table 4.1 below.

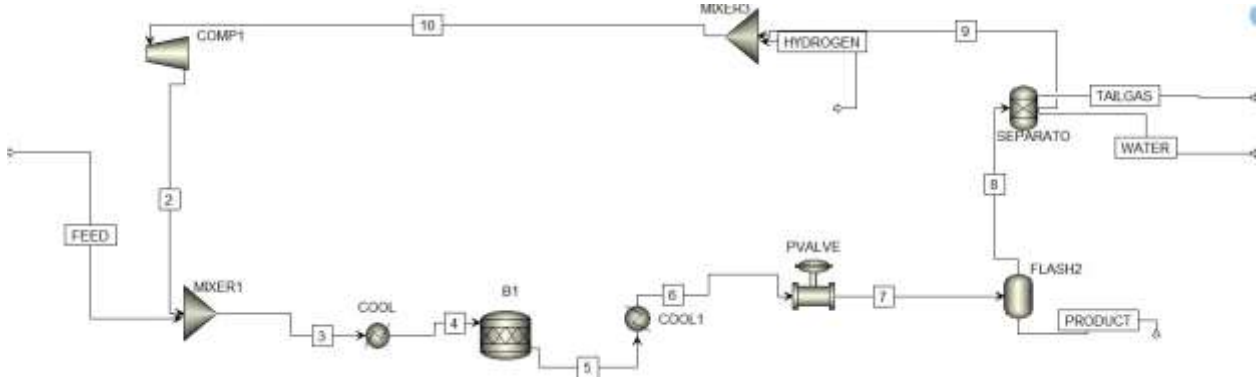


Figure 4.1 Green Diesel production flowsheet.

The results for the scenarios modelled will be presented in the sequence as illustrated in Table 4.1 below:

Table 4.1 Scenarios for Green Diesel modelling.

Case	Mass Flow(kg/hr)	Catalyst	Process Conditions for Reactor	Conversion (%)
Base	100	Alumina (Al_2O_3)	345˚C and 30 bar	99.35
1	1000	Alumina (Al_2O_3)	345˚C and 30 bar	99.35
2	100	25% Ni/SAPO-11	300˚C and 30bar	99
3	1000	25% Ni/SAPO-11	300˚C and 30bar	99

Process mass and energy balances were developed for all the scenarios in Table 4.1. The Process Flow diagram for the base case is presented in Figure 4.1 (a). Below and the mass balance results are presented in Table 4.2

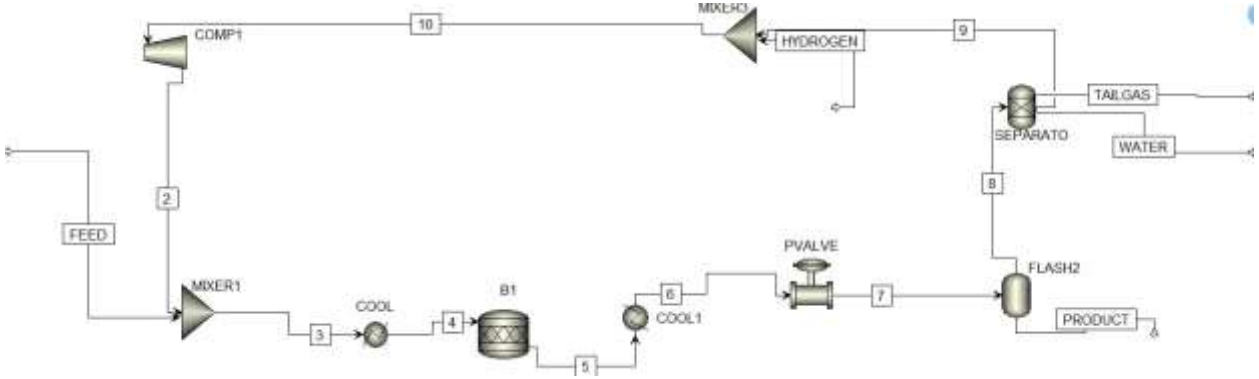


Figure 4.1(a) Green diesel production process.

Table 4.2 Base Case: Mass and Energy Balance 100kg/hr with Alumina Catalyst

Description	Units	2	3	4	5	6	7	8	9	10	FEED	HYDROGEN	PRODUCT	TAILGAS	WATER
Phase		Vapour	Vapour	Vapour	Vapour	Mix	Vapour	Vapour	Vapour	Vapour	Liquid	Vapour	Liquid	Vapour	Liquid Phase
Temperature	K	766.42	763.82	618.15	618.15	293.15	293.48	293.15	293.15	293.15	298.15	298.15	293.15	293.15	293.15
Pressure	N/sqm	3000000.00	3000000.00	3000000.00	3000000.00	3000000.00	200000.00	200000.00	200000.00	200000.00	3500000.00	200000.00	200000.00	200000.00	200000.00
Mass Enthalpy	J/kg	6820028.66	6581194.50	4498176.00	4477502.95	-147533.60	-147533.60	-121590.90	-70501.98	-70484.48	-3160960.47	855.42	-2001858.76	-4548772.20	-16030548.78
Mass Entropy	J/kg-K	-284.20	-479.47	-3504.96	-3422.12	-14031.01	-3075.24	-3021.84	-3047.33	-3047.27	-9508.63	-2805.97	-7464.11	2523.80	-9126.91
Mass Density	kg/cum	0.94	0.97	1.20	1.20	2.50	0.17	0.17	0.17	0.17	1517.58	0.16	765.23	2.45	963.76
Enthalpy Flow	Watt	7727558.32	7639753.86	5221689.99	5199640.72	-171328.02	-171328.02	-138383.32	-79863.97	-79863.74	-87804.46	0.24	-46394.03	-6593.07	-61973.10
Average MW		2.02	2.06	2.06	2.07	2.07	2.07	2.02	2.02	2.02	296.03	2.02	246.63	29.72	18.02
Mole Flows	kmol/sec	0.56	0.56	0.56	0.56	0.56	0.56	0.56	0.56	0.56	0.00	0.00	0.00	0.00	0.00
Mass Flows	kg/sec	1.13	1.16	1.16	1.16	1.16	1.16	1.14	1.13	1.13	0.03	0.00	0.02	0.00	0.00
Total Mass Flows	kg/hr	4079.05	4179.05	4179.05	4180.61	4180.61	4180.61	4097.18	4078.05	4079.05	100.00	1.00	83.43	5.22	13.92
Component Mass Flow(kg/hr)															
Heptadecane	kg/hr				41.58	41.58	41.58	0.05					41.53	0.05	
Octadecane	kg/hr				40.54	40.54	40.54	0.02					40.52	0.02	
Hydrogen	kg/hr	4079.05	4079.05	4079.05	4078.05	4078.05	4078.05	4078.05	4078.05	4079.05		1.00			
Water	kg/hr				13.92	13.92	13.92	13.92							13.92
Carbon Dioxide	kg/hr				0.65	0.65	0.65	0.65						0.65	
Carbon Monoxide	kg/hr				4.49	4.49	4.49	4.49						4.49	
Pentadecane	kg/hr				0.50	0.50	0.50	0.01					0.50	0.01	
Hexadecane	kg/hr				0.27	0.27	0.27	0.27	0.01					0.26	0.01
Ricinoleic Acid	kg/hr		87.47	87.47	0.52	0.52	0.52				87.47		0.52		
Linoleic Acid	kg/hr		3.12	3.12	0.02	0.02	0.02				3.12		0.02		
Oleic Acid	kg/hr		7.46	7.46	0.05	0.05	0.05				7.46		0.05		
Hexadecanoic Acid	kg/hr		0.91	0.91	0.01	0.01	0.01				0.91		0.01		
Stearic Acid	kg/hr		1.04	1.04	0.01	0.01	0.01				1.04		0.01		

4.1.1 Material Balance in Hydrotreating Reactor

The material balance for the conversion of castor oil in the hydrotreating reactor is shown in Table 4.3 below for the base case of 100kg/hr with Alumina catalyst. A conversion of 99.35% of castor oil occurs in the hydrotreating reactor through the different castor oil components, i.e. Ricinoleic acid, Linoleic acid, Oleic acid, Stearic acid and Palmitic acid (Hexadecanoic).

The castor oil components show a related conversion rate, with Ricinoleic acid the major component, reducing from 87.47kg/hr to 0.525kg/hr. A total residual castor oil mass of 0.6kg/hr is unreacted in the hydrotreating reactor.

The products formed from the hydrotreating of castor oil represent a high percentage of Heptadecane($C_{17}H_{36}$) and Octadecane($C_{18}H_{38}$) at 41.6% and 40.5% respectively. Water is the next component with 13.9% representation in the final product stream, followed by Carbon Dioxide at 4.5% and Carbon Monoxide at 0.65%.

Table 4.3: Material balance across the hydrotreating reactor.

	Component	Feed Stream(kg/hr)	Product Stream(kg/hr)
Castor Oil	Ricinoleic-Acid	87.472	0.525
	Linoleic-Acid	3.117	0.020
	Oleic-Acid	7.460	0.048
	Stearic-Acid	1.036	0.007
	Hexadecanoic-Acid	0.915	0.006
Products	Hexadecane	-	0.268
	Heptadecane	-	41.584
	Octadecane	-	40.540
	Pentadecane	-	0.502
	Water	-	13.921
	Carbon monoxide	-	0.652
	Carbon dioxide	-	4.495
		100.000	100.000

The results obtained are consistent with results from the simulation of castor oil for bio-jet fuel production study by Gutierrez-Antonio, et al. (2013). The hydrotreating step produced 38% heptadecane, 40% octadecane, 10% Water and 6.9% Carbon dioxide. The difference is in the production of propane in the hydrotreating step, where Gutierrez Antonio et al. (2013) show a 4.7% of propane in the final product, which can be an outcome in the hydrotreating of triglycerides.

The hydrotreating reactor products are separated into final products downstream of the reactor process in a flash separator to produce Green Diesel.

4.1.2 Product Separation

4.1.2.1 Green Diesel

The green diesel obtained from the castor oil hydrotreating is compared to Petroleum diesel, Biodiesel and Renewable diesel products in Table 4.4 below. The green diesel has a carbon content of 86.8% which is comparable to the Petroleum diesel (86.8%). The hydrogen content of 13.1% is also comparable to that of Petroleum diesel. The green diesel doesn't contain any oxygen as comparable to the Petroleum and Renewable diesel. The minimal oxygen is important to be maintained to ensure the thermal stability of the fuel (Gutierrez-Antonio, et al., 2013).

Table 4.4 Green Diesel Quality.

Property	Petroleum diesel	Biodiesel (FAME)	Renewable Diesel	**Castor Oil Green Diesel Results Aspen Simulation**
Carbon, wt.%	86.8	76.2	84.9	86.8
Hydrogen, wt.%	13.2	12.6	15.1	13.1
Oxygen, wt.%	0.0	11.2	0.0	0.0
Specific gravity	0.85	0.88	0.78	0.765
Cetane No.	40-45	45-55	70-90	114

The specific gravity of the green diesel is 0.765, which is comparable to the renewable diesel at 0.78.

Cetane Number for the Castor oil green diesel was simulated to be 114, which is higher than the diesel species for Petroleum diesel (45), Biodiesel (55), and Renewable diesel (90). According to (Cavalcanti et al., 2022), green diesel has a cetane number of 68 to 94.8. The cetane number is on the higher side than the expected green diesel; however, it is a positive difference. A lower cetane number would be of concern than a higher cetane number. According to (Sonthalia & Kumar, 2017), low volatility, boiling point, and cetane number cause issues such as incomplete combustion, engine oil contamination, and high stroke emission. Renewable/Green diesel is closely comparable with petroleum diesel in most properties. The specific gravity is lower with a higher viscosity than that of petroleum diesel. The cetane number is higher than that of petroleum diesel (Hoekman et al., 2012). The cetane number is a relative measure of the interval between the

beginning of injection and auto ignition of the fuel. The higher the cetane number, the shorter the delay interval and the greater its combustibility (Navale et al., 2011).

4.1.2.2 Water

The final separation step produced 13.9kg/hr of water from the 100kg/hr of Castor Oil; the water steam indicates a 100% mass fraction of water with no notable contaminants.

Hydrodeoxygenation, Decarboxylation, and decarbonylation occur in the hydrotreating step. Hydrodeoxygenation (HDO) is the process of removing oxygen from oxygenated feedstock in the form of water to increase the energy value of the oil. Water is formed as a byproduct in the process of Hydrodeoxygenation and Decarboxylation reactions of the Castor oil components i.e. Stearic acid in Equation(3.1) and (3.3), linoleic acid in equation(3.4) and (3.6), ricinoleic acid in Equation(3.7) and (3.8), oleic acid in Equation (3.9) and (3.11) and Palmitic Acid in Equation(3.12) and (3.14). The water can be further repurposed for cooling in the process. The cooling water circuit for the process is not included in the scope for this study.

4.1.2.3 Tail gas

The tail gas stream consists of various gases, Carbon Monoxide (81.6%) and Carbon Dioxide (11.8%) as illustrated in Table 4.5 below.

Table 4.5: Tail Gas Composition.

Mass Flow	Kg/hr	5.5
Mass Percentage	%	
Stearic Acid	$C_{18}H_{36}O_2$	
Heptadecane	$C_{17}H_{36}$	4.5
Octadecane	$C_{18}H_{38}$	1.5
Carbon dioxide	CO_2	11.8
Carbon monoxide	CO	81.6
Pentadecane	$C_{15}H_{32}$	0.5
Hexadecane	$C_{16}H_{34}$	0.1

The decarbonylation reactions of the hydrotreating steps result in the formation of Carbon Monoxide (CO) from the different castor oil components, i.e., Stearic Acid in Equation (3.2), Linoleic Acid in Equation (3.5), Oleic acid in Equation (3.10), and Palmitic acid in Equation (3.13)

Carbon Dioxide (CO_2) is formed from the decarboxylation reactions of the various castor oil components, i.e., stearic acid in Equation (3.3), linoleic Acid in Equation (3.6),

Ricinoleic Acid in Equation (3.8), Oleic Acid in Equation (3.11) and Palmitic Acid in Equation (3.14). The CO_2 represents 12% of the tail gas stream of 5kg/hr. In effect, 0.6kg/hr of carbon dioxide is produced from 100kg/hr of castor oil in the process. Carbon dioxide is a greenhouse gas, and the use of Biofuels is seen as an alternative to high emissions of carbon dioxide, often encountered in the production of fuels from other sources such as fossil fuels.

There are traces of hydrocarbons in the tail gas stream from the flash drum separation of the final product. The components include Heptadecane (4.5%), Octadecane (1.5%), Hexadecane (0.1%), and Pentadecane (0.5%). The tail gas stream is 5.5kg/hr, which is approximately 5% of the castor oil feed stream. The presence of hydrocarbons makes this stream a potential energy source before being released into the atmosphere.

4.1.3 Optimisation

4.1.3.1 Energy Consumption

From the simulation results, the main energy user in the process is the hydrogen compressor that compresses hydrogen to the required pressure for the hydrotreating process. For the base case, the compressor requires 7.8MW of energy as illustrated in Table 4.6 below.

Table 4.6 Hydrogen Compressor Energy Requirement.

Compressor: Isentropic		
Vapour Phase calculations	Units	
Indicated horsepower	kW	7807.42
Brake horsepower	kW	7807.42
Net work required	kW	7807.42
Power loss	kW	0.00
Efficiency		0.72
Mechanical efficiency		1.00
Outlet pressure	bar	30
Outlet temperature	℃	493.00
Isentropic outlet temperature	℃	360.00
Vapor fraction		1.00

The outlet stream (2) of the compressor, as can be seen in Figure 4.1, which is a recycle stream, has a high temperature of 493˚C. The size of the recycle stream is important as it

determines the size of the compressor required for the Hydrogen recycle stream. It combines with the Castor oil Feed stream and is fed to the hydrotreating reactor after being cooled to 345˚C and 30bar.

4.1.3.2 Scalability

For the base case of 100kg/hr using Alumina Catalyst, the Castor Oil feed stream was scaled to 1000kg/hr to evaluate the impact of scaling up on the feed rate on the production process. As presented in Table 4.1, Case 1 was evaluated with 1000kg/hr of Alumina at 345˚C and 30 bar and castor oil conversion of 99.35%. The results for this scenario are presented in Table 4.7 and Figure 4.1(b)below.

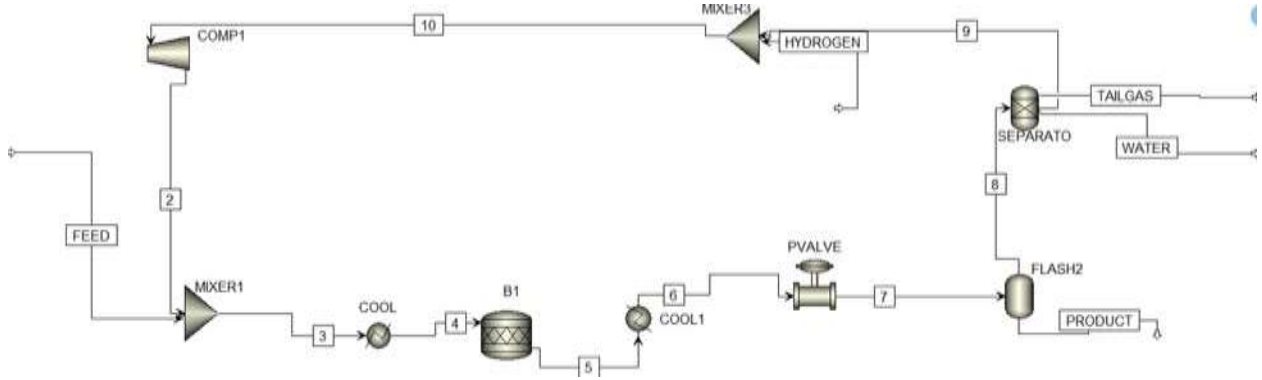


Figure 4.1(b): Green Diesel production process.

Table 4.7 Case 1: Mass and Energy Balance for 1000kg/hr with Alumina Catalyst.

Description	Units	2	3	4	5	6	7	8	9	10	FEED	HYDROGEN	PRODUCT	TAILGAS	WATER
Phase		Vapour	Vapour	Vapour	Vapour	Mix	Vapour	Vapour	Vapour	Vapour	Liquid	Vapour	Liquid	Vapour	Liquid
Temperature	K	766.54	761.36	618.15	618.15	293.15	292.97	293.15	293.15	293.20	298.15	298.15	293.15	293.15	293.15
Pressure	N/sqm	3000000.00	3000000.00	3000000.00	3000000.00	3000000.00	200000.00	200000.00	200000.00	200000.00	3500000.00	200000.00	200000.00	200000.00	200000.00
Mass Enthalpy	J/kg	6821829.23	6354841.69	4345919.12	4302152.13	-234220.94	-234220.94	-173529.86	-70501.98	-69796.10	-3161732.44	855.42	-2002335.40	-4529437.41	-16030548.78
Mass Entropy	J/kg-K	-281.85	-665.95	-3588.67	-3428.04	-13833.45	-3145.21	-2998.65	-3047.33	-3044.92	-9535.02	-2805.97	-7464.22	2612.30	-9126.91
Mass Density	kg/cum	0.94	1.00	1.22	1.22	2.56	0.17	0.17	0.17	0.17	1528.43	0.16	765.24	2.42	963.76
Enthalpy Flow	Watt	38616568.39	37738309.38	25808296.78	25338339.41	-1379488.58	-1379488.58	-981814.15	-395145.15	-395097.25	-878259.01	47.90	-464125.07	-64812.44	-622783.90
Average MW		2.02	2.11	2.11	2.12	2.12	2.12	2.03	2.02	2.02	296.14	2.02	246.52	29.46	18.02
Mole Flows	kmol/sec	2.81	2.81	2.81	2.78	2.78	2.78	2.78	2.78	2.81	0.00	0.03	0.00	0.00	0.00
Total Mass Flows	kg/sec	5.66	5.94	5.94	5.89	5.89	5.89	5.66	5.60	5.66	0.28	0.06	0.23	0.01	0.04
Total Mass Flows	kg/hr	20378.65	21378.65	21378.65	21202.88	21202.88	21202.88	20368.43	20177.06	20378.65	1000.00	201.59	834.45	51.51	139.86
Component Mass Flow															
Heptadecane	kg/hr				414.45	414.45	414.45	0.24					414.20	0.24	
Octadecane	kg/hr				406.40	406.40	406.40	0.08					406.32	0.08	
Hydrogen	kg/hr	20378.65	20378.65	20378.65	20177.07	20177.07	20177.07	20177.06	20177.06	20378.65	0.00	201.59	0.01		
Water	kg/hr				139.92	139.92	139.92	139.86					0.06		139.86
Carbon dioxide	kg/hr				6.10	6.10	6.10	6.10					0.00	6.10	
Carbon monoxide	kg/hr				45.06	45.06	45.06	45.06					0.00	45.06	
Pentadecane	kg/hr				5.06	5.06	5.06	0.03					5.04	0.03	
Hexadecane	kg/hr				2.70	2.70	2.70	0.01					2.69	0.01	
Ricinoleic acid	kg/hr		882.95	882.95	5.30	5.30	5.30				882.95		5.30		
Linoleic acid	kg/hr		31.46	31.46	0.22	0.22	0.22				31.46		0.22		
Oleic acid	kg/hr		75.30	75.30	0.53	0.53	0.53				75.30		0.53		
Hexadecanoic acid	kg/hr		9.24	9.24	0.06	0.06	0.06				9.24		0.06		
Stearic acid	kg/hr		1.05	1.05	0.01	0.01	0.01				1.05		0.01		

The Ni/SAPO11 catalyst was also simulated at 100kg/hr and 1000kg/hr at 300˚C and 30bar with a 99% conversion. The results for the 100kg/hr are presented in Figure 4.1 (c) and Table 4.8 below.

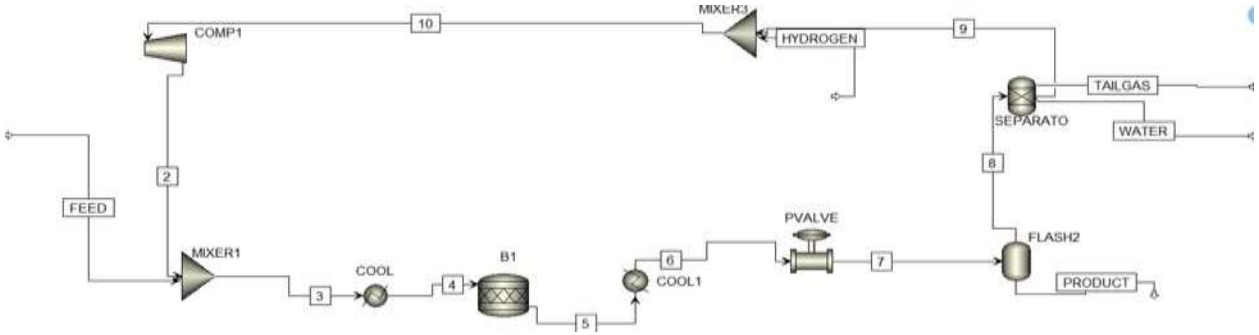


Figure 4.1(c) Green Diesel production process.

Table 4.8 Case 2: Mass and Energy Balance 100kg/hr of 25% Ni/SAPO-11.

Description	Units	2	3	4	5	6	7	8	9	10	FEED	HYDROGEN	PRODUCT	TAILGAS	WATER
Phase		Vapour	Vapour	Vapour	Vapour	Mixed	Vapour	Vapour	Vapour	Vapour	Liquid	Vapour	Liquid	Vapour	Liquid
Temperature	K	766.42	764.22	573.15	573.15	293.15	293.56	293.15	293.15	293.15	298.15	298.15	293.15	293.15	293.15
Pressure	N/sqm	3000000.00	3000000.00	3000000.00	3000000.00	3000000.00	200000.00	200000.00	200000.00	200000.00	3000000.00	200000.00	200000.00	200000.00	200000.00
Mass Enthalpy	J/kg	6820021.61	6617366.38	3878532.80	3861281.46	-133955.12	-133955.12	-113491.28	-70501.98	-70487.19	-3162095.63	855.42	-2007363.18	-4566180.32	-16030548.78
Mass Entropy	J/kg-K	-284.21	-449.45	-4572.92	-4502.70	-14062.25	-3064.82	-3025.59	-3047.33	-3047.28	-9491.86	-2805.97	-7472.40	2477.76	-9126.91
Mass Density	kg/cum	0.94	0.96	1.28	1.28	2.49	0.17	0.17	0.17	0.17	1510.46	0.16	767.13	2.46	963.76
Enthalpy Flow	Watt	9142056.05	9054219.36	5306807.07	5284863.21	-183341.85	-183341.85	-152701.43	-94486.43	-94486.19	-87836.69	0.24	-46552.31	-6646.26	-61548.46
Average MW		2.02	2.06	2.06	2.06	2.06	2.06	2.02	2.02	2.02	295.76	2.02	246.64	29.86	18.02
Mole Flows	kmol/sec	0.66	0.67	0.67	0.67	0.67	0.67	0.67	0.66	0.66	0.00	0.00	0.00	0.00	0.00
Mass Flows	kg/sec	1.34	1.37	1.37	1.37	1.37	1.37	1.35	1.34	1.34	0.03	0.00	0.02	0.00	0.00
Mass Flows	kg/hr	4825.70	4925.70	4925.70	4927.25	4927.25	4927.25	4843.77	4824.70	4825.70	100.00	1.00	83.49	5.24	13.82
Component Mass Flows(kg/hr)															
Heptadecane	kg/hr				41.18	41.18	41.18	0.06					41.12	0.06	
Octadecane	kg/hr				40.14	40.14	40.14	0.02					40.12	0.02	
Hydrogen	kg/hr	4825.70	4825.70	4825.70	4824.70	4824.70	4824.70	4824.70	4824.70	4825.70		1.00			
Water	kg/hr				13.82	13.82	13.82	13.82							13.82
Carbon Dioxide	kg/hr				0.68	0.68	0.68	0.68						0.68	
Carbon Monoxide	kg/hr				4.47	4.47	4.47	4.47						4.47	
Pentadecane	kg/hr				0.82	0.82	0.82	0.01					0.81	0.01	
Hexadecane	kg/hr				0.44	0.44	0.44						0.43		
Ricinoleic acid	kg/hr		86.96	86.96	0.87	0.87	0.87				86.96		0.87		
Linoleic acid	kg/hr		3.10	3.10	0.03	0.03	0.03				3.10		0.03		
Oleic acid	kg/hr		7.42	7.42	0.07	0.07	0.07				7.42		0.07		
Hexadecanoic acid	kg/hr		1.50	1.50	0.01	0.01	0.01				1.50		0.01		
Stearic acid	kg/hr		1.03	1.03	0.01	0.01	0.01				1.03		0.01		

The results for the 1000kg/hr of Ni/SAPO-11 catalyst at 300˚C and 30bar with 99% conversion are illustrated in Figure 4.1 (d) and Table 4.9 below.

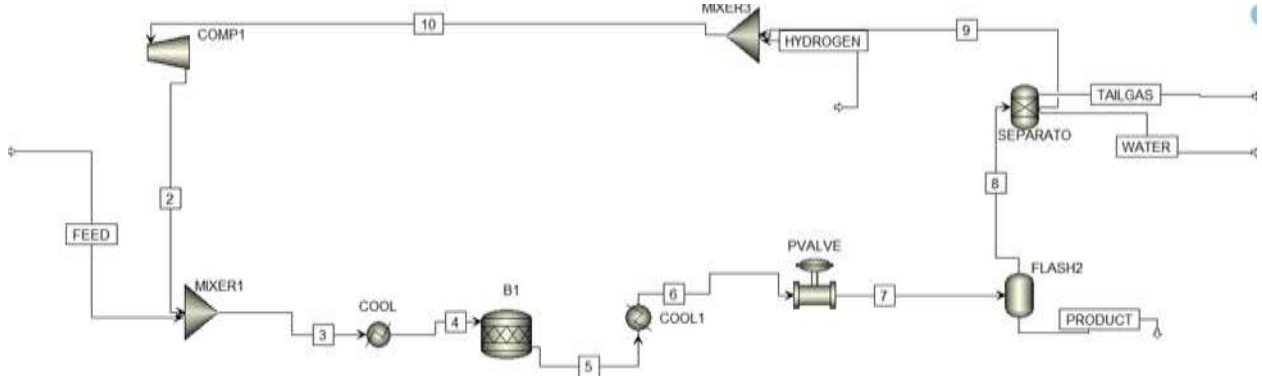


Figure 4.1(d): Green Diesel production process.

Table 4.9 Case 3: Mass and Energy Balance 1000kg/hr of 25% Ni/SAPO-11.

Description	Units	2	3	4	5	6	7	8	9	10	FEED	HYDROGEN	PRODUCT	TAILGAS	WATER
Phase		Vapour	Vapour	Vapour	Vapour	Mixed	Vapour	Vapour	Vapour	Vapour	Liquid	Vapour	Liquid	Vapour	Liquid
Temperature	K	766.48	755.18	573.15	573.15	293.15	291.75	293.15	293.15	293.18	298.15	298.15	293.15	293.15	293.15
Pressure	N/sqm	3000000.00	3000000.00	3000000.00	3000000.00	3000000.00	200000.00	200000.00	200000.00	200000.00	3000000.00	200000.00	200000.00	200000.00	200000.00
Mass Enthalpy	J/kg	6820994.80	5844404.21	3403927.30	3318944.85	-422762.25	-422762.25	-292633.79	-70501.98	-70115.11	-3162095.63	855.42	-2009079.60	-4601884.09	-16030548.78
Mass Entropy	J/kg-K	-282.94	-1085.00	-4782.10	-4456.46	-13406.45	-3305.07	-2948.55	-3047.33	-3046.01	-9491.86	-2805.97	-7472.16	2615.87	-9126.91
Mass Density	kg/cum	0.94	1.06	1.39	1.39	2.71	0.18	0.17	0.17	0.17	1510.46	0.16	767.05	2.42	963.76
Enthalpy Flow	Watt	17473855.14	16595495.24	9665631.80	9401713.26	-1197576.22	-1197576.22	-761024.74	-179631.02	-179619.14	-878359.90	11.88	-466382.08	-66061.99	-614976.11
Average MW		2.02	2.23	2.23	2.23	2.23	2.23	2.05	2.02	2.02	295.76	2.02	246.21	29.51	18.02
Mole Flows	kmol/sec	1.27	1.27	1.27	1.27	1.27	1.27	1.27	1.26	1.27	0.00	0.01	0.00	0.00	0.00
Mass Flows	kg/sec	2.56	2.84	2.84	2.83	2.83	2.83	2.60	2.55	2.56	0.28	0.01	0.23	0.01	0.04
Mass Flows	kg/hr	9222.39	10222.39	10222.39	10197.87	10197.87	10197.87	9362.18	9172.39	9222.39	1000.00	50.00	835.69	51.68	138.11
Component Mass Flow(kg/hr)															
Heptadecane	kg/hr				411.75	411.75	411.75	0.11					411.64	0.11	
Octadecane	kg/hr				401.40	401.40	401.40	0.04					401.36	0.04	
Hydrogen	kg/hr	9222.39	9222.39	9222.39	9172.40	9172.40	9172.40	9172.39	9172.39	9222.39		50.00	0.01	0.00	
Water	kg/hr				138.25	138.25	138.25	138.11					0.14	0.00	138.11
Carbon Dioxide	kg/hr				6.79	6.79	6.79	6.79					0.00	6.79	
Carbon Monoxide	kg/hr				44.72	44.72	44.72	44.72					0.00	44.72	
Pentadecane	kg/hr				8.20	8.20	8.20	0.02					8.18	0.02	
Hexadecane	kg/hr				4.37	4.37	4.37						4.36		
Ricinoleic acid	kg/hr		869.57	869.57	8.70	8.70	8.70				869.57		8.70		
Linoleic acid	kg/hr		30.98	30.98	0.31	0.31	0.31				30.98		0.31		
Oleic acid	kg/hr		74.16	74.16	0.74	0.74	0.74				74.16		0.74		
Hexadecanoic acid	kg/hr		14.99	14.99	0.15	0.15	0.15				14.99		0.15		
Stearic acid	kg/hr		10.29	10.29	0.10	0.10	0.10				10.29		0.10		

The scalability and different catalysts were evaluated for the green diesel production process, and the results are presented below in Table 4.10 for Base Case, Case 1, Case 2, and Case 3.

Table 4.10 Green Diesel Product Quality Analysis for different cases.

Product Composition (Mass% %)	Formula	Base Case	Case 1	Case 2	Case 3
Stearic Acid	$C_{18}H_{36}O_2$	0.01	0.01	0.01	0.01
Heptadecane	$C_{17}H_{36}$	49.72	49.72	49.20	49.26
Octadecane	$C_{18}H_{38}$	48.67	48.66	48.15	48.04
Pentadecane	$C_{15}H_{32}$	0.57	0.57	0.93	0.98
Ricinoleic Acid	$C_{18}H_{34}O_3$	0.63	0.63	1.05	1.04
Linoleic Acid	$C_{18}H_{32}O_2$	0.02	0.03	0.04	0.04
Oleic Acid	$C_{18}H_{34}O_2$	0.06	0.06	0.09	0.09
Hexadecanoic Acid	$C_{16}H_{32}O_2$	0.01	0.01	0.02	0.02
Hexadecane	$C_{16}H_{34}$	0.32	0.32	0.51	0.52

Base Case: 100kg/hr of castor oil processed in the Alumina catalyst.
Case 1:1000kg/hr of castor oil processed in Alumina Catalyst
Case 2: 100kg/hr of castor oil processed in 25%NiSAPO-11 catalyst.
Case 3:1000kg/hr of castor oil processed in 25% NiSAPO-11 catalyst.

The production process for the different catalysts, as presented in Table 4.10, shows a consistent product quality produced from the four cases. The difference between the Alumina cases and the NiSapo catalyst in the castor oil conversion, that 99.35% and 99% conversion are for Alumina and NiSapo, respectively. Although both processes occur at 30 bars, the hydrotreating process occurs at 345˚C and 300˚C for alumina and NiSapo, respectively. The process with the higher conversion is preferred to improve product quality and yields.

As can be seen in Table 4.10, both processes indicate a high mass percentage of Heptadecane($C_{17}H_{36}$) and Octadecane($C_{18}H_{38}$) in the final product of Green Diesel produced.

4.1.3.3 Sensitivity Analysis for Hydrogen Consumption

Hydrogen is a feedstock for the Green Diesel Production process. Although the production process for hydrogen is not modelled in detail, the consumption is optimised to ensure optimal usage of the commodity. Figure 4.2 shows the variation in hydrogen

consumption where the hydrogen recycle stream is optimised at a minimum of 18kg/hr and a maximum of 50 kg/hr for the recycle stream of 5000 kg/hr.

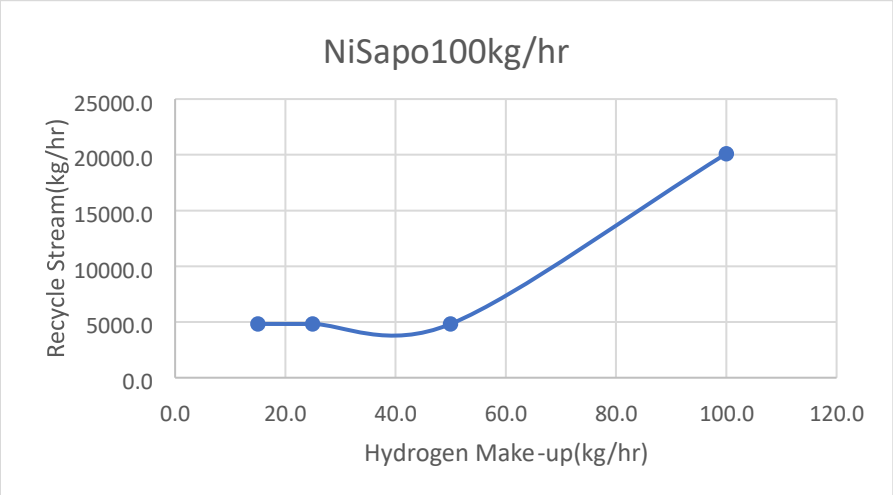


Figure 4.2: Hydrogen consumption vs recycle stream size for the 100kg/hr case of NiSapo.

The size of the hydrogen recycle stream is important to ensure that the compressor size is optimal for energy efficiency purposes.

For the 1000kg/hr NiSapo case as illustrated in Figure 4.3 below, the hydrogen consumption is optimised at a minimum of 50 kg/hr and a maximum of 100kg/hr as a make-up stream into the process for a recycle stream of 8800kg/hr.

The hydrogen make-up quantity seems to double (50 kg/hr to 100 kg/hr maximums) as compared to the 100:1000 castor oil ratio, which is ten times the base case. The hydrogen consumption is thus conservative and not directly proportional to the castor oil consumption.

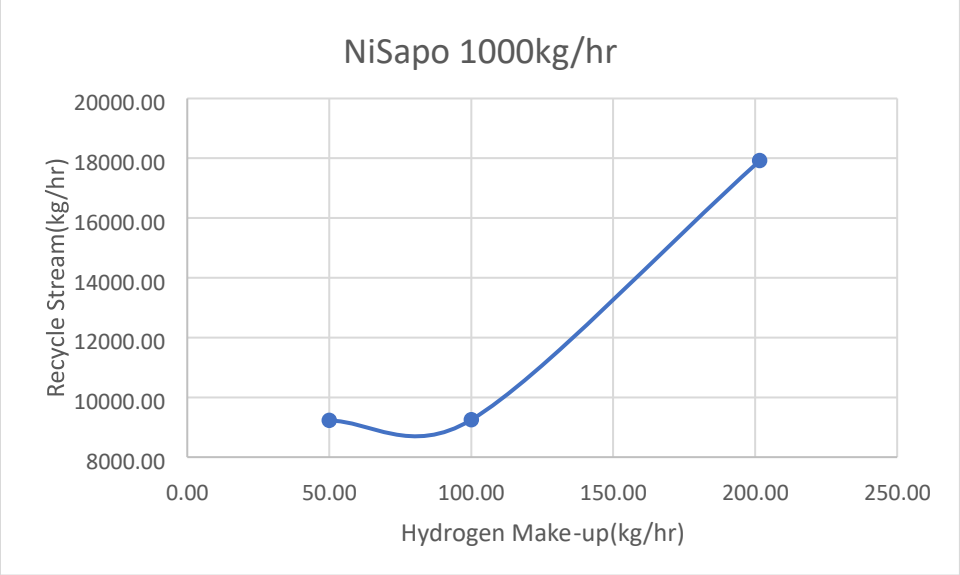


Figure 4.3: Hydrogen consumption vs recycle stream size for NiSapo.

4.1.3.4 Energy Consumption for scaling

The energy requirements for the compressor double when the castor oil stream is increased ten times from 100 kg/hr to 1000 kg/hr, as illustrated in Table 4.11 below. The energy requirements are proportional to the hydrogen in the recycle stream.

Table 4.11: Compressor results for the NiSapo 100kg/hr and 1000kg/hr.

		100kg/hr	**1000kg/hr**
Compressor model	Isentropic Compressor		
Phase calculations	Vapour phase calculation		
Indicated horsepower	MW	9.24	17.65
Brake horsepower	MW	9.24	17.65
Network required	MW	9.24	17.65
Power loss	MW	0	0
Efficiency		0.72	0.72
Mechanical efficiency		1	1
Outlet pressure	bar	30	30
Outlet temperature	C	493	493
Isentropic outlet temperature	C	361	361
Vapor fraction		1	1

4.2 Process Flowsheet for Bio-jet fuel production

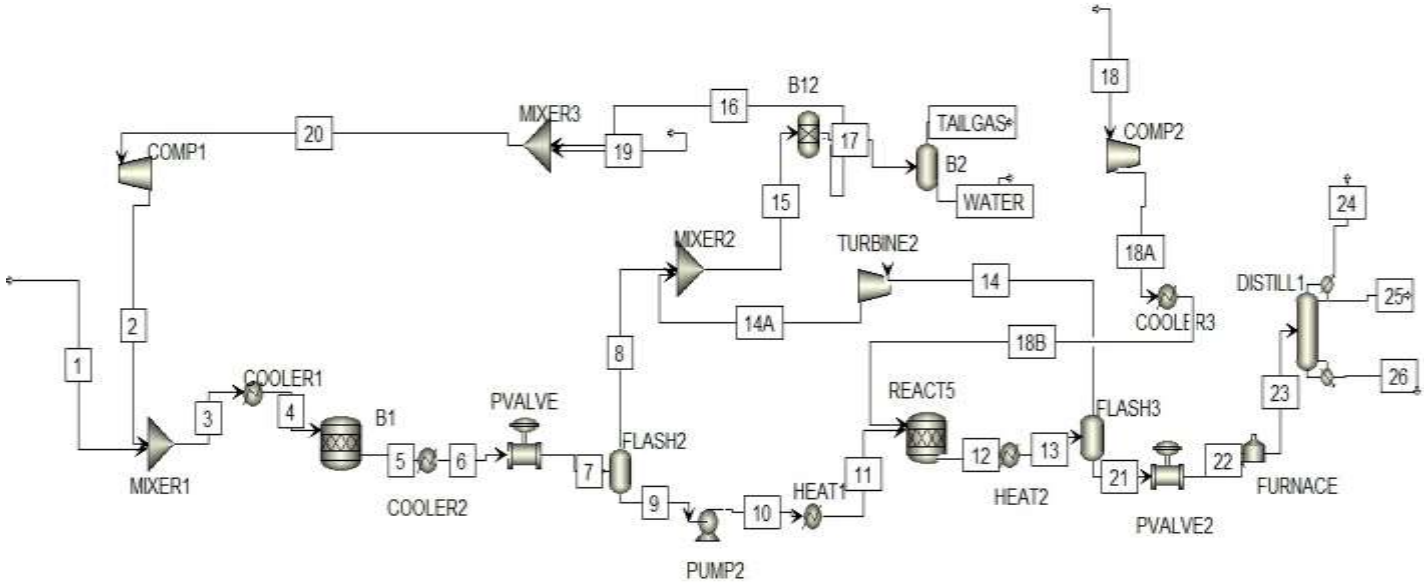


Figure 4.4 Hydrocracking flowsheet.

The hydrocracking reaction involves the further treatment of green diesel through a cracking process with Hydrogen into other products. The following products were produced from the simulation with hydrocracking and further separation by distillation. The Ni/ZSM-5 catalyst 100kg/hr case is used for the hydrocracking results analysis below.

4.2.1Hydrocracking Reactor Material Balance

The green diesel rich in heptadecane and octadecane is further treated in the hydrocracking reactor to produce a range of paraffins from propane C3 to pentadecane C15 in various concentrations as presented in the Table below. The material balance is for the Ni/ZSM-5 Catalyst at 100 kg/hr. The conversion of 99% of the feed stream is applied in the reactor for the cracking reactions (3.15) to (3.33). The input components to the hydrocracking reactor are slightly lower in mass percentage as compared to the products due to a loss of hydrocarbons to the tail gas stream in the flash separator.

The hydrogen consumed in the hydrocracking reactor is 0.546kg/hr (the difference between the Feed and Product stream). These represent 0.5% of the Castor Oil feed stream (100kg/hr). The flash drum downstream of the reactor separates the liquid products and the unreacted gaseous Hydrogen. The liquids are separated into final products in the distillation column; the unreacted hydrogen is recovered with a Turbine and recycled to the Hydrogen loop as illustrated in Figure 4.4.

Table 4.12: Material balance in the hydrocracking reactor.

	Components	Feed(kg/hr)	Products(kg/hr)
Inputs	Hexadecane	0.264	0.047
	Heptadecane	40.966	7.292
	Octadecane	39.973	7.235
	Pentadecane	0.489	3.992
	Hydrogen	10.079	9.533
Products	Propane	-	1.863
	Butane	-	2.456
	Pentane	-	3.049
	Hexane	-	3.641
	Heptane	-	4.234
	Octane	-	4.845
	Nonane	-	7.776
	Decane	-	6.012
	Undecane	-	6.605
	Dodecane	-	7.197
	Tridecane	-	8.276
	Tetradecane	-	7.720
		93.646	93.646

The high pressure of 30 bar applied through compression to feed hydrogen to the hydrocracking reactor consumes 29.5 kW of electricity. The energy recovered through the Turbine is 4.69 kW as presented in Table 4.13 below. The energy consumption is for a minimum of 10 kg/hr of Hydrogen simulated. Although the reactor uses less hydrogen, this minimum was kept for practical purposes of sizing equipment for pilot scale.

Table 4.13: Turbine and compressor for Hydrocracking for 100 kg/hr Ni/ZSM-5.

Isentropic	**Turbine**	**Compressor**	
Phase calculations	Two phase	Vapor phase	Units
Indicated horsepower	-4.69	29.53	kW
Brake horsepower	-4.69	29.53	kW
Net work required	-4.69	29.53	kW
Power loss	0	0	kW
Efficiency	0.72	0.72	
Mechanical efficiency	1	1	
Outlet pressure	2	30	bar
Outlet temperature	-90.82	744.83	℃
Isentropic outlet temperature	-133.76	545.89	℃
Vapor fraction	0.99	1.00	
Mass Flow(kg/hr)	12.85		

4.2.2 Final Products

The flash separator separates liquid products fed to the distillation column for further separation into final products. Three product streams are emerging from the RadFrac Separator, i.e. Gaseous Light hydrocarbon stream, Liquid light hydrocarbons and heavy liquid hydrocarbons as discussed below.

- **Gaseous light hydrocarbon stream** (24): For the 100kg/hr of Castor Oil simulated, 5kg/hr was produced as gaseous hydrocarbons, representing 5% of the feed stream. The stream is composed of light hydrocarbons, C3 to C7
- **Liquid light hydrocarbons (25)**: The liquid light hydrocarbons are the top distillate product of the RadFrac column. The stream is composed of C3 to C7 hydrocarbons in liquid form. The stream is 7.7kg/hr, representing 7% of the overall Castor oil feed stream.
- **Heavy hydrocarbons (26):** The heavy hydrocarbons produced as bottoms of the distillation column represent 68% of the castor oil feed stream at 68kg/hr. This is the main final product and contains components of C8 to C15. This is the typical Bio Jet fuel product.

Figure 4.5 below illustrates the distribution of Hydrocarbons to the three final product streams. The separation of the products into different streams is discussed in detail in the Distillation Section 4.2.5

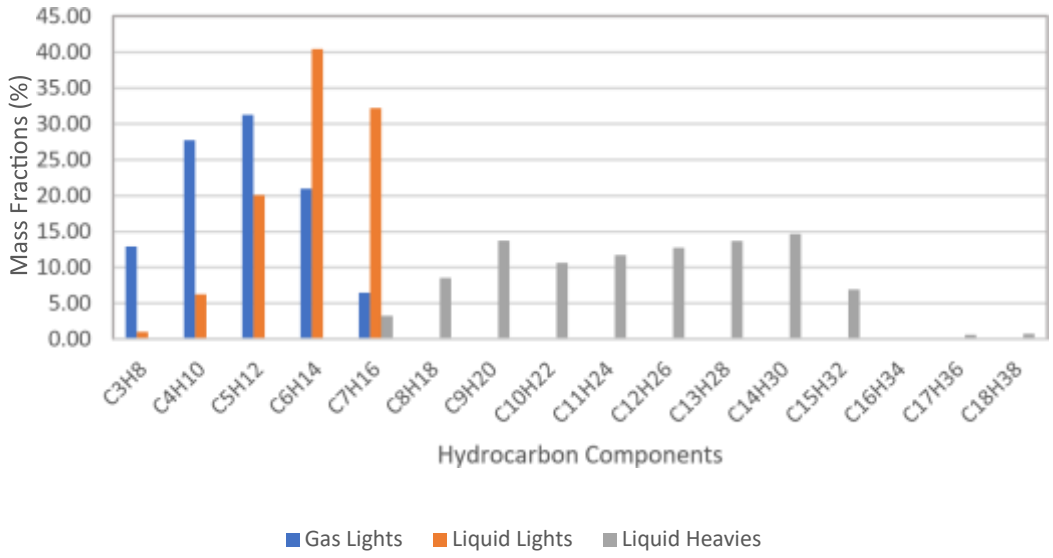


Figure 4.5: Hydrocarbon distribution to the final product stream.

4.2.3 Waste Streams

- **Tail Gas**: The hydrogenation process produces tail gas consisting of Carbon Monoxide, Carbon Dioxide and Water. Traces of hydrocarbons are present in this stream due to the imperfect separation in the Flash 2 and Flash 3 after the hydrodeoxygenation and hydrodeoxygenation processes, respectively. Hydrogen is extracted and recycled from this stream before being discarded. The tail gas is 8.7kg/hr, representing 8.7% of the castor oil feedstock.
- **Waste Water**: The water produced is from the hydrodeoxygenation process and represents 13.7% of the castor oil stream fed to the process.

4.2.4 Scalability

The various scenarios modelled for hydrocracking Bio-jet Fuel production are presented in Table 4.15 below for the alumina and Ni/ZSM-5 catalyst at different pressures, temperatures and mass flows of 100 kg/hr and 1000 kg/hr as presented in Table 4.15 below.

Table 4.15: Scenarios for process Optimisation.

Case	Mass Flow(kg/hr)	Catalyst	Process Conditions for Reactor	Conversion (%)
Base	100	Alumina (Al_2O_3)	240℃ and 60 bar	82
1	1000	Alumina (Al_2O_3)	240℃ and 60 bar	82
2	100	25% Ni/ZSM-5	300℃ and 30bar	99
3	1000	25% Ni/ZSM-5	300℃ and 30bar	99

4.2.4.1 Product quality

The product quality of the bio-jet fuel product was evaluated for the two main catalysts, i.e. Ni/ZSM-5 and Alumina, for the 100kg/hr case and the 1000kg/hr case to evaluate the impact of scalability on product quality. The flow sheets, mass and energy balances produced from the two catalysts at varying flow rates are presented in Tables 4.16,4.17,4.18, and 4.19, where each mass balance is represented by a summary of feedstock, final products and waste streams.

As it can be seen in Tables 4.16,4.17,4.18, and 4.19, the scalability does not vary the final product composition, the product quantities that affect the blend in final products are proportionate to the mass flow rates of the Castor oil produced for the same type of catalyst used i.e. Alumina 100 kg/hr and Alumina 1000kg/hr product qualities are consistent. The same applies to the Ni/ZSM-5 100kg/hr and 1000kg/hr. The same phenomenon is observed with the waste streams, where the qualities remain the same and the stream mass flow rates are proportionate to the scaling factors. The results for the bio-jet fuel production for the 100kg/hr of Alumina Catalyst case are illustrated in

Figure 4.6 and Tables 4.16 and 4.17 below

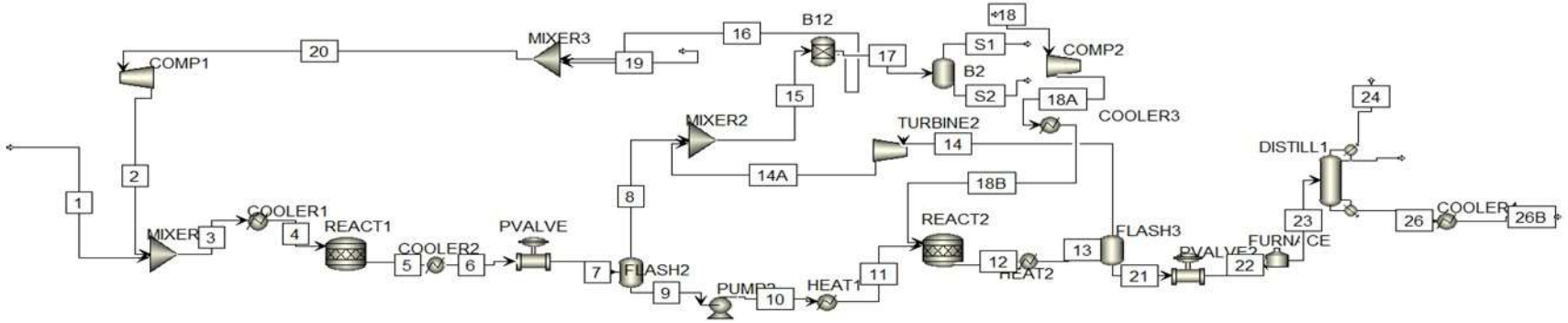


Figure 4.6 Bio-jet fuel production process flowsheet.

Table 4.16: Base Case: Alumina 100kg/hr Mass and Energy Balance.

Description	Units	1	2	3	4	5	6	7	8	9	10	11	12	13	14	14A	15	16	17	18	18A	18B	19	20	21	22	23	24	25	26	26B	S1	S2
Phase		Liquid	Vapor	Vapor	Vapor	Vapor		Vapor	Vapor	Liquid	Liquid	Liquid			Vapor		Vapor	Vapor		Vapor	Vapor	Vapor	Vapor	Vapor	Liquid			Vapor	Liquid	Liquid	Liquid	Vapor	Liquid
Temperature	C	25.00	493.17	492.03	345.00	345.00	20.00	20.60	20.00	20.00	27.97	240.00	240.00	25.00	25.00	-105.86	19.86	19.86	19.86	25.00	924.80	240.00	25.00	19.97	25.00	28.28	60.00	45.17	45.17	206.04	25.00	20.00	20.00
Pressure	bar	30.00	30.00	30.00	30.00	30.00	30.00	2.00	2.00	2.00	60.00	60.00	60.00	60.00	60.00	2.00	2.00	2.00	2.00	1.00	60.00	60.00	2.00	2.00	60.00	2.00	2.00	2.00	2.00	2.00	2.00	2.00	2.00
Mass Enthalpy	cal/gm	-755.15	1628.60	1603.16	1095.48	1092.86	-23.67	-23.67	-22.28	-482.37	-476.30	-349.07	-237.36	-456.19	-96.60	-480.08	-22.87	-17.31	-2800.18	0.10	3177.22	752.28	0.20	-16.93	-507.61	-507.61	-490.21	-490.08	-546.50	-392.25	-500.40	-924.79	-3828.79
Mass Entropy	cal/gm-K	-2.27	-0.07	-0.09	-0.83	-0.82	-3.38	-0.73	-0.72	-1.79	-1.78	-1.46	-1.44	-1.99	-3.53	-2.47	-0.73	-0.73	-1.41	0.01	0.84	-2.15	-0.67	-0.73	-1.77	-1.76	-1.70	-1.43	-1.74	-1.49	-1.77	-0.02	-2.18
Mass Density	gm/cc	1.52	0.00	0.00	0.00	0.00	0.00	0.00	0.00	0.77	0.77	0.66	0.02	0.04	0.01	0.00	0.00	0.00	0.01	0.00	0.00	0.00	0.00	0.00	0.74	0.16	0.11	0.00	0.63	0.61	0.76	0.00	0.96
Enthalpy Flow	cal/sec	-20976.45	4194652.65	4173676.20	2851965.55	2781850.84	-60248.77	-60248.77	-56188.55	-11196.27	-11055.34	-8102.13	-6173.94	-11865.86	-314.32	-1562.10	-57750.66	-43614.62	-16496.45	0.29	8895.70	2106.27	11.44	-43603.18	-11551.54	-11551.54	-11155.63	-542.27	-1108.02	-7697.05	-9819.17	-1929.99	-14565.72
Average MW		296.03	2.02	2.04	2.04	2.04	2.04	2.04	2.02	247.34	247.34	247.34	17.54	17.54	2.47	2.47	2.02	2.02	21.69	2.02	2.02	2.02	2.02	2.02	138.12	138.12	138.12	44.77	82.04	170.14	170.14	34.50	18.02
Mole Flows	kmol/hr	0.34	4599.61	4599.94	4599.94	4496.18	4496.18	4496.18	4495.84	0.34	0.34	0.34	5.34	5.34	4.74	4.74	4500.58	4499.61	0.98	5.00	5.00	5.00	100.00	4599.61	0.59	0.59	0.59	0.09	0.09	0.42	0.42	0.22	0.76
Mass Flows	kg/hr	100.00	9272.25	9372.25	9372.25	9163.72	9163.72	9163.72	9080.16	83.56	83.56	83.56	93.64	93.64	11.71	11.71	9091.87	9070.67	21.21	10.08	10.08	10.08	201.59	9272.25	81.92	81.92	81.92	3.98	7.30	70.64	70.64	7.51	13.70
Mass Components flow																																	
Heptane	kg/hr					41.07	41.07	41.07	0.11	40.96	40.96	40.96	7.29	7.29			0.11		0.11						7.29	7.29	7.29			7.29	7.29	0.11	
Octane	kg/hr					40.00	40.00	40.00	0.03	39.97	39.97	39.97	7.23	7.23			0.03		0.03						7.23	7.23	7.23			7.23	7.23	0.03	
Hydrogen	kg/hr		9272.25	9272.25	9272.25	9061.19	9061.19	9061.19	9061.19				9.53	9.53	9.48	9.48	9070.67	9070.67	0.00	10.08	10.08	10.08	201.59	9272.25	0.05	0.05	0.05	0.05					
Water	kg/hr					13.73	13.73	13.73	13.73				0.00	0.00	0.00	0.00	13.73		13.73													0.04	13.70
Propane	kg/hr					0.00	0.00	0.00	0.00				1.86	1.86	1.07	1.07	1.07		1.07						0.80	0.80	0.80	0.70	0.10			1.07	
Carbon Monoxide	kg/hr					0.65	0.65	0.65	0.65								0.65		0.65													0.65	
Carbon Dioxide	kg/hr					4.44	4.44	4.44	4.44								4.44		4.44													4.44	
Butane	kg/hr												2.46	2.46	0.66	0.66	0.66		0.66						1.80	1.80	1.80	1.24	0.56			0.66	
Pentane	kg/hr												3.05	3.05	0.32	0.32	0.32		0.32						2.73	2.73	2.73	1.16	1.57			0.32	
Hexane	kg/hr												3.64	3.64	0.12	0.12	0.12		0.12						3.52	3.52	3.52	0.65	2.87			0.12	
Heptane	kg/hr												4.23	4.23	0.04	0.04	0.04		0.04						4.19	4.19	4.19	0.18	2.20	1.81	1.81	0.04	
Octane	kg/hr												4.84	4.84	0.02	0.02	0.02		0.02						4.83	4.83	4.83			4.83	4.83	0.02	
Nonane	kg/hr												7.78	7.78	0.01	0.01	0.01		0.01						7.77	7.77	7.77			7.77	7.77	0.01	
Decane	kg/hr												6.01	6.01											6.01	6.01	6.01			6.01	6.01		
Undecane	kg/hr												6.60	6.60											6.60	6.60	6.60			6.60	6.60		
Dodecane	kg/hr												7.20	7.20											7.20	7.20	7.20			7.20	7.20		
Tetradecane	kg/hr												8.27	8.27											8.27	8.27	8.27			8.27	8.27		
Tridecane	kg/hr												7.72	7.72											7.72	7.72	7.72			7.72	7.72		
Pentadecane	kg/hr					0.50	0.50	0.50	0.01	0.49	0.49	0.49	3.99	3.99			0.01		0.01						3.99	3.99	3.99			3.99	3.99	0.01	
Hexadecane	kg/hr	3.12		3.12	3.12	0.03	0.03	0.03		0.03	0.03	0.03	0.03	0.03											0.03	0.03	0.03			0.03	0.03		
Linoleic acid	kg/hr	87.47		87.47	87.47	1.75	1.75	1.75		1.75	1.75	1.75	1.75	1.75											1.75	1.75	1.75			1.75	1.75		
Ricinoleic acid	kg/hr	7.46		7.46	7.46	0.07	0.07	0.07		0.07	0.07	0.07	0.07	0.07											0.07	0.07	0.07			0.07	0.07		
Oleic acid	kg/hr	0.91		0.91	0.91	0.01	0.01	0.01		0.01	0.01	0.01	0.01	0.01											0.01	0.01	0.01			0.01	0.01		
Hexadecanoic acid	kg/hr	0.00				0.27	0.27	0.27		0.26	0.26	0.26	0.05	0.05											0.05	0.05	0.05			0.05	0.05		
Stearic acid	kg/hr	1.04		1.04	1.04	0.01	0.01	0.01		0.01	0.01	0.01	0.01	0.01											0.01	0.01	0.01			0.01	0.01		

Table 4.17: Alumina 100kg/hr Feedstock and Product Quality Analysis.

	Feedstock			Products			Waste Streams	
	Castor Oil	**H2 Hydrotreating**	**H2 Hydrocracki**	**Gaseous C3-C7**	**Liquid C3-C7**	**Liquid C8-C15**	**Tail Gas**	**Waste Water**
Mass(kg/hr)	100.000	201.588	10.079	4.820	7.394	68.920	8.283	13.693
Mass Fractions								
Stearic Acid	0.010							
Heptane						0.106	0.012	
Octane						0.105	0.004	
Hydrogen		1.000	1.000	0.006				
Water							0.005	1.000
Propane				0.108	0.007		0.156	
Carbon Monoxide							0.078	
Carbon Dioxide							0.536	
Butane				0.242	0.047		0.113	
Pentane				0.299	0.152		0.059	
Hexane				0.219	0.325		0.023	
Heptane				0.125	0.469	0.001	0.008	
Octane						0.070	0.003	
Nonane						0.113	0.002	
Decane						0.087		
Undecane						0.096		
Dodecane						0.104		
Tetradecane						0.120		
Tridecane						0.112		
Pentadecane						0.058	0.001	
Linoleic acid	0.031					0.000		
Ricinoleic acid	0.875					0.025		
Oleic acid	0.075					0.001		
Hexadecanoic acid	0.009					0.000		
Hexadecane						0.001		

The results for the bio-jet fuel production for the 1000kg/hr of Alumina Catalyst case are illustrated in Figure 4.7 and Tables 4.18 and 4.19 below.

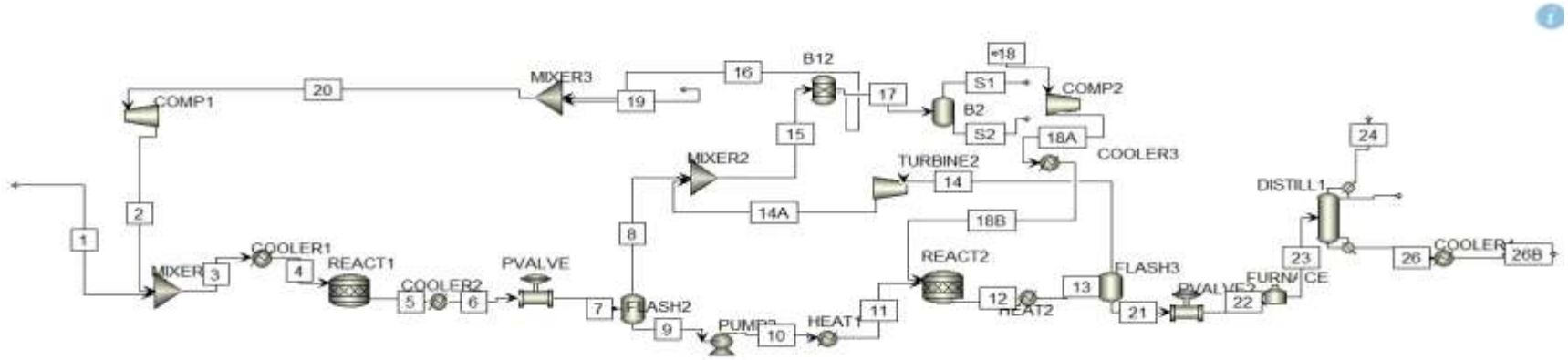


Figure 4.7 Bio-jet fuel production process flow.

Table 4.18: Case 1: Alumina 1000kg/hr Mass and Energy Balance.

Description	Units	1	2	3	4	5	6	7	8	9	10	11	12	13	14	14A	15	16	17	18	18A	18B	19	20	21	22	23	24	25	26	26B	S1	S2
Phase		Liquid	Vapor	Vapor	Vapor	Vapor		Vapor	Vapor	Liquid	Liquid	Liquid			Vapor		Vapor	Vapor		Vapor	Vapor	Vapor	Vapor	Vapor				Vapor	Liquid	Liquid	Liquid	Vapor	Liquid
Temperature	C	25.00	493.37	481.76	345.00	345.00	20.00	18.49	20.00	20.00	27.97	240.00	240.00	25.00	25.00	-103.45	19.94	19.94	19.94	25.00	924.80	240.00	25.00	20.05	25.00	27.50	60.00	19.75	19.75	192.90	25.00	20.00	20.00
Pressure	bar	30.00	30.00	30.00	30.00	30.00	30.00	2.00	2.00	2.00	60.00	60.00	60.00	60.00	60.00	2.00	2.00	2.00	2.00	1.00	60.00	60.00	2.00	2.00	60.00	2.00	2.00	2.00	2.00	2.00	2.00	2.00	2.00
Mass Enthalpy	cal/gm	-755.15	1629.29	1390.35	952.95	929.17	-104.45	-104.45	-71.83	-482.85	-476.77	-349.52	-367.18	-508.41	-146.61	-495.58	-72.10	-17.05	-3066.03	0.10	3177.22	752.28	0.20	-16.66	-510.81	-510.81	-492.32	-525.75	-580.97	-402.50	-501.82	-1090.12	-3828.79
Mass Entropy	cal/gm-K	-2.27	-0.07	-0.26	-0.90	-0.82	-3.19	-0.79	-0.70	-1.79	-1.78	-1.46	-1.43	-1.78	-3.31	-2.37	-0.70	-0.73	-1.41	0.01	0.84	-2.15	-0.67	-0.73	-1.77	-1.76	-1.70	-1.44	-1.79	-1.51	-1.77	0.57	-2.18
Mass Density	gm/cc	1.52	0.00	0.00	0.00	0.00	0.00	0.00	0.00	0.77	0.77	0.66	0.26	0.42	0.01	0.00	0.00	0.00	0.01	0.00	0.00	0.00	0.00	0.00	0.73	0.13	0.08	0.00	0.63	0.62	0.75	0.00	0.96
Enthalpy Flow	cal/sec	-209764.44	4063716.28	3853951.84	2641518.26	2529061.60	-284285.77	-284285.77	-178810.45	-112279.91	-110867.84	-81277.87	-86412.17	-119648.37	-227.50	-769.00	-179579.45	-41570.87	-161596.40	0.29	8895.70	2106.27	11.44	-41559.43	-119420.88	-119420.88	-115098.41	-5440.58	-11024.93	-82295.45	-102603.52	-16003.29	-145589.99
Average MW		296.03	2.02	2.24	2.24	2.24	2.24	2.24	2.05	246.83	246.83	246.83	100.96	100.96	2.74	2.74	2.06	2.02	20.23	2.02	2.02	2.02	2.02	2.02	132.42	132.42	132.42	39.08	71.66	165.44	165.44	29.70	18.02
Mole Flows	kmol/hr	3.38	4454.12	4457.50	4457.50	4364.86	4364.86	4364.86	4361.47	3.39	3.39	3.39	8.39	8.39	2.04	2.04	4363.50	4354.12	9.38	5.00	5.00	5.00	100.00	4454.12	6.36	6.36	6.36	0.95	0.95	4.45	4.45	1.78	7.60
Mass Flows	kg/hr	1000.00	8978.98	9978.98	9978.98	9798.68	9798.68	9798.68	8961.54	837.14	837.14	837.14	847.22	847.22	5.59	5.59	8967.13	8777.39	189.74	10.08	10.08	10.08	201.59	8978.98	841.63	841.63	841.63	37.25	68.32	736.06	736.06	52.85	136.89
Component Mass Flow																																	
Heptane	kg/hr					410.67	410.67	410.67	0.10	410.56	410.56	410.56	73.08	73.08			0.10		0.10						73.08	73.08	73.08			73.08	73.08	0.10	
Octane	kg/hr					400.05	400.05	400.05	0.03	400.01	400.01	400.01	72.40	72.40			0.03		0.03						72.40	72.40	72.40			72.40	72.40	0.03	
Hydrogen	kg/hr		8978.98	8978.98	8978.98	8773.36	8773.36	8773.36	8773.35	0.01	0.01	0.01	4.61	4.61	4.04	4.04	8777.39	8777.39	0.00	10.08	10.08	10.08	201.59	8978.98	0.57	0.57	0.57	0.57				0.00	
Water	kg/hr					137.33	137.33	137.33	137.19	0.15	0.15	0.15	0.15	0.15	0.00	0.00	137.19		137.19						0.14	0.14	0.14	0.06	0.09			0.30	136.89
Propane	kg/hr												18.66	18.66	0.96	0.96	0.96		0.96						17.71	17.71	17.71	13.92	3.79			0.96	
Carbon Monoxide	kg/hr					6.50	6.50	6.50	6.50								6.50		6.50													6.49	
Carbon Dioxide	kg/hr					44.36	44.36	44.36	44.36								44.36		44.36													44.36	
Butane	kg/hr												24.60	24.60	0.36	0.36	0.36		0.36						24.24	24.24	24.24	13.22	11.02			0.36	
Pentane	kg/hr												30.54	30.54	0.14	0.14	0.14		0.14						30.39	30.39	30.39	7.07	23.32			0.14	
Hexane	kg/hr												36.48	36.48	0.05	0.05	0.05		0.05						36.43	36.43	36.43	2.42	30.09	3.91	3.91	0.05	
Heptane	kg/hr												42.41	42.41	0.02	0.02	0.02		0.02						42.39	42.39	42.39			42.39	42.39	0.02	
Octane	kg/hr												48.53	48.53	0.01	0.01	0.01		0.01						48.53	48.53	48.53			48.53	48.53	0.01	
Nonane	kg/hr												77.87	77.87											77.87	77.87	77.87			77.87	77.87		
Decane	kg/hr												60.22	60.22											60.22	60.22	60.22			60.22	60.22		
Undecane	kg/hr												66.16	66.16											66.16	66.16	66.16			66.16	66.16		
Dodecane	kg/hr												72.10	72.10											72.10	72.10	72.10			72.10	72.10		
Tetradecane	kg/hr												82.89	82.89											82.89	82.89	82.89			82.89	82.89		
Tridecane	kg/hr												77.32	77.32											77.32	77.32	77.32			77.32	77.32		
Pentadecane	kg/hr					5.00	5.00	5.00	0.01	4.99	4.99	4.99	39.96	39.96			0.01		0.01						39.96	39.96	39.96			39.96	39.96	0.01	
Hexadecane	kg/hr	31.17		31.17	31.17	0.31	0.31	0.31		0.31	0.31	0.31	0.31	0.31											0.31	0.31	0.31			0.31	0.31		
Linoleic acid	kg/hr	874.72		874.72	874.72	17.49	17.49	17.49		17.49	17.49	17.49	17.49	17.49											17.49	17.49	17.49			17.49	17.49		
Ricinoleic acid	kg/hr	74.60		74.60	74.60	0.75	0.75	0.75		0.75	0.75	0.75	0.75	0.75											0.75	0.75	0.75			0.75	0.75		
Oleic acid	kg/hr	9.15		9.15	9.15	0.09	0.09	0.09		0.09	0.09	0.09	0.09	0.09											0.09	0.09	0.09			0.09	0.09		
Hexadecanoic ac	kg/hr	0.00		0.00	0.00	2.67	2.67	2.67		2.66	2.66	2.66	0.47	0.47											0.47	0.47	0.47			0.47	0.47		
Stearic acid	kg/hr	10.36		10.36	10.36	0.10	0.10	0.10	0.00	0.10	0.10	0.10	0.10	0.10											0.10	0.10	0.10			0.10	0.10		

Table 4.19: Alumina 1000 kg/hr Feedstock and Product Analysis.

	Feedstock			Final Products			Waste Streams	
	Castor Oil	H2 Hydrotreatin	H2 Hydrocracking	Gaseous C3-C7	Liquid C3-C7	Liquid C8-C15	Tail Gas	Waste Water
Mass Flows(kg/hr)	1000.000	201.588	10.079	43.771	69.634	726.914	53.928	136.885
Mass Fractions								
Stearic Acid	0.010							
Heptane						0.101	0.002	
Octane						0.100	0.001	
Hydrogen	0.000	1.000	1.000	0.008				
Water				0.002	0.001		0.006	1.000
Propane				0.324	0.041		0.030	
Carbon Monoxide				0.000	0.000		0.120	
Carbon Dioxide							0.823	
Butane				0.342	0.129		0.012	
Pentane				0.221	0.296		0.005	
Hexane				0.099	0.460		0.002	
Heptane				0.005	0.072	0.051	0.001	
Octane						0.067		
Nonane						0.107		
Decane						0.083		
Undecane						0.091		
Dodecane						0.099		
Tetradecane						0.114		
Tridecane						0.106		
Pentadecane						0.055		
Linoleic acid	0.031					0.000		
Ricinoleic acid	0.875					0.024		
Oleic acid	0.075					0.001		
Hexadecanoic acid	0.009					0.000		
Hexadecane	0.000					0.001		

The results for the bio-jet fuel production for the 100kg/hr of Ni/ZSM-5 Catalyst case are illustrated in Figure 4.8 and Tables 4.20 and 4.21 below.

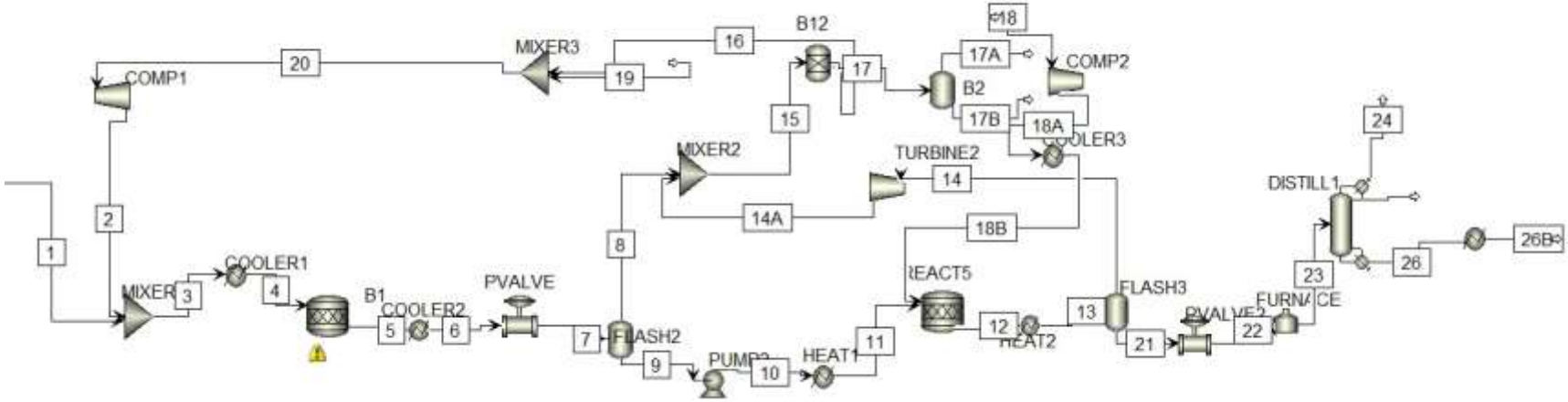


Figure 4.8 Bio-jet fuel production process.

Table 4.20 Case 2: Mass and Energy Balance Ni/ZSM-5 100kg/hr.

Description	Units	1	2	3	4	5	6	7	8	9	10	11	12	13	14	14A	15	16	17	18	18A	18B	19	20	21	22	23	24	25	26	26B	S1	S2
Phase		Liquid	Vapor	Vapor	Vapor	Vapor		Vapor	Vapor	Liquid	Liquid	Liquid			Vapor		Vapor	Vapor		Vapor	Vapor	Vapor	Vapor	Vapor	Liquid			Vapor	Liquid	Liquid	Liquid	Vapor	Liquid
Temperature	C	25.00	493.22	492.14	300.00	300.00	20.00	20.62	20.00	20.00	23.86	300.00	300.00	25.00	25.00	-86.34	19.89	19.89	19.89	25.00	697.48	300.00	25.00	19.99	25.00	26.57	60.00	61.14	61.14	199.82	25.00	20.00	20.00
Pressure	bar	30.00	30.00	30.00	30.00	30.00	30.00	2.00	2.00	2.00	30.00	30.00	30.00	30.00	30.00	2.00	2.00	2.00	2.00	1.00	30.00	30.00	2.00	2.00	30.00	2.00	2.00	2.00	2.00	2.00	2.00	2.00	2.00
Mass Enthalpy	cal/gm	-755.15	1628.76	1604.91	941.43	939.05	-23.05	-23.05	-21.93	-482.37	-479.44	-306.22	-162.68	-462.75	-148.84	-445.01	-22.50	-17.22	-2645.74	0.10	2349.25	956.06	0.20	-16.87	-514.08	-514.08	-496.01	-477.94	-533.77	-401.02	-505.42	-857.50	-3828.80
Mass Entropy	cal/gm-K	-2.27	-0.07	-0.09	-1.09	-1.08	-3.38	-0.73	-0.73	-1.79	-1.79	-1.38	-1.21	-1.91	-2.78	-2.09	-0.73	-0.73	-1.41	0.01	0.76	-1.08	-0.67	-0.73	-1.77	-1.76	-1.71	-1.43	-1.72	-1.50	-1.77	-0.26	-2.18
Mass Density	gm/cc	1.52	0.00	0.00	0.00	0.00	0.00	0.00	0.00	0.77	0.77	0.60	0.01	0.02	0.00	0.00	0.00	0.00	0.01	0.00	0.00	0.00	0.00	0.00	0.73	0.26	0.19	0.00	0.62	0.61	0.76	0.00	0.96
Enthalpy Flow	cal/sec	-20976.45	4477818.72	4456842.27	2614357.75	2553374.79	-62680.12	-62680.12	-59113.38	-11194.75	-11126.72	-7106.61	-4230.95	-12034.88	-544.01	-1626.51	-60739.90	-46380.61	-16719.22	0.29	6577.50	2676.80	11.44	-46369.16	-11490.87	-11490.87	-11087.12	-697.62	-1145.58	-7517.77	-9474.86	-2157.74	-14560.85
Average MW		296.03	2.02	2.04	2.04	2.04	2.04	2.04	2.02	247.35	247.35	247.35	17.54	17.54	2.78	2.78	2.02	2.02	22.64	2.02	2.02	2.02	2.02	2.02	132.17	132.17	132.17	57.54	84.61	158.36	158.36	36.97	18.02
Mole Flows	kmol/hr	0.34	4909.61	4909.95	4909.95	4806.23	4806.23	4806.23	4805.89	0.34	0.34	0.34	5.34	5.34	4.73	4.73	4810.62	4809.61	1.00	5.00	5.00	5.00	100.00	4909.61	0.61	0.61	0.61	0.09	0.09	0.43	0.43	0.25	0.76
Mass Flows	kg/hr	100.00	9897.19	9997.19	9997.19	9788.74	9788.74	9788.74	9705.20	83.55	83.55	83.55	93.63	93.63	13.16	13.16	9718.35	9695.60	22.75	10.08	10.08	10.08	201.59	9897.19	80.47	80.47	80.47	5.25	7.73	67.49	67.49	9.06	13.69
Component Mass Flow																																	
Heptane	kg/hr					41.07	41.07	41.07	0.12	40.95	40.95	40.95	0.41	0.41			0.12		0.12						0.41	0.41	0.41	0.00	0.00	0.41	0.41	0.12	
Octane	kg/hr					40.00	40.00	40.00	0.04	39.97	39.97	39.97	0.52	0.52			0.04		0.04						0.52	0.52	0.52	0.00	0.00	0.52	0.52	0.04	
Hydrogen	kg/hr		9897.19	9897.19	9897.19	9686.21	9686.21	9686.21	9686.21				9.42	9.42	9.39	9.39	9695.60	9695.60		10.08	10.08	10.08	201.59	9897.19	0.03	0.03	0.03	0.03	0.00				
Water	kg/hr					13.73	13.73	13.73	13.73								13.73		13.73						0.00	0.00	0.00	0.00	0.00			0.04	13.69
Propane	kg/hr					0.00	0.00	0.00	0.00				2.24	2.24	1.59	1.59	1.59		1.59						0.66	0.66	0.66	0.59	0.06			1.59	
Carbon Monoxide	kg/hr					0.65	0.65	0.65									0.65		0.65						0.00	0.00	0.00	0.00	0.00			0.65	
Carbon Dioxide	kg/hr					4.44	4.44	4.44	4.44								4.44		4.44						0.00	0.00	0.00	0.00	0.00			4.44	
Butane	kg/hr												2.96	2.96	1.18	1.18	1.18		1.18						1.78	1.78	1.78	1.35	0.43			1.18	
Pentane	kg/hr												3.67	3.67	0.62	0.62	0.62		0.62						3.06	3.06	3.06	1.65	1.41			0.62	
Hexane	kg/hr												4.39	4.39	0.24	0.24	0.24		0.24						4.15	4.15	4.15	1.18	2.97			0.24	
Heptane	kg/hr												5.10	5.10	0.09	0.09	0.09		0.09						5.01	5.01	5.01	0.45	2.86	1.70	1.70	0.09	
Octane	kg/hr												5.84	5.84	0.03	0.03	0.03		0.03						5.80	5.80	5.80			5.80	5.80	0.03	
Nonane	kg/hr												9.37	9.37	0.02	0.02	0.02		0.02						9.35	9.35	9.35			9.35	9.35		
Decane	kg/hr												7.24	7.24											7.24	7.24	7.24			7.24	7.24		
Undecane	kg/hr												7.95	7.95											7.95	7.95	7.95			7.95	7.95		
Dodecane	kg/hr												8.67	8.67											8.67	8.67	8.67			8.67	8.67		
Tetradecane	kg/hr												9.97	9.97											9.97	9.97	9.97			9.97	9.97		
Tridecane	kg/hr												9.30	9.30											9.30	9.30	9.30			9.30	9.30		
Pentadecane	kg/hr					0.50	0.50	0.50	0.01	0.49	0.49	0.49	4.71	4.71			0.01		0.01						4.71	4.71	4.71			4.71	4.71	0.01	
Hexadecane	kg/hr	3.12		3.12	3.12	0.03	0.03	0.03		0.03	0.03	0.03	0.03	0.03											0.03	0.03	0.03			0.03	0.03		
Linoleic acid	kg/hr	87.47		87.47	87.47	1.75	1.75	1.75		1.75	1.75	1.75	1.75	1.75											1.75	1.75	1.75			1.75	1.75		
Ricinoleic acid	kg/hr	7.46		7.46	7.46	0.07	0.07	0.07		0.07	0.07	0.07	0.07	0.07											0.07	0.07	0.07			0.07	0.07		
Oleic acid	kg/hr	0.91		0.91	0.91	0.01	0.01	0.01		0.01	0.01	0.01	0.01	0.01											0.01	0.01	0.01			0.01	0.01		
Hexadecanoic acid	kg/hr	0.00				0.27	0.27	0.27		0.26	0.26	0.26																					
Stearic acid	kg/hr	1.04		1.04	1.04	0.01	0.01	0.01		0.01	0.01	0.01	0.01	0.01											0.01	0.01	0.01			0.01	0.01		

Table 4.21: Ni/ZSM-5 100kg/hr Summary of Feedstock and Final Products.

	Feedstock			Final Products			Waste Streams	
Compound	**Castor Oil**	**H2 Hydrotreating**	**H2 Hydrocracking**	**Gaseous C3-C7**	**Liquid C3-C7**	**Liquid C8-C15**	**Tail Gas**	**Waste Water**
Mass Flows(Kg/hr)	100.000	201.588	10.079	5.066	7.703	68.025	8.739	13.691
Mass Fractions								
Stearic Acid	1.036					0.02	0.00	
Heptane						0.60	1.18	
Octane						0.76	0.38	
Hydrogen		100.000	100.000	0.63				
Water				0.01			0.47	100.00
Propane				12.92	1.01		17.31	
Carbon Monoxide							7.43	
Carbon Dioxide							50.76	
Butane				27.73	6.28		12.25	
Pentane				31.25	20.06		6.22	
Hexane				20.98	40.45		2.38	
Heptane				6.47	32.20	3.26	0.87	
Octane						8.54	0.34	
Nonane						13.75	0.18	
Decane						10.64	0.05	
Undecane						11.69	0.02	
Dodecane						12.75	0.01	
Tetradecane						14.66		
Tridecane						13.67		
Pentadecane						6.92	0.13	
Linoleic acid	3.117					0.05		
Ricinoleic acid	87.472					2.57		
Oleic acid	7.460					0.11		
Hexadecanoic acid	0.915					0.01		
Hexadecane							0.03	

The results for the bio-jet fuel production for the 1000kg/hr of Ni/ZSM-5 Catalyst case are illustrated in Figure 4.9 and Tables 4.22 and 4.23 below.

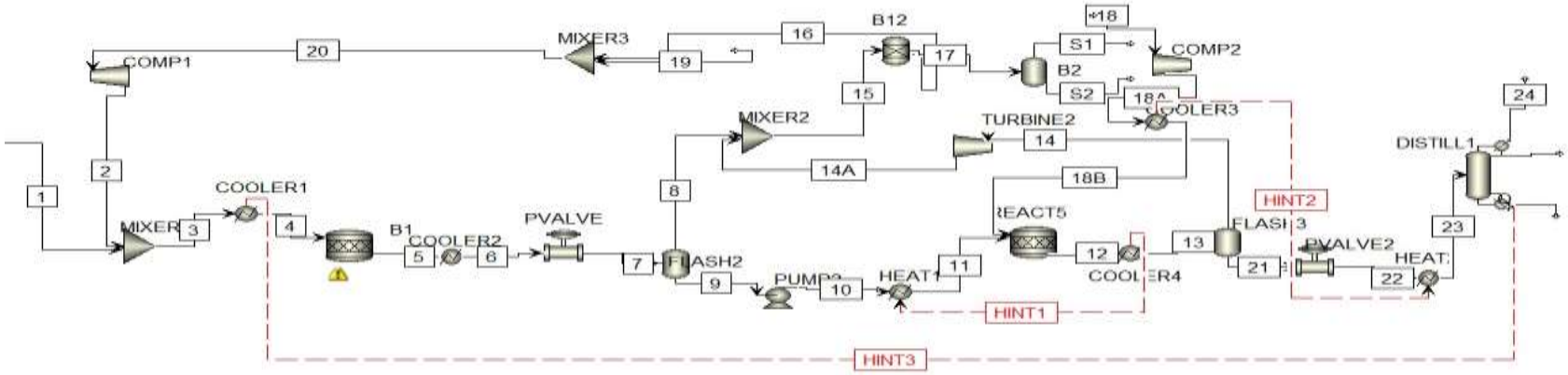


Figure 4.9 Bio-jet fuel production process.

Table 4.22 Case 3: Ni/ZSM-5 1000kg/hr Mass and Energy Balance.

Description	Units	1	2	3	4	5	6	7	8	9	10	11	12	13	14	14A	15	16	17	18	18A	18B	19	20	21	22	23	24	25	26	S1	S2	S3
Phase		Liquid	Vapor	Vapor	Vapor	Vapor		Vapor	Vapor	Liquid	Liquid	Liquid			Vapor		Vapor	Vapor		Vapor	Vapor	Vapor	Vapor	Vapor	Liquid			Vapor	Liquid	Liquid	Liquid	Vapor	Liquid
Temperature	C	25.00	493.42	482.06	300.00	300.00	20.00	18.56	20.00	20.00	23.91	342.49	300.00	25.00	25.00	-82.29	19.96	19.96	19.96	25.00	697.48	300.00	25.00	20.07	25.00	25.88	55.38	25.91	25.91	180.96	20.00	20.00	25.00
Pressure	bar	30.00	30.00	30.00	30.00	30.00	30.00	2.00	2.00	2.00	30.00	30.00	30.00	30.00	30.00	2.00	2.00	2.00	2.00	1.00	30.00	30.00	2.00	2.00	30.00	2.00	2.00	2.00	2.00	2.00	2.00	2.00	2.00
Mass Enthalpy	cal/gm	-755.15	1629.45	1395.30	812.50	789.41	-102.78	-102.78	-71.30	-478.54	-475.59	-269.49	-309.59	-513.22	-242.40	-480.19	-71.55	-16.98	-3054.18	0.10	2349.25	956.06	0.20	-16.60	-515.03	-515.03	-498.30	-525.63	-577.78	-411.11	-1079.46	-3828.79	-503.03
Mass Entropy	cal/gm-K	-2.27	-0.07	-0.26	-1.14	-1.06	-3.20	-0.79	-0.70	-1.78	-1.78	-1.32	-1.30	-1.76	-2.48	-1.95	-0.70	-0.73	-1.41	0.01	0.76	-1.08	-0.67	-0.73	-1.76	-1.75	-1.70	-1.46	-1.78	-1.52	0.54	-2.18	-1.76
Mass Density	gm/cc	1.52	0.00	0.00	0.00	0.00	0.00	0.00	0.00	0.77	0.77	0.55	0.10	0.34	0.00	0.00	0.00	0.00	0.01	0.00	0.00	0.00	0.00	0.00	0.72	0.20	0.11	0.00	0.62	0.61	0.00	0.96	0.74
Enthalpy Flow	cal/sec	-209764.51	4156928.31	3947163.80	2298473.21	2193922.07	-285637.01	-285637.01	-181611.92	-110993.28	-110307.62	-62506.80	-72673.59	-120473.82	-377.66	-748.13	-182360.04	-42367.85	-163901.61	0.29	6577.50	2676.80	11.44	-42356.41	-120096.15	-120096.15	-116195.45	-7055.18	-11674.74	-82038.87	-16321.76	-147577.72	-100380.91
Average MW		296.03	2.02	2.23	2.23	2.24	2.24	2.24	2.05	246.21	246.21	246.21	100.71	100.71	3.53	3.53	2.05	2.02	20.29	2.02	2.02	2.02	2.02	2.02	123.38	123.38	123.38	47.35	71.27	150.84	29.90	18.02	150.84
Mole Flows	kmol/hr	3.38	4555.85	4559.23	4559.23	4467.18	4467.18	4467.18	4463.79	3.39	3.39	3.39	8.39	8.39	1.59	1.59	4465.38	4455.85	9.52	5.00	5.00	5.00	100.00	4555.85	6.80	6.80	6.80	1.02	1.02	4.76	1.82	7.70	4.76
Mass Flows	kg/hr	1000.00	9184.05	10184.05	10184.05	10005.04	10005.04	10005.04	9170.05	834.99	834.99	834.99	845.07	845.07	5.61	5.61	9175.66	8982.47	193.19	10.08	10.08	10.08	201.59	9184.05	839.46	839.46	839.46	48.32	72.74	718.40	54.43	138.76	718.40
Component Mass flows																																	
Heptane	kg/hr					415.80	415.80	415.80	0.11	415.69	415.69	415.69	4.16	4.16			0.11		0.11						4.16	4.16	4.16			4.16	0.11		4.16
Octane	kg/hr					405.37	405.37	405.37	0.03	405.34	405.34	405.34	5.27	5.27			0.03		0.03						5.27	5.27	5.27			5.27	0.03		5.27
Hydrogen	kg/hr		9184.05	9184.05	9184.05	8979.38	8979.38	8979.38	8979.37	0.01	0.01	0.01	3.40	3.40	3.10	3.10	8982.47	8982.47	0.00	10.08	10.08	10.08	201.59	9184.05	0.30	0.30	0.30	0.30					
Water	kg/hr					139.21	139.21	139.21	139.06	0.14	0.14	0.14	0.14	0.14			139.06		139.06						0.14	0.14	0.14	0.06	0.08		0.31	138.76	
Propane	kg/hr					0.00	0.00	0.00	0.00	0.00	0.00	0.00	22.77	22.77	1.55	1.55	1.55		1.55						21.22	21.22	21.22	17.15	4.07		1.55		
Carbon Monoxide	kg/hr					6.52	6.52	6.52	6.52	0.00	0.00	0.00	0.00	0.00	0.00	0.00	6.52		6.52												6.51		
Carbon Dioxide	kg/hr					44.95	44.95	44.95	44.95	0.00	0.00	0.00	0.00	0.00	0.00	0.00	44.95		44.95												44.95		
Butane	kg/hr												30.02	30.02	0.60	0.60	0.60		0.60						29.42	29.42	29.42	17.39	12.02		0.60		
Pentane	kg/hr												37.26	37.26	0.23	0.23	0.23		0.23						37.03	37.03	37.03	10.24	26.79		0.23		
Hexane	kg/hr												44.50	44.50	0.08	0.08	0.08		0.08						44.42	44.42	44.42	3.17	29.78	11.47	0.08		11.47
Heptane	kg/hr												51.75	51.75	0.03	0.03	0.03		0.03						51.72	51.72	51.72			51.72	0.03		51.72
Octane	kg/hr												59.21	59.21	0.01	0.01	0.01		0.01						59.20	59.20	59.20			59.20	0.01		59.20
Nonane	kg/hr												95.04	95.04	0.01	0.01	0.01		0.01						95.03	95.03	95.03			95.03	0.01		95.03
Decane	kg/hr												73.48	73.48											73.48	73.48	73.48			73.48			73.48
Undecane	kg/hr												80.72	80.72											80.72	80.72	80.72			80.72			80.72
Dodecane	kg/hr												87.96	87.96											87.96	87.96	87.96			87.96			87.96
Tetradecane	kg/hr												101.14	101.14											101.14	101.14	101.14			101.14			101.14
Tridecane	kg/hr												94.35	94.35											94.35	94.35	94.35			94.35			94.35
Pentadecane	kg/hr					5.02	5.02	5.02	0.01	5.01	5.01	5.01	47.75	47.75			0.01		0.01						47.75	47.75	47.75			47.75	0.01		47.75
Hexadecane	kg/hr	31.17		31.17	31.17	0.22	0.22	0.22		0.22	0.22	0.22	0.22	0.22											0.22	0.22	0.22			0.22			0.22
Linoleic acid	kg/hr	874.72		874.72	874.72	5.25	5.25	5.25		5.25	5.25	5.25	5.25	5.25											5.25	5.25	5.25			5.25			5.25
Ricinoleic acid	kg/hr	74.60		74.60	74.60	0.52	0.52	0.52		0.52	0.52	0.52	0.52	0.52											0.52	0.52	0.52			0.52			0.52
Oleic acid	kg/hr	9.15		9.15	9.15	0.06	0.06	0.06		0.06	0.06	0.06	0.06	0.06											0.06	0.06	0.06			0.06			0.06
Hexadecanoic ac	kg/hr	0.00		0.00	0.00	2.67	2.67	2.67		2.67	2.67	2.67	0.03	0.03											0.03	0.03	0.03			0.03			0.03
Stearic acid	kg/hr	10.36		10.36	10.36	0.07	0.07	0.07		0.07	0.07	0.07	0.07	0.07											0.07	0.07	0.07			0.07			0.07

Table 4.23: Ni/ZSM-5 1000kg/hr Feedstock and Final Products.

	Feedstock			Final Products			Waste Streams	
Compound	**Castor Oil**	**H2 Hydrotreating**	**H2 Hydrocracking**	**Gaseous C3-C7**	**Liquid C3-C7**	**Liquid C8-C15**	**Tail Gas**	**Waste Water**
Mass Flow(kg/hr)	1000.000	201.588	10.079	46.916	72.564	720.403	54.062	138.758
Mass %								
Stearic Acid	1.036					0.010		
Heptane						0.577	0.196	
Octane						0.731	0.063	
Hydrogen		100.000	100.000	0.756	0.001		0.000	
Water				0.130	0.115		0.568	99.997
Propane				36.548	5.920		2.459	
Carbon Monoxide							12.046	0.003
Carbon Dioxide							83.139	
Butane				36.171	17.279		0.938	
Pentane				20.592	37.762		0.364	
Hexane				5.803	38.923	1.870	0.125	
Heptane						7.180	0.045	
Octane						8.218	0.017	
Nonane						13.191	0.009	
Decane						10.199	0.002	
Undecane						11.205	0.001	
Dodecane						12.210		
Tetradecane						14.039		
Tridecane						13.097		
Pentadecane						6.629	0.022	
Linoleic acid	3.117					0.030		
Ricinoleic acid	87.472					0.729		
Oleic acid	7.460					0.072		
Hexadecanoic acid	0.915					0.009		
Hexadecane						0.004	0.005	

4.2.4.2 Hydrogen Consumption

The material balance across the hydrotreating reactor shows a feed of 10kg/hr and unreacted hydrogen of 3.4 kg/hr in the product stream; a total of 6.68 kg/hr of hydrogen is consumed in the hydrotreating reactor. This consumption is twelve times the amount of hydrogen consumed in the 100kg/hr case of 0.546kg/hr.

Table 4.24: Material balance across the hydrocracking reactor for the 1000kg/hr Ni/ZSM-5 case.

Stream	**Hydrocarbons**	**Hydrogen**	**Products**
Mass Flows(kg/hr)	834.48	10.08	845.07
Stearic Acid			0.07
Heptadecane	415.692		4.16
Octadecane	405.340		5.27
Hydrogen	-	10.08	3.40
Water	-	-	0.15
Propane	-	-	22.77
Butane	-	-	30.02
Pentane	-	-	37.26
Hexane	-	-	44.50
Heptane	-	-	51.75
Octane	-	-	59.21
Nonane	-	-	95.04
Decane	-	-	73.48
Undecane	-	-	80.72
Dodecane	-	-	87.96
Tetra Decane	-	-	101.14
Tri decane	-	-	94.35
Pentadecane	5.005	-	47.75
Linoleic Acid	0.000	-	0.22
Ricinoleic Acid	5.248	-	5.25
Oleic Acid	0.522	-	0.52
Hexadecane	0.000	-	0.06
Hexadecanoic acid	2.672	-	0.03

For both the 100 kg/hr and the 1000 kg/hr case, the amount of hydrogen fed to the hydrocracking reactor was maintained the same at 10 kg/hr. The high consumption in

the 1000 kg/hr case results in less mass flow to the turbine of 5.19 kg/hr vs the 12 to.85 kg/hr as illustrated in Table 4.25 and Table 4.13, respectively.

4.2.5 Energy Efficiency

The Ni/ZSM-5 1000 kg/hr case with a fully developed flowsheet was used for the evaluation of energy efficiency optimisation; the principles are applicable to the other 100 kg/hr case. Due to the same amount of hydrogen used for the hydrotreating steps for both 100 and 1000 kg/hr cases, the compressor energy requirements remained the same, whilst the turbine power out was less than the compressor power, as illustrated in Table 4.25 below. There is less residual hydrogen for recycling to the hydrogen loop. The turbine recycles unreacted hydrogen and traces of hydrocarbons from the flash separator to the hydrogen loop for hydrogen recovery.

Table 4.25: Turbine and compressor for 1000 kg/hr Ni/ZSM-5.

Isentropic	**Turbine**	**Compressor**	
Phase calculations	Two phase	Vapor phase	
Indicated horsepower	-1.55	17.58	MW
Brake horsepower	-1.55	17.58	MW
Network required	-1.55	17.58	MW
Power loss	0.00	0.00	kW
Efficiency	0.72	0.72	
Mechanical efficiency	1.00	1.00	
Outlet pressure	2.00	30.00	bar
Outlet temperature	-82.29	493.42	°C
Isentropic outlet temperature	-114.89	361.12	°C
Vapor fraction	0.99	1.00	
Mass Flow kg/hr	5.60	9184	

4.2.5.1 Hydrotreating Pinch Analysis

The heat exchanger system for the hydrotreating section consists of two coolers due to the high outlet temperatures from the hydrogen recycle compressor. The compressor has a high outlet temperature of 493˚C; thermodynamically streams incur a high temperature after compression in the compressor. The reactor is set at 300˚C, and thus, cooling is required as part of feed preparation in Cooler 1; cooling is further required in Cooler 2 to

enable the cooling of the reactor products for flash separation. Table 4.26 below shows the hot streams in the hydrotreating section.

Table 4.26: Hot streams for the hydrotreating section.

Equipment	Stream Number	Stream type	Start Temperature (℃)	Target Temperature (℃)	Heat Duty(kW)
Cooler 1	3	Hot	482.0	300.0	-6902.7
Cooler 2	5	Hot	280	20.0	-10381.4

There is no cold stream in the hydrotreating section; there is integration with other streams, especially reboilers in the distillation columns. There is an overall 17MW cooling requirement that can be achieved using cooling water as a utility.

4.2.5.2 Hydrocracking Pinch Analysis

The hydrocracking section consists of 2 heaters and 2 coolers, excluding the distillation reboiler and condensers. These coolers and heat exchangers represent a set of cold and hot streams for pinch analysis. Pinch analysis will be done to ensure that the process is optimal from an energy efficiency point of view and to reduce the need for additional cooling capacity and additional heating capacity. Cooling would normally be provided from a cooling water stream, and heating from a steam supply. The process design for the cooling water and steam production system is not studied in detail in this study; however, it will be referred.

Shell and Tube exchangers are used throughout the process to facilitate heat optimisation and process integration. A list of cold and hot streams is displayed in the Table 4.27 below.

Table 4.27: Hot and Cold Stream temperatures.

Equipment	Stream Number	Stream type	Start Temperature (℃)	Target Temperature (℃)	Heat Duty (kW)
Cooler 4	12	Hot	300.0	25.0	-200.1
Cooler 3	18A	Hot	697.5	300.0	-16.3
Heat 1	10	Cold	24.0	300.0	200.1
Heat 2	22	Cold	26.0	60.0	16.3

From Table 4.27 above, Cooler 3 and Heat 2 require the same amount of duty for cooling and for heating, respectively. The approach temperatures between the two streams should also not be less than 10˚C, as is the case with the two streams. These streams are therefore integrated for heating and cooling with a net duty of 0kW, i.e. there will be no additional cooling or heating after the integration, which is a reduction in utility requirements. Figure 4.10 below shows the heat integration as HINT 2 in the process.

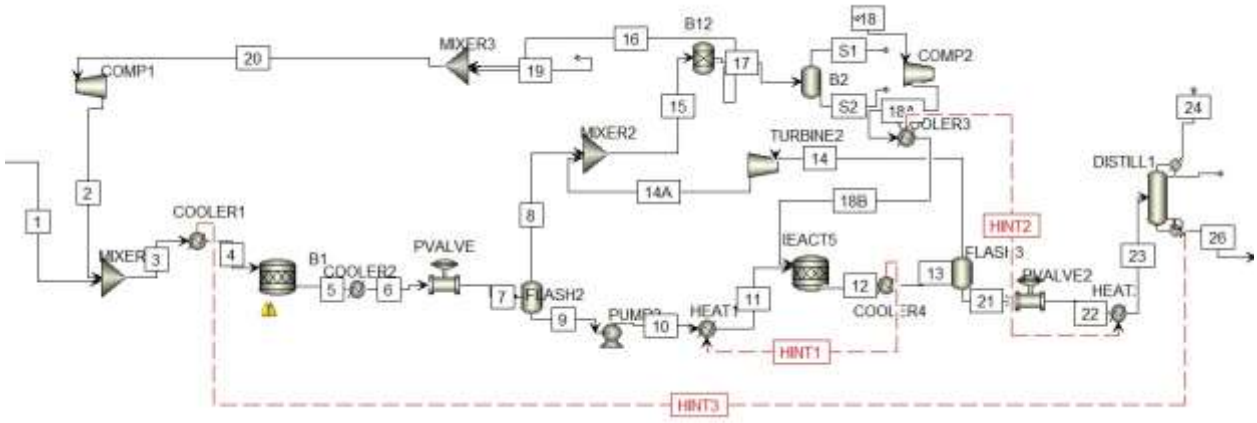


Figure 4.6: Heat integration illustrated on the Castor Oil Aspen Simulation.

Cooler 4 and Heat 1 will also be integrated, where Stream 12, a hot stream, will be cooled and Stream 10, a cold stream, will be heated. The cold stream is heated completely without additional need for utilities, i.e. steam. The hot stream is also cooled completely, as an integration of the two streams results in an overall net duty of 0kW. Without heat integration, 200kW was required for cooling through cooling water, and 200kW was also required from steam for heating purposes. Figure 4.10 shows the heat integration in the process as HINT 1.

4.2.5.3 Distillation Pinch

The main heat exchangers on the distillation column are the condenser and reboiler. The heat duties are presented in Table 4.28 below. Where the Reboiler requires 145.1kW of heat energy, which would normally come from steam, and the condenser requires -80.5kW of cooling from cooling water.

Table 4.28: Distillation Column cold and hot streams.

	Condenser	Reboiler
Outlet Temperature, ℃	25.9	180.9
Heat duty (kW)	-80.5	145.1

There are several ways of optimising the energy efficiency of a distillation column, which include reduction in reflux ratio, feed conditioning and side condensing or reboiling

(March, 1998). The column already has optimised products; for simplicity, the pinch was performed separately. The available duty from the upstream hydrotreating process is abundantly available for the reboiler. The Cooler1 in Table 4.26 has 6902kW of energy available for integration with the reboiler that requires 141.8kW, and the approach temperatures are compatible for a pinch integration by being above 10 degrees Celsius. Figure 4.6 demonstrates the heat integration as HINT3 in the process. Based on the results derived from HINT 1, 2, and 3, a total of 358 MW has been conserved due to the implementation of pinch technology energy efficiency measures.

4.2.5.4 Comparison to petroleum refining energy consumption

The heat integration through pinch for the hydrotreating and hydrocracking sections has optimised the process from an energy consumption perspective. The net energy requirement for the castor oil process remains the electrical energy for the hydrogen compressor in the hydrotreating section, which is 17.58MW(MJ/s) for the 1000kg/hr castor oil process. With the castor oil at 961kg/m^3, the volumetric flow rate is 6.55bbl/hr. energy density for the process is 9669.6MJ/barrel. The process is at a high level, and hydraulic equipment such as pumps, utility processes and housing amenities have not been considered in the estimation.

The petroleum refining process with hydrotreating, hydrocracking and distillation sections has an average energy density of 500MJ/bbl (Bergh, 2012). The energy density for the castor oil process seems higher than the conventional petroleum refining process. For the process to be renewable, sources of green hydrogen and other green electricity sources are recommended.

4.2.6 Distillation

There is a distillation column installed for the separation process of the final products. The Radfrac column separates the feed stream into gaseous stream, tops and bottom liquid streams. Appendix B contains details of the distillation profiles related to the separation process. The split fractions for the various components in the column are presented in Table 4.29 below.

Table 4.29 Split fractions in the Distillation column for the 100kg/hr Ni/ZSM-5.

	Stream	**Top -24**	**Top -25**	**Bottoms-26**
Component	Formula	Gaseous	Liquid	Liquid
Stearic Acid	$C_{18}H_{36}O_2$			1.00
Heptadecane	$C_{17}H_{36}$			1.00
Octadecane	$C_{18}H_{38}$			1.00
Hydrogen	H_2	1.00		
Water	H_2O	0.82	0.18	
Propane	C_3H_8	0.94	0.06	
Carbon dioxide	CO_2	0.98	0.02	
Butane	C_4H_{10}	0.85	0.15	
Pentane	C_5H_{12}	0.72	0.28	
Hexane	C_6H14	0.52	0.48	
Heptane	C_7H_{16}	0.32	0.68	
Octane	C_8H_{18}	0.10	0.48	0.42
Nonane	C_9H_{20}			1.00
Decane	$C_{10}H_{22}$			1.00
Undecane	$C_{11}H_{24}$			1.00
Dodecane	$C_{12}H_{26}$			1.00
Tetra Decane	$C_{14}H_{30}$			1.00
Tri decane	$C_{13}H_{28}$			1.00
Pentadecane	$C_{15}H_{32}$			1.00
Linoleic Acid	$C_{18}H_{32}O_2$			1.00
Ricinoleic Acid	$C_{18}H_{34}O_3$			1.00
Oleic Acid	$C_{18}H_{34}O_2$			1.00
Hexadecanoic acid	$C_{16}H_{32}O_2$			1.00
Hexadecane acid	$C_{16}H_{34}$			1.00

4.2.6.1 Product Streams

Stream 24: The gaseous stream contains residual hydrogen from the hydrocracking reaction, residual water, and residual Carbon Dioxide from the hydrocracking process. The flash separator removes the gases, i.e. hydrogen, water, and carbon dioxide, from the hydrocarbon stream before the distillation process. These components are preferentially directed towards the gaseous stream. 100%Hydrogen, 82% Water and 98% Carbon Dioxide. The hydrocarbon splits in the gaseous stream include light hydrocarbons, i.e. Propane(C_3H_8), Butane(C_4H_{10}) and Pentane(C_5H_{12}), with preferential split towards the gaseous stream, i.e. Propane 94%, Butane 85% and 72% Pentane, with residual components reporting to the Top liquid stream. Hexane(C_6H_{14}) indicates an almost equal split between the gaseous phase and the liquid phase, with 52% reporting to the gaseous stream.

Stream 25: The top distillate separates Heptane and Octane, with distribution ratios of 68% for Heptane and 48% for Octane. Octane is the one component represented in all the streams in the 10% Gas stream, the 48% top distillate and the 42% Bottoms products.

Stream 26: This stream represents Bio-jet fuel, containing heavy components from C8 to C15 in the final product pool. Table 4.30 below shows a comparison between the various Bio-jet fuels and the simulated Castor oil produced jet fuel.

Table 4.30: Bio-jet fuel product comparison.

Properties	Commercial Jet Fuel	Bio-jet Fuel I*	Bio-jet Fuel II**	Bio-jet Fuel **Castor Oil Simulation**
Density(g/cm3)	0.797	0.87	0.81	0.743
Carbon content(wt.%)	86.3	89.7	85.7	86.5
Hydrogen content(wt.%)	13.4	10.3	14.3	13.4
Total Oxygen(wt.%)	-	0.03	ud+	-
Total sulphur(wt.%)	0.04	ud	ud	-
Average carbon number	11.0	11.5	11.6	10.8
H/C (mol ratio)	1.98	1.4	1.9	2.17
Average molecular weight	C11H21	C11.5H15.7	C11.9H21.9	C10.8H23.4

The jet fuel is comparable to the commercial jet fuel as tabulated concerning the density (0.743 vs 0.797), the carbon content wt.% (86.5 vs 86.3), Hydrogen content wt.% of 13.4%.

Hydrotreating removes both oxygen and sulphur. Although this simulation does not address sulphur removal, it also occurs during the hydrotreating step. Hydrotreating involves the saturation of olefins for a particular petroleum feed as well as the removal of sulphur, nitrogen, and other impurities (Gary, et al., 2007). Biofuel feedstock typically has low levels of sulphur and nitrogen but contains a significant amount of oxygen that must be removed. Therefore, the focus for hydrotreating was on Hydrodesulphurisation (HDS) or Hydrodenitrogenation (HDN), but on Hydrodeoxygenation (HDO) (Molefe, et al., 2019)

The molecular weight for the castor oil jet fuel is C10.8H23, which is also closely related to the commercial jet fuel of C11H21.

4.2.7 Bio-gasoline production process.

Optimising the separation section of the Bio-jet production process enables Bio-gasoline production. The hydrocracking reactor produces a varied range of Hydrocarbons from C3-C16. The Bio-gasoline is composed of C4 to C12 components, as illustrated in Table 4.24. Consequently, different distillation optimisations can be executed to ascertain the product slate to produce either Bio-jet fuel or Bio-Gasoline. Bio-jet fuel composition includes C7 to C15 components. A second distillation column is added to the bio-jet fuel process to produce Bio-gasoline, as shown in Figure 4.11 below.

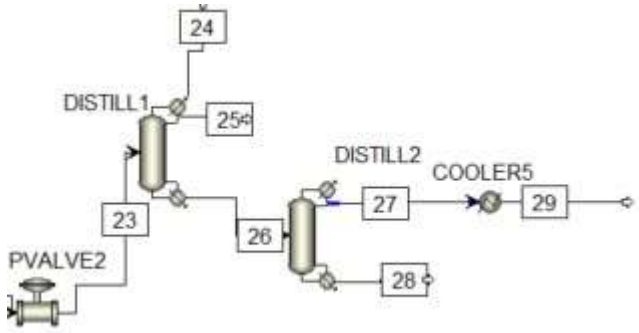


Figure 4.11: Separation process of the Bio-jet/ Bio-gasoline fuel.

The following optimisation steps were implemented on the bio-jet fuel process to achieve Bio-gasoline production:

- The feed temperature into the Distillation column was reduced from 60˚C to 25˚C, which resulted in the removal of Heat 2, a heater which was installed before the Distillation 1 separation process.
- The distillate to feed ratio was reduced from 0.3 to 0.1 as shown in Figure 4.12 below.

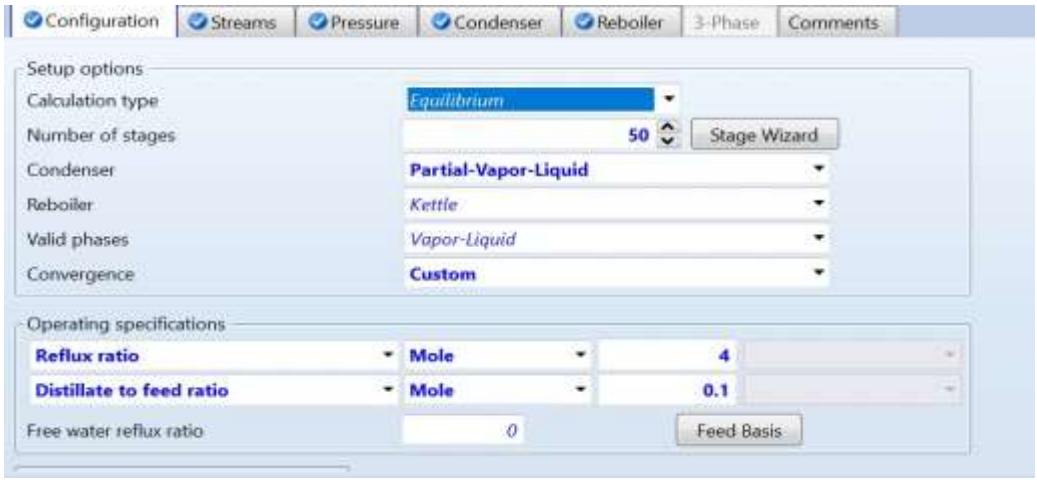


Figure 4.12: Distillation 1 column specification.

- The final distillation column is installed with specifications as listed in Figure 4.13 below.

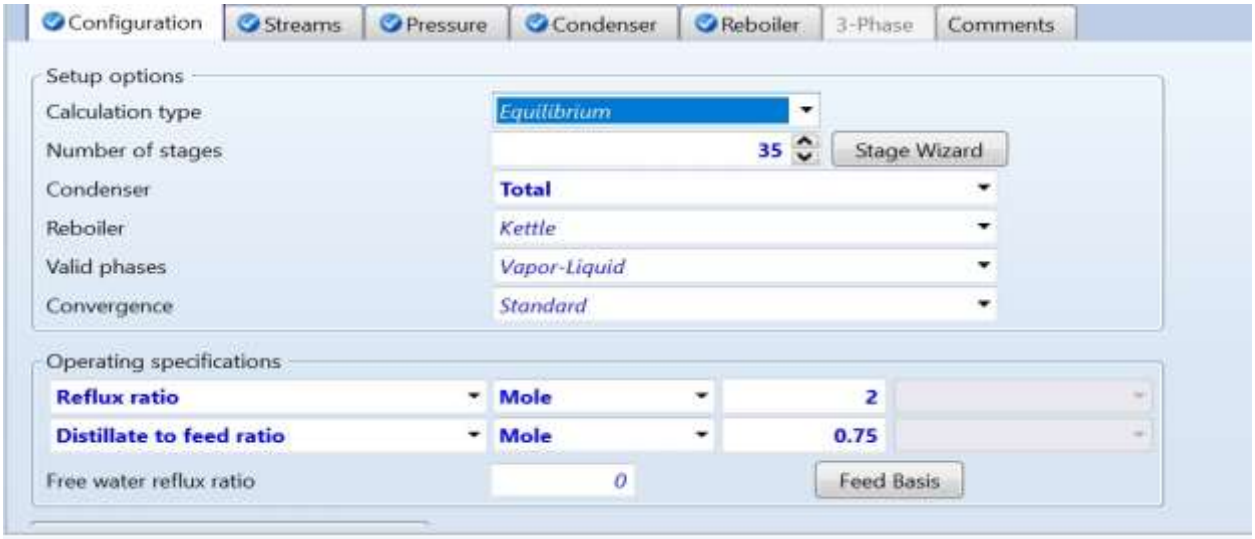


Figure 4.13: Distillation 2, second and final distillation column specifications.

The results for the separation process, as shown in Figure 4.11, are displayed in Table 4.33 below.

Table 4.33: Results for Bio-gasoline Production as illustrated in Figure 4.11.

	Stream	**23**	**24**	**25**	**26**	**27**	**28**
Phase	Units		Vapor Phase	Liquid Phase	Liquid Phase	Liquid Phase	Liquid Phase
Temperature	C	26.04	-41.95	-41.95	102.97	60.00	273.90
Pressure	bar	2.00	2.00	2.00	2.00	2.00	2.00
Mass Liquid Fraction		0.99	0.00	1.00	1.00	1.00	1.00
Molar Enthalpy	cal/mol	-63246.02	-12981.22	-31098.28	-62322.67	-56822.62	-64985.69
Mass Enthalpy	cal/gm	-516.71	-575.47	-691.53	-471.25	-508.80	-335.04
Molar Density	mol/cc	0.00	0.00	0.01	0.01	0.01	0.00
Mass Density	gm/cc	0.18	0.00	0.59	0.66	0.67	0.56
Enthalpy Flow	cal/sec	-120640.19	-1238.07	-2965.96	-106991.04	-73161.71	-27890.68
Average MW		122.40	22.56	44.97	132.25	111.68	193.96
Mole Flows	kmol/hr	6.87	0.34	0.34	6.18	4.64	1.55
Mass Flows	kg/hr	840.52	7.75	15.44	817.34	517.65	299.68
Mass Fractions							
Heptadecane		0.005			0.005		0.014
Octadecane		0.006			0.006		0.018
Hydrogen		0.000	0.046				
Water		0.001			0.001	0.001	
Propane		0.026	0.941	0.917			
Butane		0.035	0.013	0.083	0.034	0.054	
Pentane		0.044			0.045	0.072	
Hexane		0.053			0.054	0.086	
Heptane		0.062			0.063	0.100	
Octane		0.070			0.072	0.114	
Nonane		0.113			0.116	0.184	
Decane		0.087			0.090	0.142	
Undecane		0.096			0.099	0.156	
Dodecane		0.105			0.108	0.091	0.136
Tetra Decane		0.120			0.124		0.338
Tri decane		0.112			0.115		0.315
Pentadecane		0.057			0.058		0.159
Linoleic acid							0.001
Ricinoleic acid		0.006			0.006		0.018
Oleic acid		0.001			0.001		0.002

Final Product streams are discussed below:

- **Stream 27(Bio-gasoline):** The Bio-gasoline is represented in Stream 27, which contains hydrocarbons C4 to C12, which is a typical bio-gasoline composition as displayed in Table 2.4. The density of the stream is 0.67 as compared to 0.77g/mL at 288K. The difference in density can be attributed to the temperature difference, with Stream 27 currently at 60˚C(333K). The final product is cooled down to a final temperature of 288K, and the density is 0.7. The stream does not contain any oxygen, as expected for the thermal stability of the fuel. This steam is 518kg/hr, representing 62% of the feed to the distillation process and 51.8%of the Castor Oil feed.

- **Stream 28**: The bottom's product contains C12-15 products, with the Bio-gasoline stream produced as the distillate product. The stream has a specific gravity of 0.56, which is lighter than the expected 0.78 for a diesel product. Green diesel produced contains the range of C17-C18 alkanes. The bio-jet fuel specific gravity is also heavier at 0.81**.** The stream can be recycled to the hydrocracking reactor for further cracking to produce more C4 to C12 products and to maximise the Bio-gasoline production rate. This stream is 299kg/hr, representing 36% of feed to the distillation process(840kg/hr) and 30 of % Castor oil feed.

- **Stream 24 and Stream 25:** Streams 24 and 25 contain high percentages (94% and 91%) of Propane with traces of Butane, with Stream 24 being Gas phase and Stream 25 being a Liquid. Traces of Hydrogen also appear in the gaseous Stream 24 at 4.6% of the mass flow. The combined mass flow rate of the two streams is 23kg/hr, which is 2% of the Castor Oil feed to the process. The observed properties in these streams can allow the usage of the products as Petroleum Gas and Liquefied Petroleum Gas. According to (Testbook, 2023), the main components of liquefied petroleum gas, or LPG, are Propane, Butane, Isobutane, Butylene, Propylene, and combinations of these gases. Natural gas processing and crude oil refining are used to create the components of LPG gas. Under normal pressure and temperature, they are a liquid and a gas, respectively. LPG percentage composition is 100% Propane, 60% Propane and 40% Butane, or 35% Propane and 65% Butane.

Chapter 5: Conclusions

The research aimed to develop a process simulation for the pilot-scale production of green diesel, bio-jet fuel and bio-gasoline from castor oil using hydrotreating and hydrocracking in the presence of catalysts such as alumina and nickel-based composites. Green diesel was synthesised by hydrotreating castor oil under conditions of 345˚C and 30 bar using an Alumina catalyst, and at 300˚C and 30 bar with a NiSapo-11 catalyst. Bio-jet fuel and bio-gasoline were produced through the hydrocracking process with Alumina at 240˚C and 60bar and Ni/ZSM-5 catalyst at 300˚C and 30bar. The process simulation for biofuels production from castor oil was developed in Aspen Plus Version 14. Process flowsheets for the development of these processes are available and converged.

The simulation was performed for castor oil flow rates at 100kg/hr and 1000kg/hr. From the results obtained, the process flowsheets are similar with slight differences due to the conversion rates, and for both catalysts, being similar and stoichiometric reactors were used for modelling. Thus, the conversion of the castor oil was applied in the reactor/s based on the catalyst employed. The impact of scaling through increasing castor oil mass flow rates from 100kg/hr to 1000kg/hr showed no variation in product quality. The pilot-scale production of biofuels from castor was scaled up without major variations in product quality and yields.

The energy efficiency of the process was optimised using the pinch technology. A total of 358MW was saved through heat integration. The process of biofuels production uses hydrogen as feedstock for both hydrotreating and hydrocracking reactors. From the results obtained, the compression of hydrogen is the major energy consumption in the process, with both hydrotreating and hydrocracking processes occurring at high pressures. The hydrogen used was recycled in the loop to recover unreacted hydrogen and make-up for consumption only. The hydrogen for the hydrocracking section has different compressors due to the need to operate at different pressures for the hydrotreating and hydrocracking sections. A turbine was installed to recover the unreacted hydrogen in the hydrocracking section, which is also a recovery of energy through electricity generation.

Chapter 6: Recommendations

The biofuels production process from castor oil is recommended for fuel production for environmental impact as well as economic development in Africa. There is a choice to produce Green Diesel, Bio-jet Fuel or Bio-gasoline, and the plant can be established at various feed flows of castor oil. The extra benefit of Liquid Petroleum Gas is an added benefit to the entrepreneur who seeks to maximise profits and yields from the castor oil production process. It is recommended that the flowsheets be used for further equipment sizing and business development purposes, feasibility studies and funding applications for entrepreneurs.

The further process improvements to be performed to the flowsheet include quantifying the utility requirements for the process, i.e. steam, cooling, water and electricity. The waste management strategy can also be further developed to responsibly manage emissions from the process, especially carbon dioxide. The use of carbon capture and storage technology can be explored to reduce carbon dioxide emissions to zero.

A collaboration with the agricultural sector is recommended to produce castor oil feedstock to feed the process plants for fuel production from castor oil. At large castor oil feed rates, a large feedstock will be required to maintain the demand for the process plant. It is yet another opportunity to create jobs and economic development in the agricultural sector. The cultivation of land to grow castor oil seeds and, extraction of castor oil from the seeds are enablers for the success of biofuels production from castor oil.

Alternative feedstock, such as waste cooking oil, can be studied as a variation to castor oil to maximise the use of the process plant in cases of feedstock limitations. For applications in other regions, alternative crops such as Jatropha can also be explored as an alternative feedstock for the process.

References

Amigun, B., Muller-Langer, F., Weber, M. & von Blottnitz, H., 2008. Predicting the costs of biodiesel production in Africa: learning from Germany. *Energy for Sustainable Development,* Volume 12, pp. 31-47.

Amigun, B., Musango, J. & Stafford, W., 2010. Biofuels and sustainability in Africa. *Renewable and Sustainable Energy Reviews,* Volume 1156, p. 13.

Atlas, W. D., 2022. *Knoema.* [Online]
Available at: https://knoema.com/atlas/South-Africa/topics/Energy/Oil [Accessed 26 May 2023].

Baroutian, S., Aroua, M. & Raman, A., 2010. Viscosities and densities of binary and ternary blends of palm oil, palm biodiesel, and diesel fuel at various temperatures. *Journal of Chemical and Engineering Data,* 55(1), pp. 504-507.

D.S., O., 2005. Castor Oil: A vital industrial raw material.

Dermibas, A., Bafail, A., Ahmad, W. & Sheikh, M., 2016. Biodiesel production from non-edible plant oils. *Energy Exploration & Exploitation,* 34(2), pp. 290-318.

Dermibas, A. et al., 2015. Octane rating of gasoline and octane booster additives. *Petroleum Science and Technology,* 33(11), pp. 1190-1197.

Dermirbas, A., 2003. Biodiesel fuels from vegetable oils via catalytic and non-catalytic supercritical alcohol transesterifications and other methods: a survey. *Energy Convers. Manage,* Volume 44, pp. 20932109.

De, S. & Luque, R., 2014. Upgrading of waste oils into transportation fuels using hydrotreating technologies. *Biofuel Research journal,* 4(1), pp. 107-109.

Douvartzides, S., Charisiou, N., Papageridis, K. & Goula, M., 2019. Green Diesel: Biomass Feedstocks, Production technologies, Catalytic research, Fuel Properties and Performance in compression ignition internal combustion engines. *Energies,* 12(809).

Forero, C., 2004. *Biodiesel from castor oil: A promising fuel for cold weather.,* Columbia: Santander University.

Gary, J., Handwerk, G. & Kaiser, M., 2007. Petroleum refining technology and economics. *CRC Press,* Volume 5th Edition.

Gutierrez-Antonio, C., Gomez-Castro, F. & Segovia-Hernandez, J., 2013. *Simulation and optimisation of a bio-jet fuel production process.* Lappeenranta, Finland, Elsevier.

Hoekman, S. et al., 2012. Review of biodiesel composition, properties, and specifications. *Renewable and Sustainable Energy Reviews,* Volume 16, pp. 143-169.

J.J., W., 1993. Genetic Improvement and commercialisation of the African perennial castor (Ricinus communis) plant. *Zimbabwe Sci.News,* Volume 27, pp. 42-45.

Kaur, R. & Bhaskar, T., 2020. Potential of castor plant (Ricinus communis) for production of biofuels, chemicals and value-added products. *Elsevier,* pp. 269-310.

Kiri-Othmer, 1979. *Encyclopaedia of Chemical Technology,* Volume 5.

Klerk, A., 2011. Fischer-Tropsch Refining. *Wiley-VCH Verlag&Co.*

Kubicka, D. & Tukac, V., 2013. Hydrotreating of Triglyceride-based Feedstocks in Refineries. *Advances in Chemical Engineering,* Volume 42, pp. 141-194.

Laura, M., David, A., Sanchez, L. & Rios, L., 2017. Second-generation green diesel from castor oil: Development of a new and efficient continuous-production process. *Chemical Engineering Journal,* Volume 322, pp. 149-156.

Linganiso, E. et al., 2022. Biodiesel production from waste oils: A South African outlook. *Sustainability,* Issue 14.

Liu, S. et al., 2015. Bio-aviation fuel production from hydro processing of castor oil promoted by the nickel-based bifunctional catalysts. *Bioresource Technology,* Volume 183, pp. 93-100.

Lovas, P., Hudec, P., Hadvinova, M. & Haz, A., 2015. Conversion of rapeseed oil via catalytic cracking: effect of the ZSM-5 catalyst on the deoxygenation process. *Fuel Process Technology,* Volume 134, pp. 223-230.

Ma, F. & Hanna, M., 1999. Biodiesel production: a review. *Bioresource Technology,* Volume 70, pp. 1-15.

McCall, M. et al., 2011. *Production of aviation fuel from renewable feedstocks.* United States, Patent No. US 8,039,682 B2.

Mohammad, M., Hari, T., Yaako, Z. Y. & Sopian, K., 2013. Overview on the production of paraffin-based biofuels via catalytic hydrodeoxygenation. *Renewable Sustainable Energy,* 22(1), pp. 121-132.

Molefe, M., Diakanua, N. & Hembe, E., 2019. Method selection for Bio-jet and Bio-gasoline Fuel Production from Castor Oil: A Review. *Energy & Fuels,* Volume 33, pp. 5918-5932.

Murzin, D., 2013. Hydrotreating of triglyceride-based feedstocks in refineries. In Advances in Chemical Engineering. *Academic Press: London,* Volume 42, pp. 141-194.

Navale, P. et al., 2011. *Review of vegetable oil as an alternative fuel for internal combustion engines.* Mumbai, Fr.C. Rodrigues Institute of Technology.

Navale, P. et al., 2011. *Review of Vegetable Oil as an Alternative Fuel for Internal Combustion Engine (CI).* Mumbai, India, Research Gate.

Ogunniyi, D., 2005. Castor Oil: A Vital Industrial Raw Material. *Pak.J. Sci.Ind.Res. Res,* Volume 48, pp. 143-148.

Oluwe, F., Abdulrahim, A., Aviara, N. & Ndahi, N., 2012. Traditional Method of Extracting Castor Oil. *Continent.J.Eng.Sci.,* 7(3), pp. 6-10.

Ong & Bhatia, 2010. The current status and perspectives of biofuel production via catalytic cracking of edible and non-edible oils. *Energy,* 35(1), pp. 111-119.

Osorio-Gonzalez, C. et al., 2020. Production of Biodiesel from Castor Oil: A Review. *Energies,* 13(2467).

Rajagopal, D., 2007. *Rethinking current strategies for biofuel production in India.* Hyderabad, India, IWMI.

Rodionova, M., 2017. *Review article Biofuel production: Challenges and opportunities.* s.l., Science Direct.

Sebos, I., Matsoukas, A., Apostolopoulos, V. & Papayannakos, N., 2009. Catalytic hydrocracking of cottonseed oil in petroleum diesel mixtures for the production of renewable diesel. *Fuel,* Volume 88, pp. 144-149.

Shrirame, H., Panwar, N. & Bamniya, B., 2011. Biodiesel from Castor Oil- A Green Energy Option. *LCE,* 2(1), pp. 1-6.

Shrirame, H., Panwar, N. & Bamniya, B., 2011. Diesel from Castor Oil - A Green Energy Option. *LCE,* 2(1), pp. 1-6.

Sotelo-Boyas, R., Trejo-Zarraga, F. & Hernandez-Loyo, F., 2012. Hydro conversion of triglycerides into green liquid fuels. *Intech Open,* Volume 1.

Szeto, W. & Leung, D., 2022. Is hydrotreated vegetable oil a superior substitute for fossil diesel? A comprehensive review on physicochemical properties, engine performance and emissions. *Fuel,* Volume 327.

Taufiqurrahmi & Bhatia, 2011. Catalytic cracking of edible and non-edible oils for the production of biofuels. *Energy Environmental Science,* Volume 4, pp. 1087-1112.

Tvaronaviciene, M., 2021. *Effects of climate change on environmental sustainability.* Silo, E3SWeb of Conferences 250.

UNIDO, 2009. *Round Table Towards Sustainable Biofuels in Africa.* Vienna, United Nations Industrial Development Organisation.

Veza, I., Said, M. & Latiff, Z., 2019. Progress of acetone-butanol-ethanol (ABE) as biofuel in gasoline and diesel engines: A review. *Fuel Processing Technology,* Volume 196.

Visagie, E. & Prasad, G., 2006. *Renewable energy technologies for poverty alleviation,* Cape Town: s.n.

Woodend, J., 1993. Genetic improvement and commercialisation of the African perennial castor (Ricinus communis) plant. *Zimbabwe Sci. News,* Volume 27, pp. 42-45.

Wu, X. et al., 2016. Production of bio-jet fuels by catalytic transformation of triglyceride-based oils. *Fuel,* 16(2361).

Zhang, A. et al., 2020. *Preparation of Biodiesel based on Alkaline Ionic Liquid.* s.l., IOP.

Appendix A: Catalysis research on hydrotreating of vegetable oils, waste cooking oil

Catalyst Reactor	Reactor	Oil	H2/Oil Ratio	T(°C)	Pressure(bar)	LHSV ()	Duration(hr)	Conversion (%)	Selectivity among oil product(wt.%)	Main product
Ni/Al2O3	Continuous	Rapeseed	50	260–280	35	0.25–4	n.a.	98	59 (C17)	C17 (zero C18)
Mo/Al2O3	Continuous	Rapeseed	50	260–280	35	0.25–4	n.a.	100	82 (C18)	C18 (only 2 wt.% C17)
Ni–Mo/Al2O3	Continuous	Rapeseed	50	260–280	35	0.25–4	n.a.	100	94 (C17 and C18)	C15–C18 (C17/C18 = 0.36)
Ni–Mo/Al2O3	Continuous	Rapeseed	250	340	40	1	n.a.	n.a.	91.64 (C15–C18)	C15–C18(C17/C18 = 1.32)
Ni–Mo/Al2O3	Batch	Rapeseed	n.a.	350	80	n.a.	3	n.a.	70 (C15–C18)	C15–C18 (C17/C18 = 1.63)
Ni–Mo/Al2O3	Continuous	Rapeseed	100	310	70	1.5	n.a.	100	>90 (C17 and C18)	C17–C18 (C17/C18 = 0.25)
Ni–Mo/MCM-41	Continuous	Rapeseed	100	310	70	1.5	n.a.	100	>90 (C17 and C18)	C17–C18 (C17/C18 = 0.5)
Ni–Mo/OMA	Continuous	Rapeseed	100	310	70	1.5	n.a.	100	>90 (C17 and C18)	C17–C18 (C17/C18 = 0.07)
Pt/HZSM-5	Batch	Rapeseed	n.a.	380	110	n.a.	3	n.a.	43 (C5–C12)	Gasoline (C5–C12)
FCC equilibrium catalyst	Continuous	Rapeseed	n.a.	525	1	n.a.	n.a.	n.a.	15.7 (C12–C20)	Gasoline (C5–C12) 32.4 wt.%
FCC-ZSM-5	Continuous 2	Rapeseed	n.a.	525	1	n.a.	n.a.	n.a.	13.2 (C12–C20)	Gasoline (C5–C12) 32.3 wt.%
Ni–Mo/Al2O3	Continuous	Palm	n.a.	350	40	2	n.a.	n.a.	80(C15–C18)	C15-C18(C17/C18 = 0.58)
Ni–Mo/Al2O3	Continuous	Palm	250	350	45	0.6	n.a.	n.a.	92.69 (C15–C18)	C15–C18 (C17/C18 = 0.78)
Ni–Mo/zeolite	Batch	Palm	n.a.	300–320	1	n.a.	n.a.	n.a.	47.24 (C15–C19)	C15–C19 and 52.76% C8–C13
MCM-41		Palm	n.a.	450	1	2.5	n.a.	n.a.	26 (Diesel)	Also, gasoline 23.9% and kerosene 13 wt.%
Al–MCM-41	Continuous	Palm	n.a.	450	1	2.5	n.a.	n.a.	11.2–20.3 (Diesel)	Gasoline 30.1–31.7% and kerosene 10.6–20.7 wt.%
Ni–Mo/Al2O3	Batch	Soybean	n.a.	400	92	n.a.	2	92.9	64.45 (C15–C18)	C15–C18 (C17/C18 = 2.49)
Pd/Al2O3	Batch	Soybean	n.a.	400	92	n.a.	2	91.9	79.22 (C15–C18)	C15–C18 (C17/C18 = 11.9)
Co–Mo/Al2O3	Batch	Soybean	n.a.	400	92	n.a.	2	78.9	33.67 (C15–C18)	C15–C18 (C17/C18 = 2.16)
Ni/Al2O3-SiO2	Batch	Soybean	n.a.	400	92	n.a.	2	60.8	39.24 (C15–C18)	C15–C18 (C17/C18 = 29.3))
Pt/Al2O3	Batch	Soybean	n.a.	400	92	n.a.	2	50.8	37.71 (C15–C18)	C15–C18 (C17/C18 = 0.92)
Ru/Al2O3	Batch	Soybean	n.a.	400	92	n.a.	2	39.7	32.00 (C15–C18)	C15–C18 (C17/C18 = 39.6)
Ni/Al2O3	Batch	Soybean	n.a.	350	6.9	n.a.	4	68	51.20 (>C18)	>C18
Ni–Al/LDH	Batch	Soybean	n.a.	350	6.9	n.a.	4	74	52.90 (C8–C17)	C8–C17
Ni–Mg–Al/LDH	Batch	Soybean	n.a.	350	6.9	n.a.	4	49	54.1 (>C18)	>C18
Mg–Al/LDH	Batch	Soybean	n.a.	350	6.9	n.a.	4	72	47.80 (C8–C17)	C8–C17
Co–Mo/Al2O3	Continuous	Sunflower	450	340–350	50–80	1	n.a.	94.0–99.8	63.1–71.5	91 cetane number Diesel
Co–Mo/Al2O3	Continuous	Sunflower	500–600	380	40–60	1	n.a.	100	83.1–89.2	C15–C18 (C17/C18 = 0.15)
Ni–Mo/Al2O3	Continuous	Sunflower	450	340–350	50–80	1	n.a.	81.8–97.4	42.0–51.9	92 cetane number Diesel fuel
Ni–Mo/	Al2O3	Continuous	Sunflower	500	350	45	0.8	n.a.	n.a.	86.59 (C15–C18)
Ni–W/Al2O3	Continuous	Sunflower	450	340–350	50–80	1	n.a.	86.7–95.6	39.4–49.3	91 cetane number Diesel fuel
Ni–Mo/Al2O3-F	Continuous	Sunflower	500	350–370	20–40	1	n.a.	91–96	73.2–75.6	C15–C18, of which 37–38% isomers
Pd/SAPO-31	Continuous	Sunflower	1000	310–350	20	0.9–1.6	n.a.	n.a.	83.4–100	nSH 1 and iSH 1, of which 46.8–90.7% C17 and C18
V2O5/ -Al2O3	Batch	Sunflower	n.a.	355	1	n.a.	0.66	92.1	48 (Heavy Diesel)	Also, about 23% gasoline and 4% kerosene
V2O5/ -Al2O3	Batch	Sunflower	n.a.	390	1	n.a.	0.5	85	68 (b.p > 200 °C)	Liquid oil products with a boiling point > 200 °C 11
Co3O4/ -Al2O3	Batch	Sunflower	n.a.	390	1	n.a.	0.5	68	60(b.p > 200 °C)	Liquid oil products with a boiling point > 200 °C
KOH/ -Al2O3	Batch	Sunflower	n.a.	390	1	n.a.	0.5	65	53 (b.p > 200°C)	Liquid oil products with a boiling point > 200 °C°C
MoO3/ -Al2O3	Batch	Sunflower	n.a.	390	1	n.a.	0.5	56	59 (b.p > 200 °C)	Liquid oil products with a boiling point > 200 °C
NiO/ -Al2O3	Batch	Sunflower	n.a.	390	1	n.a.	0.5	66	57 (b.p > 200 °C)	Liquid oil products with a boiling point > 200 °C
ZnO/ -Al2O3	Batch	Sunflower	n.a.	390	1	n.a.	0.5	84	70 (b.p > 200 °C)	Liquid oil products with a boiling point > 200 °C
Ni–Mo/Al2O3	Continuous	Jatropha	800	350	40	7.6	n.a.	100	97.2 (C11–C20)	C11–C20 (iSH/nSH 1 = 0.08)
Ni–Mo/SiO2	Continuous	Jatropha	800	350	40	7.6	n.a.	100	99.1 (C11–C20)	C11–C20 (iSH/nSH 1 = 0.03)
Ni–Mo/Al2O3-SiO2	Continuous	Jatropha	800	350	40	7.6	n.a.	100	89.6 (C11–C20)	C11–C20 and also 9.8 wt.% C5–C10 (iSH/nSH 1 = 0.26)
Ni–Mo/H-Y	Continuous	Jatropha	800	350	40	7.6	n.a.	100	50.9 (C11–C20)	C11–C20 and also 48.9 wt.% C5–C10 (iSH/nSH 1 = 0.87)
Ni–Mo/H-ZSM-5	Continuous	Jatropha	800	350	40	7.6	n.a.	100	22.1 (C11–C20)	Also 77.8 wt.% C5–C10 (iSH/nSH 1 = 1.21)
Ni–HPW(30%)/nHA	Continuous	Jatropha	600	360	30	2	n.a.	100	83.4	[(C15 + C17)/(C16 + C18)] = 4.4, (iSH/nSH

Appendix B: Distillation profiles

The column consists of 50 stages, with the feed stage at stage 15. The temperature profile in Figure A.1 shows a top stage temperature of 95˚C and a bottom temperature of 215˚C. The feed stream at stage 15 shows a cooling effect with a drop in temperature from 160˚C to 140˚C. The feed stream to the column is at 60˚C, which explains the cooling effect on the temperature profile.

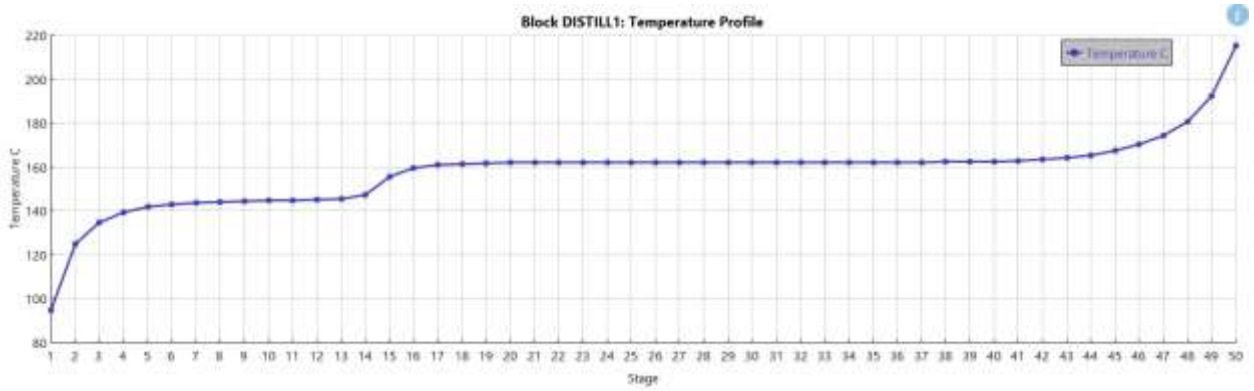


Figure A.1: Temperature profile in the distillation column.

The column condenser performance is illustrated in Table A. 1 below, with a reflux ratio of 4 and a distillate to feed ratio of 0.30.

Table A.1: Condenser/Top Stage Performance.

Name	Value	Units
Temperature	94.93	C
Heat duty	-302.06	cal/sec
Distillate rate	0.03	kmol/hr
Reflux rate	0.11	kmol/hr
Reflux ratio	4.00	
Distillate to feed ratio	0.30	

The column reboiler info is in Table A.2 below, indicating a boil-up ratio of 3.00 and a bottoms-to-feed ratio of 0.70.

Table A.2: Reboiler/Bottom stage performance.

Name	Value	Units
Temperature	215.46	C
Heat duty	608.57	cal/sec
Bottoms rate	0.06	kmol/hr
Boil-up rate	0.19	kmol/hr
Boil-up ratio	3.00	
Bottoms to feed ratio	0.70	

The liquid mass fraction of Octane is the highest of all components throughout the column profile as indicated in Figure A.2 below. Octane shows an almost equal (48/42) split between the bottoms and the top distillate product as presented in Table A.2 above.

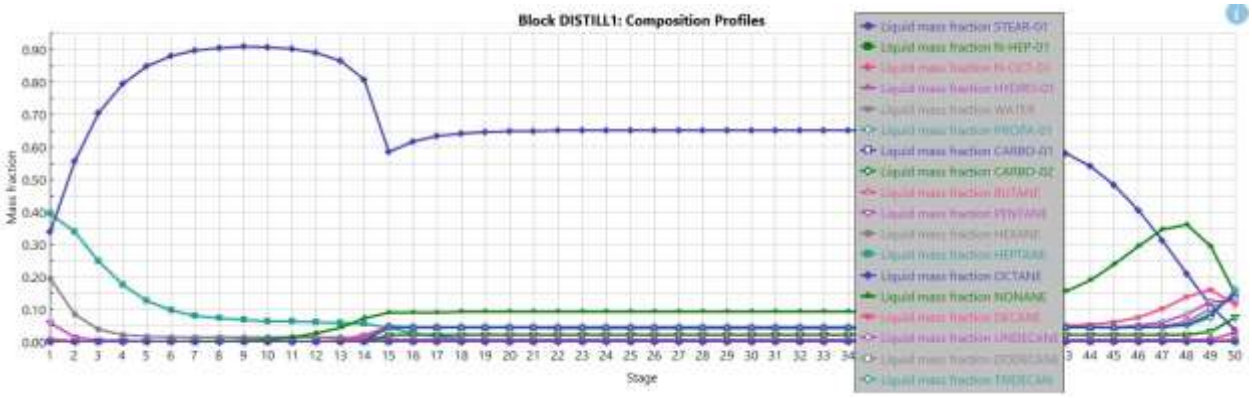


Figure A.2: Liquid mass composition profiles in the distillation column.

In the top stages, liquid heptane is the second most present, the split towards the bottoms stream was higher than all the other components at 68% vs the top at 32%. Heptane is then followed by hexane as the most present component in the bottom product.

In the bottom stages, nonane is the second most present component, followed by decane. Although octane is present throughout the column, towards the bottom, nonane and decane exceed the octane presence. Both components have a 100% preferential split towards the bottom's product.

The partial vapour-liquid condenser was used for the simulation, and a close to zero vapour-to-liquid ratio is observed in the top stage. A ratio of 1.25 is maintained until the feed stage 15, where the liquid feed stream enters the column, dropping the ratio to 0.75.

At the bottom stage 50, the boil off in the reboiler increases the ratio to 2.5, closer to the reboiler boil up ratio of 3.0 as in Table A.2 above.

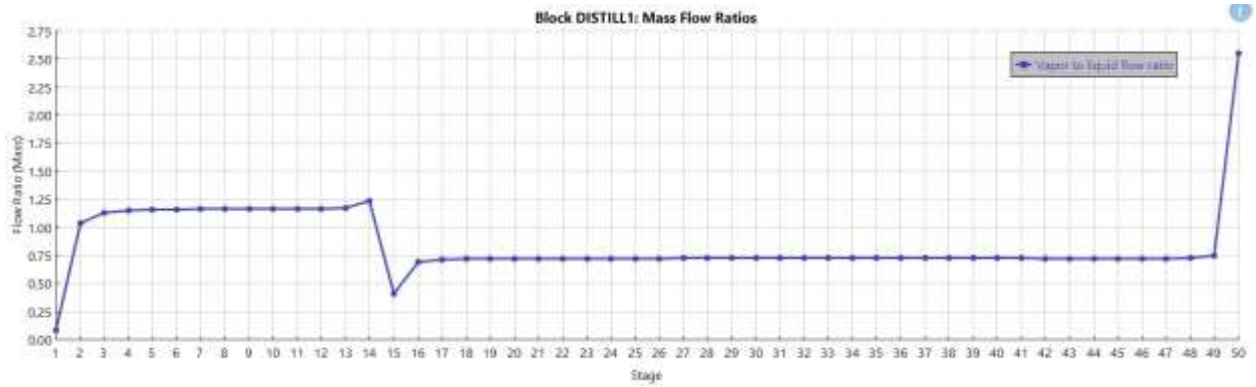


Figure A.3: The Mass Flow vapour to liquid ratios in the distillation column.

The K-Value profiles for the different components are illustrated in Figure A. 4 below. The k-values represent the relative volatility of the different components. It explains the high K-values for the Hydrogen, Carbon Monoxide, Carbon Dioxide and Propane, which are the gaseous components in the column. The remainder of the liquid components remains lowered.

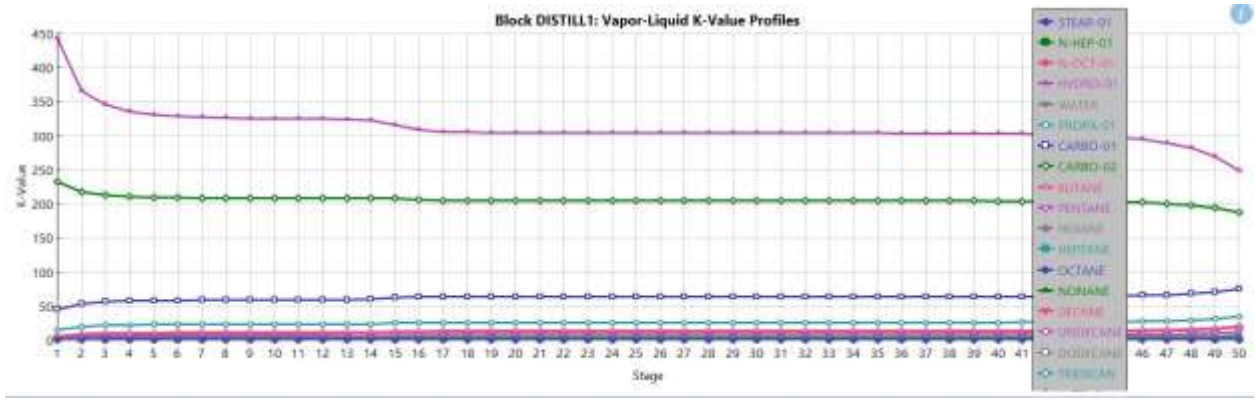


Figure A.4: K-value components in the distillation column.